NASA TECHNICAL MEMORANDUM

NASA TM X-1678

NASA TM X-1678

ATLAS-CENTAUR AC-12 FLIGHT PERFORMANCE FOR SURVEYOR III

Lewis Research Center
Cleveland, Ohio

NATIONAL AERONAUTICS AND SPACE ADMINISTRATION • WASHINGTON, D. C. • NOVEMBER 1968

ATLAS-CENTAUR AC-12 FLIGHT PERFORMANCE FOR SURVEYOR III

Lewis Research Center
Cleveland, Ohio

NATIONAL AERONAUTICS AND SPACE ADMINISTRATION

ABSTRACT

Atlas-Centaur vehicle AC-12, launched on April 17, 1967, was the third operational flight in the Centaur program. The vehicle carried Surveyor III, which was boosted into a lunar-intercept trajectory by the parking-orbit mode of ascent. This mode of ascent included placing the Centaur in a circular orbit, coasting under low-gravity conditions, and restarting the Centaur main engines to supply energy to attain the proper lunar-intercept trajectory. This report includes a flight performance evaluation of the Atlas-Centaur launch vehicle system from lift-off through Centaur retromaneuver.

CONTENTS

I. SUMMARY

The Atlas-Centaur vehicle AC-12, with Surveyor III spacecraft, was successfully launched from Eastern Test Range Complex 36B on April 17, 1967 at 0205:01 hours eastern standard time. The Centaur, with Surveyor, was first injected into a 90-nautical-mile (167-km) parking orbit. After a 22-minute coast, the Centaur main engines were restarted, and the Surveyor was placed in a lunar-transfer orbit. Orbital insertion was accurate and only a slight midcourse velocity correction of 3.9 meters per second (for miss only) would have been required to place the Surveyor on the prelaunch selected target. The Surveyor successfully touched down on the lunar surface at 1904 hours eastern standard time on April 19, 1967, after an elapsed flight time of 65 hours.

AC-12 was the third operational Atlas-Centaur vehicle. It was also the first of the operational Centaurs designed for main engine restart capability in space, as required for parking-orbit mode-of-ascent missions. The vehicle configuration, as developed on the research and development flights, provided successful control of the cryogenic propellants throughout the orbital coast. Centaur main engine restart and second burn were successful. A performance evaluation of the Atlas and Centaur vehicle systems in support of this flight is given in this report.

2

II. INTRODUCTION

by John J. Nieberding

The flight of Atlas-Centaur vehicle AC-12 and Surveyor III was the first operational Centaur flight to use an indirect (parking-orbit) mode of ascent. Surveyors I and II were launched by an Atlas-Centaur combination which used a direct mode of ascent. The parking-orbit mode consisted of first launching the Centaur-Surveyor into an approximately 90-nautical-mile (167-km) circular parking orbit. The vehicle then coasted for about 22 minutes under very low thrust. This coast period was followed by the restart of the Centaur main engines to transfer the Centaur-Surveyor from the nearly circular parking orbit into a highly elliptical lunar-intercept trajectory. The objective of the launch was to inject Surveyor III into this lunar trajectory with sufficient accuracy so that the midcourse velocity correction performed by the spacecraft was within the Surveyor III capability. The lunar-landing location selected prior to launch was 3.33^O South latitude, 23.17^O West longitude. This region is of interest to the Apollo manned lunar-landing program.

The development of the parking-orbit, or two-burn, mode of ascent was undertaken to provide greater launch flexibility than was provided by the one-burn, direct-ascent mode. With direct ascent, for example, lunar launches were restricted to the summer months. The parking-orbit ascent permits launches every month of the year. In addition to providing more launch days for lunar missions, the parking orbit allows longer launch periods on each day in the launch opportunity.

Two research and development vehicles, AC-8 and AC-9, were assigned to support the development of the Centaur two-burn mission capability. These vehicles successfully demonstrated the ability of Centaur to provide the propellant control during the low-gravity coast phase. This propellant control was essential for a Centaur main engine restart.

This report presents an evaluation of the Atlas-Centaur launch vehicle systems performance and the results of flight AC-12, showing how launch vehicle performance supported the objectives of Surveyor III.

III. LAUNCH VEHICLE DESCRIPTION

by Eugene E. Coffey

The Atlas-Centaur AC-12 was a two-stage launch vehicle consisting of an Atlas first stage and a Centaur second stage connected by an interstage adapter. Both stages were 10 feet (3.05 m) in diameter and the composite vehicle was 113 feet (34.44 m) in length. The vehicle weight at lift-off was 303 000 pounds (137 000 kg). The basic structure of the Atlas and the Centaur stages utilized thin-wall, pressurized, main propellant tank sections of monocoque construction.

The first-stage Atlas vehicle, as shown in figure III-1, was 65 feet (19.81 m) long. It was powered by a standard Rocketdyne MA-5 propulsion system consisting of two booster engines with 330 000 pounds (146.784×10^4 N) thrust total, a single sustainer engine of 57 000 pounds (253.55×10^3 N) thrust, and two small vernier engines of 670 pounds (2980 N) thrust each. All engines burned liquid oxygen and kerosene (RP-1) and were ignited simultaneously on the ground. The booster engines were gimbaled for pitch, yaw, and roll control during the booster phase of the flight. This phase was completed when the vehicle acceleration equaled about 5.7 g's and the booster engines were cut off. The booster engines were jettisoned 3.1 seconds after booster engine cutoff. The sustainer engine and the vernier engines continued to burn after booster engine cutoff for the Atlas sustainer phase of the flight. During this phase, the sustainer engine gimbaled for pitch and yaw control while the vernier engines gimbaled for roll control only. The sustainer and vernier engines burned until propellant depletion, which completed the sustainer phase. The Atlas was then separated from the Centaur by the firing of a shaped-charge severance system located on the interstage adapter. The firing of a retrorocket system, required to back the Atlas and the interstage adapter away from the Centaur, completed the separation of these stages.

The second-stage Centaur vehicle is shown in figure III-2. This stage, including the nose fairing, was 48 feet (14.63 m) long. Centaur is a high performance stage (specific impulse, 442 sec). It was powered by two Pratt & Whitney RL10A3-3 engines which generated 30 000 pounds (133.45×10^3 N) thrust total. These engines burned liquid hydrogen and liquid oxygen. The Centaur main engines gimbaled to provide pitch, yaw, and roll control during Centaur powered flight. Fourteen hydrogen peroxide engines of various thrust levels, mounted on the aft periphery of the tank, provided attitude control, propellant settling and retention, and vehicle reorientation after spacecraft separation. The Centaur hydrogen tank was equipped with four insulation panels 1-inch (2.54-cm) thick.

5

The panels consisted of glass fabric lamination and a polyurethane foam core. A fiberglass nose fairing was used to provide an aerodynamic shield for the Surveyor spacecraft, guidance equipment, and electronic packages during ascent. The insulation panels and nose fairing were jettisoned during the Atlas sustainer phase.

The AC-12 vehicle was designed for a parking-orbit mode-of-ascent trajectory. As such, the hydrogen tank was equipped with a slosh baffle and energy-dissipating devices on the propellant return lines to inhibit disturbances in the liquid residuals at engine shutdown. Suppression of liquid disturbance after main engine first cutoff and the retention of the liquid residuals during the low-gravity coast period were provided by continuous thrust from the hydrogen peroxide engines. This propellant control was required to support main engine restart.

AC-12 was similar to AC-9 (see ref. 1). The major systems, as they were configured for the Atlas-Centaur launch vehicle AC-12, are delineated in the subsequent sections of this report.

Oxidizer boiloff valve

Forward bulkhead

Liquid oxygen tank

Oxidizer tank pressurization line

Wiring tunnel

Antislosh baffle assembly

Intermediate bulkhead

Equipment pod (upper pod in flight)

Fuel tank

Equipment pod (lower pod in flight)

Oxidizer duct

Antivortex baffle

Retrorockets (eight)

Vernier thrust chamber 1

B-2 booster thrust chamber

Gas generator exhaust

B-1 booster thrust chamber

Sustainer thrust chamber

Down range or down in flight

Quadrant II

-y

x

Quadrant I

y

Quadrant III

-x

Quadrant IV

Figure III-1. - General arrangement of Atlas launch vehicle, AC-12.
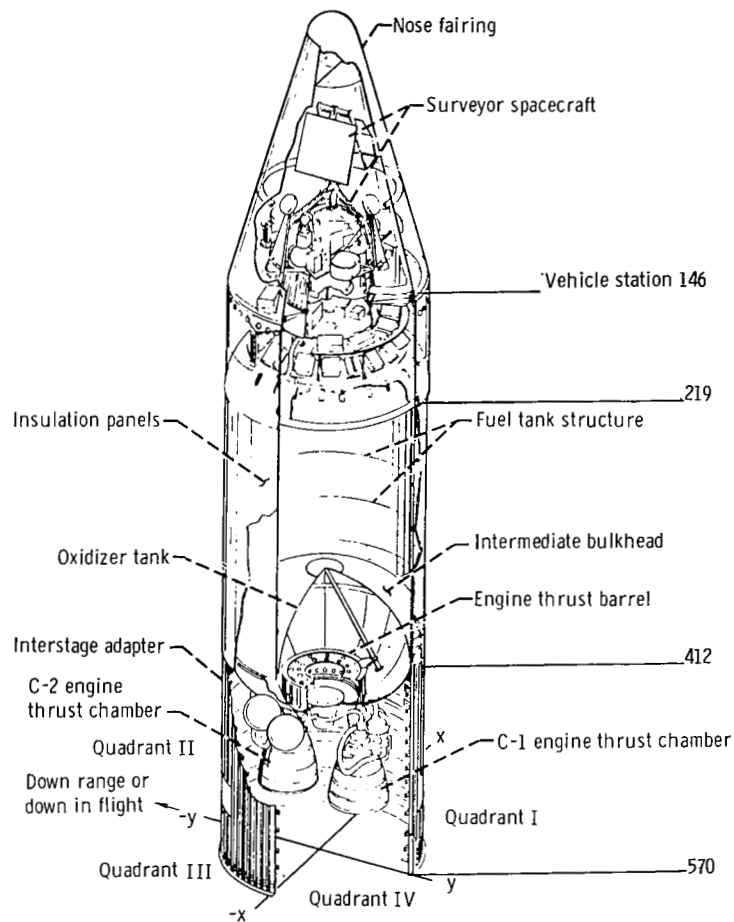
Figure III-2. – General arrangement of Centaur vehicle, AC-12.

Nose fairing

Surveyor spacecraft

Vehicle station 146

219

Fuel tank structure

Insulation panels

Intermediate bulkhead

Oxidizer tank

Engine thrust barrel

Interstage adapter

412

C-2 engine thrust chamber

C-1 engine thrust chamber

Quadrant II

x

Down range or down in flight   -y

Quadrant I

Quadrant III

570

y

Quadrant IV

-x

IV. MISSION PERFORMANCE

by William A. Groesbeck

The third operational Atlas-Centaur vehicle AC-12, with Surveyor III, was successfully launched from Eastern Test Range Complex 36B on April 17, 1967 at 0205:01 hours eastern standard time. This flight was the first operational vehicle to employ the indirect (parking-orbit) mode of ascent. All programmed mission objectives were successfully achieved: The Centaur and Surveyor were injected into an approximately 90-nautical-mile (167-km) orbit, coasted under low-gravity conditions for about 22 minutes, restarted the Centaur main engines, and injected the Surveyor into a lunar-transfer orbit.

A compendium of the AC-12 mission profile and the lunar-transfer trajectory are shown in figures IV-1 and IV-2. For reference also, a listing of the postflight vehicle weights summary, atmospheric sounding data, trajectory data, surveyor launch window, and flight events record are given in the appendix.

ATLAS FLIGHT PHASE

Ignition and thrust buildup of the Atlas engines were normal, and the vehicle lifted off (T + 0 sec) with a combined vehicle weight of 303 000 pounds (137 000 kg) and a thrust to weight ratio of 1.28. Two seconds after lift-off, the vehicle initiated a programmed roll from the launcher fixed azimuth of 115° to the required flight azimuth of 100.81^O. At T + 15 seconds, the vehicle had rolled to the flight azimuth and it began a preprogrammed pitchover maneuver which lasted through booster engine cutoff. The inertial guidance system was functioning during this time, but steering commands were not admitted to the flight control systems until after booster staging.

The preset Atlas pitch program used to command the vehicle during the booster flight was augmented by supplemental pitch and yaw inputs which acted to reduce vehicle bending loads due to winds. This supplemental program, one of a series selected on the basis of measured prelaunch upper air soundings, was stored in the airborne computer. The incremental values were algebraically summed with the fixed program stored in the Atlas flight programmer. Booster engine gimbal angles for thrust vector control were accordingly reduced and did not exceed 1.16^O during the atmospheric ascent.

Vehicle acceleration during the boost phase proceeded according to the mission plan. Centaur guidance issued the booster engine cutoff signal when the vehicle acceleration

reached 5.62 g's. Three seconds later at T + 145.3 seconds, the Atlas programmer issued the staging command causing separation of the booster engine stage from the vehicle. Staging transients were small, and the maximum vehicle angular rate in pitch, yaw, or roll did not exceed 1.08 degrees per second. Low amplitude "slosh" was excited in the Atlas liquid-oxygen tank but it was damped out within a few seconds.

Vehicle steering by the inertial guidance system was initiated about 4 seconds following Atlas booster staging. At the start of guidance steering, the vehicle was slightly off the required steering vector by about 11° nose high in pitch and 1^O nose left in yaw. This correction was made within 7 seconds as the guidance system issued commands to continue the pitchover maneuver during the Atlas sustainer flight phase.

Insulation panels were jettisoned during the sustainer flight phase at T + 176.2 seconds. All four panels were completely severed by the shaped charge and fell away from the vehicle. The nose fairing unlatch command was given at T + 202.4 seconds and the thruster bottles, firing 0.5 second later, rotated the fairing halves away from the vehicle. Vehicle angular rates, due to the jettisoning of the insulation panels and nose fairing, were insignificant.

Sustainer and vernier engine system performance was satisfactory throughout the flight. Sustainer engine cutoff was initiated because of liquid-oxygen depletion at T + 237.7 seconds. Maximum vehicle acceleration just prior to sustainer cutoff was 1.78 g's.

Coincident with sustainer engine cutoff, the guidance steering commands to the flight control system were discontinued, allowing the vehicle to coast in a noncontrolled flight mode. This guidance mode prevented gimbaling the Centaur main engines and allowed the engines to be centered to maintain clearance between the engines and the interstage adapter during staging.

The Atlas staging command was issued by the flight programmer at T + 239.6 seconds. A shaped-charge firing cut the interstage adapter to separate the two stages. Eight retrorockets on the Atlas then fired to push the Atlas stage away from the Centaur. The staging transients were small and the maximum angular rate imparted to the vehicle did not exceed 0.2 degree per second.

CENTAUR FLIGHT PHASE

Centaur Main Engine First Burn

The main engine start sequence for the Centaur stage was initiated prior to sustainer engine cutoff. Propellant boost pumps were started at T + 203.9 seconds and allowed to come up to speed. To prevent boost pump cavitation during the near-zero-gravity period

from sustainer engine cutoff until main engine start at T + 249.2 seconds, the required net positive suction pressure was provided by pressure pulsing the propellant tanks with helium. Eight seconds prior to main engine start, the Centaur programmer issued prestart commands for engine firing. Centaur main engines were gimbaled to zero. Engine prestart valves were opened to flow liquid hydrogen through the lines and thereby chill down the engine turbopumps. Chilldown of the turbopumps ensured against cavitation during pump acceleration and made possible a uniform and rapid thrust buildup after engine ignition. At T + 249.2 seconds, the ignition command was issued by the flight programmer and engine thrust increased to full flight levels.

Guidance steering for the Centaur stage was initiated at T + 253.2 seconds. The discontinuance of guidance steering commands during the engine start sequence prevented engine gimbaling which could cause excessive vehicle angular rates during the start transient. The total residual angular rates and disturbing torques induced during this staging interval resulted in only a slight vehicle drift off the steering vector. This attitude drift error was corrected within 4 seconds after start of guidance steering.

Through the remainder of the Centaur main engine burn, the guidance steering commands were required to provide the necessary pitchdown rate to acquire the injection velocity vector for the desired parking orbit. At T + 589.7 seconds, the guidance-computed velocity for injection was attained and the engines were commanded off. Orbital insertion at an altitude of about 90 nautical miles (167 km) occurred approximately 1200 nautical miles (2220 km) southeast of Cape Kennedy at a velocity of 24 253 feet per second (7405 m/sec).

The Centaur engine burn time to establish the parking orbit was about 14 seconds longer than expected. The additional firing time was necessary to compensate for a lower thrust resulting from a slight shift in the thrust controller unit. The propellant utilization system performed satisfactorily and accurately controlled the fuel and oxidizer flow rates to the engines.

Centaur Coast Phase

At main engine cutoff, the vehicle began a 22-minute orbital coast. Guidance generated steering commands to the flight control system were discontinued. Vehicle control for stabilization was switched to the hydrogen peroxide attitude control system.

Control of the propellants during the coast phase was successfully accomplished by using liquid energy-dissipating devices and a programmed low-level-thrust schedule. Propellant tank configuration and propellant control technique for this phase of the mission were the same as those successfully demonstrated on the AC-9 research and development flight. Coincident with main engine cutoff, two 50-pound (222-N) thrust engines were

fired to provide an acceleration level of 6.9×10^{-3} g's for 76 seconds. This thrust level suppressed the excursions of the liquid disturbances excited by engine shutdown transients and retained the propellants in the bottom of the tanks. Energy-dissipating devices, such as baffles around the hydrogen tank and energy-dissipating diffusers on return flow lines into the tank, also attenuated and dissipated the disturbance inputs to the residual propellants. At 76 seconds into the coast, with the liquid disturbances largly damped out, the thrust level was reduced to 6 pounds (26.7 N) or an acceleration of 4.1×10^{-4} g's. This was sufficient thrust to retain the propellants in a settled condition through the remainder of the coast.

Attitude control of the vehicle through the coast phase was achieved without incident. Disturbance torques due to the firing of two 50-pound (222-N) thrust engines for propellant settling were the same as noted in previous flights (see ref. 1). Hydrogen venting through the nonpropulsive vent system did not produce any disturbing torques on the vehicle. Venting of the hydrogen tank during the coast phase did not occur until T + 1105 seconds when the ullage pressure increased to the regulating range of the primary vent valve. Hydrogen gas was then vented intermittently as required to maintain tank pressure through the remainder of the coast. The oxygen tank was not vented at any time during the coast.

Forty seconds prior to main engine restart the thrust level on the vehicle was increased back up to 100 pounds (444 N) to give added assurance of proper propellant settling. At the same time, the hydrogen tank vent valve was closed and the tank pressures were increased by injecting helium gas into the ullage. Engine prestart valves were opened 17 seconds prior to engine start to allow liquid hydrogen to flow through and chill down the lines and engine components. Tank pressurization, thermal conditioning of the engines, and control of the propellants throughout the coast phase were all completely successful and supported a restart of the main engines.

Centaur Main Engine Second Burn

The Centaur main engines were successfully restarted on command at T + 1917.3 seconds, and engine performance was satisfactory through the second burn. At engine restart, the 100-pound (444-N) thrust used for propellant control was terminated. The hydrogen peroxide attitude control was also switched off at engine restart, and 4 seconds later Centaur guidance steering was resumed to steer the vehicle toward the computed velocity vector required for injection of the spacecraft into a lunar-intercept trajectory. All systems performed properly. At T + 2029 seconds the required injection velocity was attained, and the guidance system issued commands to shut down the engines.

The propellant utilization system controlled the propellant mixture ratio to an aver-

age value of 5.23 to 1. Burnable residual propellants would have provided an additional 8.3 seconds of engine firing. This indicated an adequate propellant reserve and satisfactory vehicle performance.

SPACECRAFT SEPARATION

Coincident with the main engine second cutoff, the guidance steering commands were temporarily discontinued, and the coast phase hydrogen peroxide attitude control system was again activated. Angular rates imparted to the vehicle by engine shutdown transients were small and were quickly damped to rates less than the control threshold of 0.2 degree per second. The residual vehicle motion below the rate threshold allowed only a negligible drift in vehicle attitude. This drift did not interfere with the subsequent spacecraft separation.

The Centaur with the Surveyor coasted in a near-zero-gravity field for about 70 seconds. During this time, any residual vehicle rates were damped out, and commands were given to prepare the spacecraft for separation. Commands were given by the Centaur programmer to the spacecraft to turn on transmitter high power, arm the spacecraft separation pyrotechnics, and extend landing gear and omniantennas. All commands were properly received by the spacecraft.

At T + 2093.3 seconds, the command for spacecraft separation was given. The hydrogen peroxide attitude control system was commanded off, the pyrotechnically operated latches were fired, and the separation springs pushed the Surveyor away from the Centaur. Full extension of all three springs occurred within 1 millisecond of each other, and the separation velocity imparted to the spacecraft was about 0.75 foot per second (0.213 m/sec). Angular rates of the spacecraft after separation did not exceed 0.56 degree per second. This rate was well below the maximum allowable of 3.0 degrees per second.

CENTAUR RETROMANEUVER

Following spacecraft separation, the Centaur stage was commanded to perform a reorientation and retrothrust maneuver. This type of maneuver was necessary to alter the Centaur orbit in order to eliminate the possibility of the Surveyor star sensor acquiring the reflected light of Centaur rather than the star Canopus. A second objective of the retromaneuver was to prevent the Centaur from impacting on the Moon.

A guidance steering vector for the turnaround was selected which was the reciprocal of the velocity vector at second main engine cutoff. Execution of the turnaround was commanded 5 seconds after spacecraft separation at T + 2098.5 seconds. Guidance sys-

tem logic accounted for any vehicle drift after main engine cutoff, and steering commands were given which rotated the vehicle in the shortest arc from its actual position to the new retrovector. Angular rates during the turnaround were limited to a maximum of 1.6 degrees per second.

About half way through the turnaround at T + 2138.4 seconds, two 50-pound (222-N) thrust hydrogen peroxide engines were fired for 20 seconds to impart lateral as well as additional longitudinal separation from the spacecraft. The lateral separation was necessary to minimize the possible impingement of frozen particles on the spacecraft during the subsequent discharge of residual Centaur propellants through the main engines. While these 50-pound (222-N) thrust engines were firing, the exhaust plumes produced high impingement forces on the vehicle causing a clockwise roll disturbing torque. To correct this disturbing roll torque, the 3.5- and 6.0-pound (15.55- and 26.6-N) thrust attitude control engines were required to operate 50 percent of the time.

The turnaround maneuver was completed at about T + 2200 seconds after rotating the vehicle through 162°. After the retrovector was acquired, the attitude control maintained the vehicle position on the vector within 1.5^O.

At T + 2333.7 seconds, the retrothrust portion of the retromaneuver was commanded by the Centaur programmer. The main engines were gimbaled to aline the thrust vector with the newly acquired steering vector, the engine prestart valves were opened, and residual propellants were allowed to discharge through the engines. The propellant discharge provided sufficient thrust to increase the separation distance from the spacecraft and to alter the Centaur orbit in order to avoid impact on the Moon. The relative separation distance between the spacecraft and the Centaur at the end of 5 hours was 1436 kilometers. This distance was about 4.3 times the required minimum.

At completion of the retromaneuver at T + 2701 seconds, the hydrogen and oxygen tank vent valves were enabled to the relief or normal regulating mode. A postmission exercise was then conducted to determine the amount of residual hydrogen peroxide. This test was accomplished by firing two of the 50-pound (222-N) thrust engines until the propellant (hydrogen peroxide) was depleted. The engines fired for 44 seconds. For normal consumption, the firing time indicated a residual of about 31 pounds (14 kg) of usable hydrogen peroxide. Following this test, all systems were deenergized and the vehicle continued in orbit in a nonstabilized flight mode.

SURVEYOR LUNAR TRANSIT

The Surveyor III was injected into its lunar-intercept trajectory with such accuracy that a lunar impact would have occurred without any midcourse correction. And to vector in on the preselected touchdown site, only a very slight midcourse velocity correction of

14

3.9 meters per second (miss only) would have been required 20 hours after injection. However, there was a target change and an actual correction of 4.19 meters per second (for miss only) was made 21 hours and 55 minutes after injection. The Surveyor III functioned successfully and touched down on the lunar surface at 1904 hours eastern standard time on April 19, 1967. Elapsed flight time for the mission was about 65 hours.

The actual touchdown point on the Moon was at a position of 2.94° South latitude and 23.3° West longitude. This position was within 5.6 kilometers of the final targeted aiming point. Surveyor III was the second spacecraft in the Surveyor program to land successfully on the Moon.
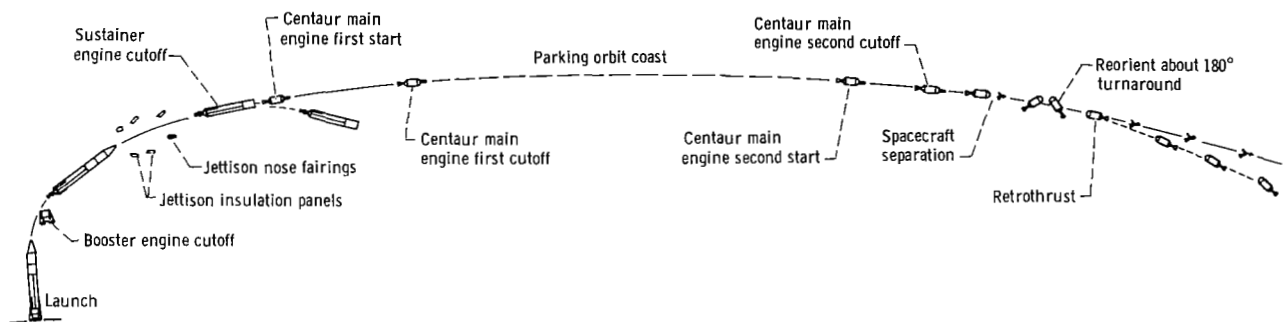
Figure IV-1. - Atlas Centaur flight compendium for indirect-ascent mode, AC-12.
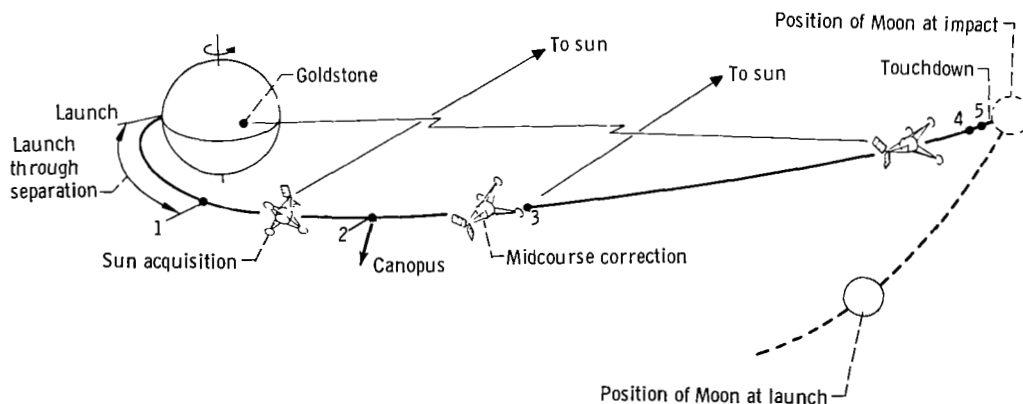
Figure IV-2. - Surveyor III-Earth-Moon trajectory. 1, injection and separation; 2, star acquisition and verification; 3, reacquisition of sun and star after midcourse correction; 4, retrophase initiated about 60 miles (96 km) from Moon; 5, vernier descent initiated 35 000 feet (10 700 m) above surface of Moon, AC-12.

V. LAUNCH VEHICLE SYSTEM ANALYSIS

PROPULSION SYSTEMS

by Steven V. Szabo, Jr., Ronald W. Ruedele, Kenneth W. Baud, and Donald B. Zelten

Atlas

System description. - The Rocketdyne MA-5 engine system utilized by the Atlas consisted of a booster engine system, a sustainer engine system, a vernier engine system, an engine start system, a logic control subsystem, and an electric subsystem. The systems are shown schematically in figure V-1.

All engines were single start using liquid oxygen (oxidizer) and RP-1 (fuel) as propellants. The engines were hypergolically ignited using pyrophoric fuel cartridges. The pyrophoric fuel preceded the RP-1 into the combustion chambers and initiated ignition with the liquid oxygen. Combustion was then sustained by the RP-1 and liquid oxygen. All thrust chambers were regeneratively cooled with RP-1.

The rated thrust values of the engines are given in the following table:

Engine	Chamber	Thrust	
		lb	N
Booster	2 (total)	328 600	14.6×10^5
Sustainer	1	57 000	25.4×10^4
Vernier	2 (total)	1 340	5.96×10^3

The booster engine system consisted of two gimbaled thrust chambers and a common power package consisting of a gas generator and two turbopumps and a supporting control system. The sustainer engine was a gimbaled engine assembly consisting of a thrust chamber, gas generator, turbopump, and supporting control system. The two vernier engines consisted of thrust chambers, propellant valves, gimbal bodies, and mounts. The self-contained engine start system consisted of an oxidizer start tank, fuel start tank, and the associated controls.

System performance. - Engine start and thrust buildup appeared normal, and engine

TABLE V-1. - ATLAS ENGINE REQUIREMENTS AT ENGINE

START, AC-12

(a) U.S. Customary Units

Parameter	Required at engine start	Value at engine start
Booster gas generator liquid-oxygen regulator reference pressure (absolute), psi	615 to 635	629
Sustainer gas generator liquid-oxygen regulator reference pressure (absolute), psi	809 to 849	834
Number 2 booster engine turbine inlet temperature, ^{o}F	>0	69
Sustainer engine turbine inlet temperature, ^{o}F	>0	52
Liquid-oxygen temperature at fill and drain valve, ^{o}F	<-283	-305.2
Sustainer lubrication oil tank temperature, ^{o}F	>45	53

(b) SI Units

Parameter	Required at engine start	Value at engine start
Booster gas generator liquid-oxygen regulator reference pressure (absolute), N/cm^2	424 to 437	434
Sustainer gas generator liquid-oxygen regulator reference pressure (absolute), N/cm^2	557 to 585	575
Number 2 booster engine turbine inlet temperature, K	>256	293
Sustainer engine turbine inlet temperature, K	>256	284
Liquid-oxygen temperature at fill and drain valve, K	<98	85
Sustainer lubrication oil tank temperature, K	>281	284

18

system requirements for start were adequately met as given in table V-1.

Booster engine system operation during flight was satisfactory. Booster engine thrust calculated from chamber pressure data is compared with predicted thrust levels in the following table:

	Thrust, lb force; N	
	T + 10 sec	Booster engine cutoff
Predicted	324 645; 14.4×10^5	374 450; 16.6×10^5
Actual	326 995; 14.5×10^5	377 476; 16.8×10^5

Booster engine cutoff occurred at T + 142.3 seconds and at an axial acceleration of 5.62 g's. Telemetered booster engine performance data are summarized in table V-2.

The in-flight operation of the sustainer and vernier engines was also satisfactory. Sustainer and vernier engine cutoff occurred at T + 237.7 seconds, and the maximum axial acceleration, which occurred just prior to sustainer engine cutoff, was 1.78 g's.

Sustainer engine shutdown occurred as planned, by activation of the pressure switches in the sustainer fuel injection manifold. These switches were activated because of liquid-oxygen depletion.

Predicted and actual combined sustainer and vernier engine axial thrust is presented in the following table:

	Thrust, lb force; N		
	T + 10 sec	Booster engine cutoff	Sustainer engine cutoff
Predicted	57 876; 25.7×10^4	81 456; 36.2×10^4	79 921; 35.5×10^4
Actual	59 635; 26.5×10^4	83 023; 36.9×10^4	82 189; 36.6×10^4

Actual thrust was calculated from chamber pressure data telemetered during flight. Telemetered sustainer and vernier engine performance data are also summarized in table V-2.

TABLE V-2. - ATLAS ENGINE SYSTEM PERFORMANCE, AC-12

(a) U.S. Customary Units

Engine parameter	Flight time, sec		
	T + 10	Booster engine cutoff[a]	Sustainer engine cutoff[a]
Number 1 booster engine:			
Chamber pressure, psi	561	561	---
Pump speed, rpm	6 300	6 280	---
Oxidizer pump inlet absolute pressure, psi	59	76	---
Fuel pump inlet absolute pressure, psi	70	55	---
Number 2 booster engine:			
Chamber pressure (absolute), psi	579	580	---
Pump speed, rpm	6 300	6 300	---
Oxidizer pump inlet absolute pressure, psi	57	81	---
Fuel pump inlet absolute pressure, psi	69	55	---
Booster:			
Gas generator combustion chamber pressure (absolute), psi	510	510	---
Liquid-oxygen regulator reference pressure (absolute), psi	638	623	---
Sustainer:			
Chamber pressure (absolute), psi	700	680	670
Pump speed, rpm	10 370	10 200	10 320
Oxidizer injection manifold pressure (absolute), psi	828	818	798
Pump discharge pressure (absolute), psi	940	933	918
Oxidizer regulator reference pressure (absolute), psi	841	841	841
Gas generator discharge pressure (absolute), psi	655	655	655
Fuel pump inlet absolute pressure, psi	73	64	43
Oxidizer pump inlet pressure (absolute), psi	62	84	32
Number 1 vernier chamber absolute pressure, psi	260	252	256
Number 2 vernier chamber absolute pressure, psi	257	257	253

[a]Data points actually taken 2 sec prior to engine cutoff.

TABLE V-2. – Concluded. ATLAS ENGINE SYSTEM PERFORMANCE, AC-12

(b) SI Units

Engine parameter	Flight time, sec		
	T + 10	Booster engine cutoff[a]	Sustainer engine cutoff[a]
Number 1 booster engine:			
Chamber pressure, N/cm^2	386	386	---
Oxidizer pump inlet absolute pressure, N/cm^2	41	52	---
Fuel pump inlet absolute pressure, N/cm^2	48	38	---
Number 2 booster engine:			
Chamber pressure (absolute), N/cm^2	399	399	---
Oxidizer pump inlet absolute pressure, N/cm^2	39	56	---
Fuel pump inlet absolute pressure, N/cm^2	47	38	---
Booster:			
Gas generator combustion chamber pressure (absolute), N/cm^2	352	352	---
Liquid-oxygen regulator reference pressure (absolute), N/cm^2	440	429	---
Sustainer:			
Chamber pressure (absolute), N/cm^2	483	469	462
Oxidizer injection manifold pressure (absolute), N/cm^2	571	564	550
Pump discharge pressure (absolute), N/cm^2	648	643	633
Oxidizer regulator reference pressure (absolute), N/cm^2	580	580	580
Gas generator discharge pressure (absolute), N/cm^2	452	452	452
Fuel pump inlet absolute pressure, N/cm^2	51	44	30
Oxidizer pump inlet pressure (absolute), N/cm^2	43	58	21
Number 1 vernier chamber absolute pressure, N/cm^2	179	174	176
Number 2 vernier chamber absolute pressure, N/cm^2	177	177	174

[a]Data points actually taken 2 sec prior to engine cutoff.

Centaur Main Engines

System description. - Two Pratt & Whitney RL10A-3-3 engines were used to provide thrust for the Centaur stage. A schematic drawing of the Centaur main engine is shown in figure V-2. Each engine was regeneratively cooled and turbopump fed with a single thrust chamber. Engine rated thrust was 15 000 pounds (66 700 N) at an altitude of 200 000 feet (61 000 m). Propellants were liquid oxygen and liquid hydrogen injected at an oxidizer-to-fuel mixture ratio of about 5.0 to 1. Rated engine thrust was achieved at a design combustion chamber absolute pressure of 400 psi (275.5 N/cm^2). The thrust chamber nozzle expansion area ratio was 57; specific impulse was a minimum of 439 seconds.

These engines used a "bootstrap" process as follows: pumped fuel, after cooling the thrust chamber, was expanded through the turbine which drives the propellant pumps. The fuel was then injected into the combustion chamber. The pumped oxidizer was supplied directly to the propellant injector through the propellant utilization valve. This valve controlled the propellant mixture ratio supplied to the thrust chamber.

Thrust control was achieved by regulating the amount of fuel bypassed around the turbine as a function of combustion chamber pressure. The turbopump speed varied thereby controlling engine thrust. Ignition was accomplished by a spark igniter recessed in the propellant injector face. Starting and stopping were controlled by pneumatic valves. Helium pressure to these valves was supplied through engine-mounted solenoid valves which were controlled by electrical signals from the flight programmer.

System performance during main engine first burn. - An engine turbopump chilldown sequence of 8 seconds duration was conducted immediately prior to main engine start. This operation satisfactorily prevented cavitation of the main engine turbopumps during the start transient.

Main engine start was commanded at T + 249.20 seconds. Main engine chamber pressures during the start transient are presented in figure V-3. Start total impulse during the 2-second period following the main engine start command was calculated to be 9690 and 8870 pound-seconds (43 100 and 39 400 N-sec) for the C-1 and C-2 engines, respectively. The differential impulse of 820 pound-seconds (3650 N-sec) between engines was well within the specification allowable of approximately 6000 pound-seconds (26 700 N-sec).

Liquid-hydrogen and liquid-oxygen pump-inlet pressure and temperature data for the first 90 seconds of main engine operation are presented in figure V-4 to V-6. The pump-inlet pressures and temperatures indicated that the propellant pressures remained well above saturation during this time period. The margin between the steady-state operating limit and the actual inlet conditions ensured satisfactory values of net positive suction pressure.

Steady-state operating conditions at 90, 200, and 335 seconds after main engine start

TABLE V-3. – CENTAUR MAIN ENGINE FIRST FIRING OPERATING CONDITIONS, AC-12

(a) U.S. Customary Units

Parameter	Expected value	Time from main engine start, sec					
		90		200		330	
		Engine					
		C-1	C-2	C-1	C-2	C-1	C-2
Liquid-hydrogen pump total inlet pressure (absolute), psi	17.2 to 37.3	31.2	32.3	30.4	30.8	28.2	29.0
Liquid-hydrogen pump inlet temperature, $^\circ$R	37.4 to 43.0	38.9	39.0	38.3	38.4	37.6	37.7
Liquid-oxygen pump total inlet pressure (absolute), psi	52.2 to 77.9	62.7	63.7	62.6	64.6	61.5	61.0
Liquid-oxygen pump inlet temperature, $^\circ$R	172.0 to 183.8	176.9	176.9	176.3	176.4	175.4	175.4
Hydrogen venturi upstream pressure (absolute), psi	[a]737±25	726	722	735	728	724	723
Hydrogen turbine inlet temperature, $^\circ$R	[a]372±22	381.7	389.0	368.2	377.1	367.9	380.2
Oxygen pump speed, rpm	[a]12 163±347	12 170	12 140	12 410	12 090	12 210	11 980
Oxygen injector differential pressure, psi	[a]46±10	38.8	45.2	41.4	45.5	39.6	46.0
Engine chamber pressure (absolute), psi	[a]392.4±5.4	388.5	381.5	386.3	382.6	386.8	384.8

(b) SI Units

Parameter	Expected value	Time from main engine start, sec					
		90		200		330	
		Engine					
		C-1	C-2	C-1	C-2	C-1	C-2
Liquid-hydrogen pump total inlet pressure (absolute), N/cm^2	11.9 to 25.7	21.5	22.3	21.0	21.2	19.5	20.0
Liquid-hydrogen pump inlet temperature, K	20.8 to 23.9	21.6	21.65	21.3	21.35	20.9	20.95
Liquid-oxygen pump total inlet pressure (absolute), N/cm^2	36.0 to 53.7	43.2	44.0	43.2	44.6	42.4	42.0
Liquid-oxygen pump inlet temperature, K	95.6 to 102.1	98.0	98.0	97.8	97.9	97.4	97.4
Hydrogen venturi upstream pressure (absolute), N/cm^2	[a]518±17	501	498	507	502	499	498
Hydrogen turbine inlet temperature, K	[a]256±15	212	216	210	209.5	204	211
Oxygen injector differential pressure, N/cm^2	[a]32±7	26.8	31.2	29.6	31.4	27.3	31.7
Engine chamber pressure (absolute), N/cm^2	[a]270.7±3.7	268	263	256.5	264	267	266

[a]Expected values at design inlet conditions and a propellant utilization valve angle of zero.

23

are compared with their corresponding predicted values in table V-3. At main engine start plus 90 seconds, chamber pressure was 7.4 and 10.4 psi (5.1 and 7.2 N/cm^2) below engine acceptance test levels for the C-1 and C-2 engines, respectively. The reduction in chamber pressure has been attributed to a performance shift within the engine thrust controller. Other engine system parameters substantiated a thrust controller performance shift. A comparison with engine acceptance data showed that hydrogen venturi upstream pressure was 12 and 18 psi (8.4 and 12.4 N/cm^2) low, and hydrogen turbine inlet temperature was 12° and 15° R (6.7 and 8.4 K) high for the C-1 and C-2 engines, respectively. These pressure and temperature differences correlate with expected values during a shift in thrust controller performance. A possible reason for a thrust controller shift was the removal of orifices within the thrust controller for a contamination inspection. This inspection was conducted following the engine final acceptance tests.

Main engine performance, determined by using the Pratt & Whitney characteristic velocity (C*) iteration technique, is presented in figures V-7 and V-8. At main engine start plus 90 seconds, thrust was 14 830 and 14 450 pounds (66 000 and 64 300 N) for the C-1 and C-2 engines, respectively. These values compare with 14 996 and 14 993 pounds (66 700 and 66 690 N) obtained during the engine acceptance tests. The lower values of thrust during flight resulted from the lower chamber pressure values previously discussed. Specific impulse and mixture ratio were not significantly affected by the reduction in thrust.

Main engine first cutoff was commanded at T + 589.69 seconds. Main engine firing time was 340.49 seconds compared with a predicted value of 326.6 seconds. Approximately 9.0 seconds of this difference can be attributed to the low engine thrust. The remaining 4.8 seconds is within previous flight experience. Cutoff total impulse was 2900 pound-seconds (12 900 N-sec) which compares favorably with the predicted value of 2997±170 pound-seconds (13 320±750 N-sec).

System performance during coast phase. - Stainless-steel heat shields were installed on the AC-12 Centaur main engines for protection from impingement heating during the coast phase. Impingement from the exhaust products of the hydrogen peroxide ullage settling engines was suspected during the flight of AC-9. The shields were installed in five locations: (1) the engine hydrogen pumps, (2) the engine oxidizer pumps, (3) the oxidizer flow control valves, (4) the hydrogen pump discharge manifolds, and (5) the cooldown valve to thrust chamber ducts.

The effectiveness of the heat shields is shown in table V-4: engine hydrogen and oxygen pump housing temperatures following main engine first cutoff and prior to main engine second start on AC-12 are compared with those of AC-9. The data indicate that the heat shields reduced the warming rates. Temperature data of the engine hydrogen pump housing, the oxygen pump housing, and the hydrogen turbine inlet taken during the flight are presented in figures V-9 to V-11.

TABLE V-4. – WARMING TREND FOLLOWING MAIN ENGINE FIRST CUTOFF, AC-12

(a) U.S. Customary Units

Engine	Pump	AC-9			AC-12		
		Main engine first cutoff	Main engine cutoff plus 75 sec	Main engine second start minus 40 sec	Main engine first cutoff	Main engine cutoff plus 75 sec	Main engine second start minus 40 sec
		Housing temperature, $^{\circ}R$					
C-1	Fuel	67	140	265	61	108	230
C-1	Oxidizer	193	360	375	178	234	276
C-2	Fuel	73	135	242	[a]96	[a]116	[a]219
C-2	Oxidizer	212	344	370	178	245	282

(b) SI Units

Engine	Pump	AC-9			AC-12		
		Main engine first start	Main engine cutoff plus 75 sec	Main engine second start minus 40 sec	Main engine first start	Main engine cutoff plus 75 sec	Main engine second start minus 40 sec
		Housing temperature, K					
C-1	Fuel	37	78	147	34	60	128
C-1	Oxidizer	108	200	214	99	130	153
C-2	Fuel	40	75	134	[a]53	[a]64	[a]122
C-2	Oxidizer	118	191	206	99	136	157

[a]Measurement accuracy and response are considered erroneous.

System performance during main engine second burn. - An engine turbopump chill-down sequence was commanded 17 seconds prior to main engine second start. The longer chilldown sequence was programmed because of the added heat content of the propellant supply ducts and the engine turbopumps which resulted from the coast phase of flight. Liquid propellant conditions were evident at the turbopump inlets within 3 seconds following the initiation of chilldown. Main engine second start was commanded at T + 1917.33 seconds. Engine thrust chamber pressure rise is presented in figure V-12. The rate of chamber pressure rise on the C-1 engine was slightly in excess of previous flight experience. A thrust rise rate of approximately 230 pounds per millisecond (1020 N/msec) was experienced. This thrust rise rate occurred over a 20-millisecond time span and was within the engine maximum allowable specification. The engine specification states that the thrust rise rate shall not exceed 250 pounds per millisecond (1110 N/msec) for any time period which exceeds 10 milliseconds. The rapid thrust rise rate has been attributed

to a combination of the long chilldown sequence and an oxidizer-rich setting of the propellant utilization valve during the engine start transient. Start total impulse from main engine second start to start plus 2 seconds was calculated to be 9760 and 9780 pound-seconds (43 400 and 43 500 N-sec) for the C-1 and C-2 engines, respectively. The differential impulse of 20 pound-seconds (90 N-sec) between engines is considered negligible.

Liquid-hydrogen and liquid-oxygen pump-inlet pressure and temperature data during the main engine second burn are presented in figures V-13 to V-15. The pump inlet pressures and temperatures remained within the steady-state operating limits during the entire main engine second burn.

Steady-state operating conditions at main engine start plus 50 and 100 seconds are presented in table V-5. Engine chamber pressures at main engine start plus 100 seconds were 3.6 and 5.6 psi (2.5 and 3.9 N/cm^2) below acceptance levels for the C-1 and C-2 engines, respectively. Hydrogen venturi upstream pressures were 8 and 20 psi (5.5 and 13.8 N/cm^2) lower than acceptance test levels, while hydrogen turbine inlet temperature was 11° and 18° R (6.1 and 10 K) warmer for the C-1 and C-2 engines, respectively. These values tend to substantiate a performance shift within the engine thrust controller, while no definite correlation can be made with oxidizer pump speed. Main engine performance in terms of thrust, specific impulse, and mixture ratio is presented in figures V-7 and V-8.

Main engine second cutoff was commanded at T + 2028.62 seconds. The duration of the main engine firing was 111.3 seconds compared with a predicted value of 108.4 seconds. Approximately 1.0 second of the longer firing time can be attributed to low engine thrust, while the remaining 1.9 seconds was within previous flight experience. Engine cutoff total impulse was calculated to be 3014 pound-seconds (13 400 N-sec) and compared favorably with a predicted level of 2894±170 pound-seconds (12 880±750 N/sec).

System performance during retrothrust. - A vehicle turnaround and retrothrust operation was commanded following spacecraft separation to increase the distance between the Centaur stage and the spacecraft. The retrothrust was provided by opening the engine inlet valves and allowing the propellants in the tanks to discharge through the main engines. This operation was commanded at approximately T + 2333.7 seconds for a period of 250 seconds.

Fuel and oxidizer pump inlet pressure and temperature data taken during retrothrust are presented in figures V-16 and V-17. Both pressure "traces" responded as expected. At approximately 20 seconds prior to the end of retrothrust operation, hydrogen pump inlet temperature became erratic. This was evidence of depletion of the liquid-hydrogen supply. Two-phase or gaseous hydrogen was discharged for the remaining 20 seconds. The oxidizer pump inlet temperature data indicated liquid throughout the retrothrust operation.

TABLE V-5. - CENTAUR MAIN ENGINE SECOND FIRING OPERATING CONDITIONS,

AC-12

(a) U.S. Customary Units

Parameter	Expected value	Time from main engine start, sec			
		50		100	
		Engine			
		C-1	C-2	C-1	C-2
Liquid-hydrogen pump total inlet pressure (absolute), psi	17.7 to 39.3	35.6	37.3	32.8	33.4
Liquid-hydrogen pump inlet temperature, ^{O}R	37.6 to 43.4	38.9	38.8	39.2	39.3
Liquid-oxygen pump total inlet pressure (absolute), psi	51.4 to 78.2	61.1	62.8	58.1	59.4
Liquid-oxygen pump inlet temperature, ^{O}R	172.5 to 184.4	175.2	175.3	174.1	174.2
Hydrogen venturi upstream pressure (absolute), psi	[a]737±25	730.2	723.4	725.6	720.9
Hydrogen turbine inlet temperature, ^{O}R	[a]372±22	364.8	371.9	380.2	391.9
Oxygen pump speed, rpm	[a]12 163±347	12 330	12 065	12 250	12 100
Oxygen injector differential pressure, psi	[a]46±10	41.8	46.1	42.8	46.5
Engine chamber pressure (absolute), psi	[a]392.4±5.4	387.8	383.6	392.3	386.3

(b) SI Units

Parameter	Expected value	Time from main engine start, sec			
		50		100	
		Engine			
		C-1	C-2	C-1	C-2
Liquid-hydrogen pump total inlet pressure (absolute), N/cm^2	12.2 to 27.1	24.6	25.9	22.6	23.0
Liquid-hydrogen pump inlet temperature, K	20.9 to 24.1	21.6	21.6	21.8	21.8
Liquid-oxygen pump total inlet pressure (absolute), N/cm^2	35.4 to 53.9	42.2	43.3	40.1	41.0
Liquid-oxygen pump inlet temperature, K	95.8 to 102.4	97.4	97.5	96.8	96.9
Hydrogen venturi upstream pressure (absolute), N/cm^2	[a]518±17	504	498	500	497
Hydrogen turbine inlet temperature, K	256±15	203.0	206.5	211.5	217.8
Oxygen injector differential pressure, N/cm^2	32±7	28.8	31.8	29.5	32.1
Engine chamber pressure (absolute), N/cm^2	270.7±3.7	267.5	264.3	270.7	266.5

[a]Design inlet conditions and a propellant utilization valve angle of zero.

27

Centaur Boost Pumps

System description. - Boost pumps were used in the liquid-oxygen and liquid-hydrogen tanks on Centaur to supply propellants to the main engine turbopumps at the required inlet pressures. Both boost pumps were mixed-flow, centrifugal types, and were powered by hot-gas-driven turbines. The hot gas consisted of superheated steam and oxygen from catalytic decomposition of hydrogen peroxide. Constant turbine input power on each unit was maintained by metering hydrogen peroxide through fixed orifices upstream of a catalyst bed. A speed-limiting control system was provided on each unit to prevent pump overspeed under abnormal operating conditions. Illustrations of the complete boost pump and hydrogen peroxide supply systems are shown in figures V-18 to V-21.

Boost pump performance. - Performance of the boost pumps was satisfactory during the entire flight. Performance data at various times during boost pump operation are presented in tables V-6 and V-7 for the main engine first and second firings, respectively. The boost pumps were started 45.2 seconds prior to main engine first start, and continued to operate until main engine cutoff at T + 589.7 seconds. The boost pumps were restarted 28 seconds prior to main engine second ignition and continued to operate until main engine cutoff at T + 2028.6 seconds. First indications of turbine inlet pressures were evident less than 1 second after boost pump start command for both engine firings. Steady-state turbine-inlet pressures were within 3 psi (2.1 N/cm^2) of expected values for both engine firings. Expected absolute pressure values of 94 psi (64.8 N/cm^2) for the liquid-oxygen boost pump, and 100 psi (69.0 N/cm^2) for the liquid-hydrogen boost pump were established from prelaunch test data.

Steady-state turbine speed for the liquid-oxygen boost pump was 1000 rpm higher (during both engine firings) than was obtained during prelaunch tests. The steady-state turbine speed for the liquid-hydrogen boost pump was 1900 rpm higher than expected for the main engine first firing, and 1000 rpm higher than expected for the main engine second firing. Expected values of turbine speed established by prelaunch tests were 32 500 rpm for the liquid-oxygen boost pump and 40 200 rpm for the liquid-hydrogen boost pump. Differences between the ground-test data and flight values were within the accuracy tolerances of the instrumentation and telemetry systems.

A momentary decrease in liquid-oxygen boost pump turbine-inlet pressure occurred 7 seconds after main engine second ignition. Similarly, a momentary decrease in liquid-hydrogen boost pump turbine-inlet pressure occurred 11 seconds after main engine second ignition. In each case, the turbine-inlet pressure recovered to the normal level within 2.5 seconds. Minimum absolute pressure values recorded during the decrease were 58 psi (40.0 N/cm^2) and 34 psi (23.4 N/cm^2) for the liquid-oxygen and liquid-hydrogen boost pumps, respectively. The liquid-hydrogen boost pump turbine speed decreased approximately 1000 rpm during the 2.5-second time period of low turbine-inlet pressure.

TABLE V-6. - BOOST PUMP PERFORMANCE DATA, CENTAUR FIRST BURN, AC-12

(a) U.S. Customary Units

Parameter	Boost pump first start	Start engine chilldown	Main engine first start	Main engine start plus 10 sec	Main engine first cutoff
Oxidizer:					
Boost pump turbine speed, rpm	0	39 000	38 700	33 200	33 500
Boost pump turbine inlet absolute pressure, psi	0	93	93	93	95
Boost pump turbine bearing temperature, $^{\circ}$F	54	57	57	60	177
Boost pump inlet temperature, $^{\circ}$F	-282.6	-282.1	-282.1	-282.8	-285.0
Fuel:					
Boost pump turbine speed, rpm	0	54 000	44 800	40 800	42 100
Boost pump turbine inlet absolute pressure, psi	0	96	96	96	96
Boost pump turbine bearing temperature, $^{\circ}$F	69	84	86	90	231
Boost pump inlet temperature, $^{\circ}$F	-420.7	-420.7	-420.9	-421.0	-422.4

(b) SI Units

Parameter	Boost pump first start	Start engine chilldown	Main engine first start	Main engine start plus 10 sec	Main engine first cutoff
Oxidizer:					
Boost pump turbine inlet absolute pressure, N/cm^2	0	64.1	64.1	64.1	65.5
Boost pump turbine bearing temperature, K	286	287	287	289	354
Boost pump inlet temperature, K	98.5	98.7	98.7	98.3	97.1
Fuel:					
Boost pump turbine inlet absolute pressure, N/cm^2	0	66.1	66.1	66.1	68.2
Boost pump turbine bearing temperature, K	294	302	303	306	384
Boost pump inlet temperature, K	21.7	21.7	21.6	21.5	20.7

TABLE V-7. – BOOST PUMP PERFORMANCE DATA, CENTAUR SECOND BURN, AC-12

(a) U.S. Customary Units

Parameter	Boost pump second start	Start engine chilldown	Main engine second start	Main engine start plus 50 sec	Main engine second cutoff
Oxidizer:					
Boost pump turbine speed, rpm	0	35 600	40 200	33 500	33 500
Boost pump turbine inlet absolute pressure, psi	0	95	95	95	95
Boost pump turbine bearing temperature, $^{\circ}$F	261	261	261	267	275
Boost pump inlet temperature, $^{\circ}$F	-284.5	-284.4	-284.0	-285.0	-286.7
Fuel:					
Boost pump turbine speed, rpm	0	36 900	42 800	41 200	41 200
Boost pump turbine inlet absolute pressure, psi	0	97	97	97	97
Boost pump turbine bearing temperature, $^{\circ}$F	276	276	279	291	306
Boost pump inlet temperature, $^{\circ}$F	-420.9	-420.9	-420.9	-421.1	-420.7

(b) SI Units

Parameter	Boost pump second start	Start engine chilldown	Main engine second start	Main engine start plus 50 sec	Main engine second cutoff
Oxidizer:					
Boost pump turbine inlet absolute pressure, N/cm^2	0	65.5	65.5	65.5	65.5
Boost pump turbine bearing temperature, K	401	401	401	404	409
Boost pump inlet temperature, K	97.5	97.5	97.7	97.1	96.2
Fuel:					
Boost pump turbine inlet absolute pressure, N/cm^2	0	66.8	66.8	66.8	66.8
Boost pump turbine bearing temperature, K	409	409	410	417	426
Boost pump inlet temperature, K	21.6	21.6	21.6	21.5	21.7

However, there was no noticeable change in liquid-oxygen boost pump turbine speed.

The cause of the momentary decreases in boost pump turbine-inlet pressures was most likely a small amount of gas being entrained in the liquid flow from the hydrogen peroxide supply bottle. The configuration of the hydrogen peroxide bottle is such that a small quantity of gas can be trapped at the top of the bottle. It is believed that this small quantity of gas was dislodged by disturbances during the engine start transient and was subsequently entrained in the liquid flow to the boost pumps. The effect on overall system performance was negligible.

Hydrogen Peroxide Supply and Engine System

System description. - The hydrogen peroxide engines were used during the non-powered portion of the flight for attitude control, propellant settling and retention, and to provide the initial thrust for the retromaneuver. The attitude control system consisted of four 3.0-pound (13-N) thrust engines, four 50-pound (222-N) thrust engines, and two clusters each of which consisted of two 3.5-pound (16-N) thrust engines and one 6.0-pound (27-N) thrust engine. Propellant was supplied to the engines from a positive expulsion, bladder-type storage tank which was pressurized to an absolute pressure of about 300 psi (207 N/cm^2) by the pneumatic system. The hydrogen peroxide was decomposed in the engine catalyst beds, and the hot decomposition products were expanded through converging-diverging nozzles to provide thrust. Hydrogen peroxide was also provided to drive the boost pump turbines. The system is shown in figures V-19 and V-22.

System performance. - Engine chamber surface temperature data were recorded for two of the 50-pound (222-N) thrust engines (V2 and V4) and two of the 3-pound (13-N) thrust engines (S2 and S4). All temperature data indicated that the hydrogen peroxide engines performed satisfactorily on command.

A postmission experiment was performed on AC-12 to provide data for determining hydrogen peroxide consumption. The experiment consisted of firing the 50-pound (222-N) engines in the V half on mode (see table V-19 in GUIDANCE AND FLIGHT CONTROL SYSTEMS section) until the hydrogen peroxide supply was depleted. The firing time was 42.2 seconds, which, for estimated consumption rates, corresponded to 31.4 pounds (14.2 kg) of hydrogen peroxide.
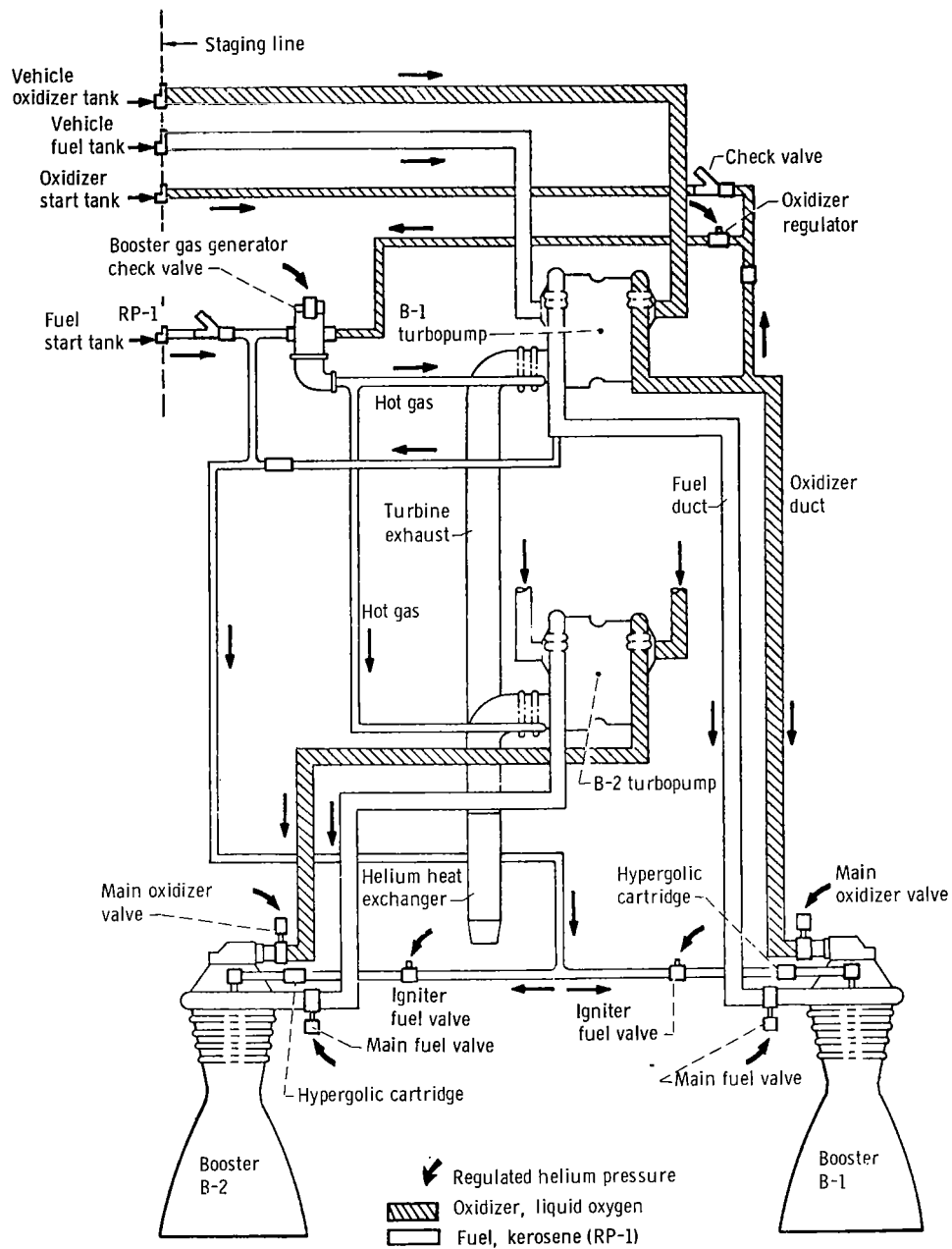
The hydrogen peroxide consumption was calculated for the various flight sequence times (see table V-8). This calculation was made by using the hydrogen peroxide experiment to determine the time of propellant depletion and the engine firing commands to establish the total engine firing times. Propellant flow rates for the individual engines were estimated. The small difference, as shown in table V-8, between total consumption and

total usable hydrogen peroxide is attributed to uncertainties in the actual tanking weight and estimated consumption rates.

TABLE V-8. - CALCULATED HYDROGEN PEROXIDE

CONSUMPTION, AC-12

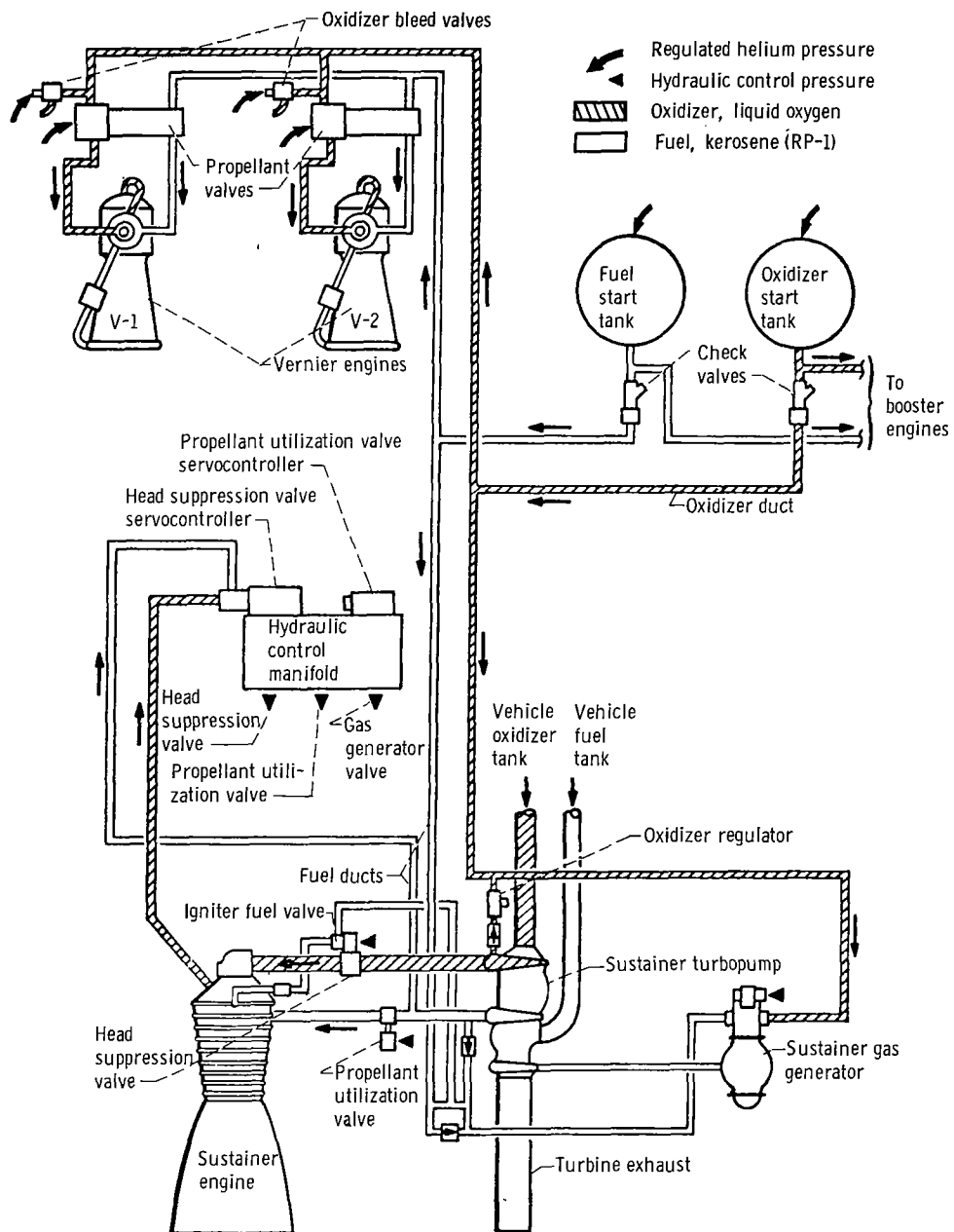| Sequence	Duration, sec	Mass	
		lb	kg
Boost pumps, first burn	385.8	31.6	14.3
First V half on mode[a]	75.1	54.3	24.6
S half on mode	1212.2	52.0	23.6
Second V half on mode	39.9	29.7	13.5
Boost pumps, second burn	139.7	11.5	5.2
Main engine second cutoff to retrothrust (excluding hydrogen peroxide use during lateral thrust time)	284.7	2.9	1.3
Lateral thrust (V half on mode)	20.0	14.9	6.8
Retrothrust	249.8	2.5	1.1
Postmission experiment (V half on mode)	42.2	31.4	14.2
Total consumption		230.8	104.6
Total tanked		236.9	107.4
Unusable residual		4.5	2.0
Total usable		232.4	105.4

[a]See table V-19 in GUIDANCE AND FLIGHT CONTROL SYSTEMS section for description of firing modes.

(a) Atlas vehicle booster engine.

Figure V-1. – Engine system schematic drawing, AC-12.

Regulated helium pressure
Hydraulic control pressure
Oxidizer, liquid oxygen
Fuel, kerosene (RP-1)

(b) Atlas vehicle sustainer and vernier engines.

Figure V-1. - Concluded.
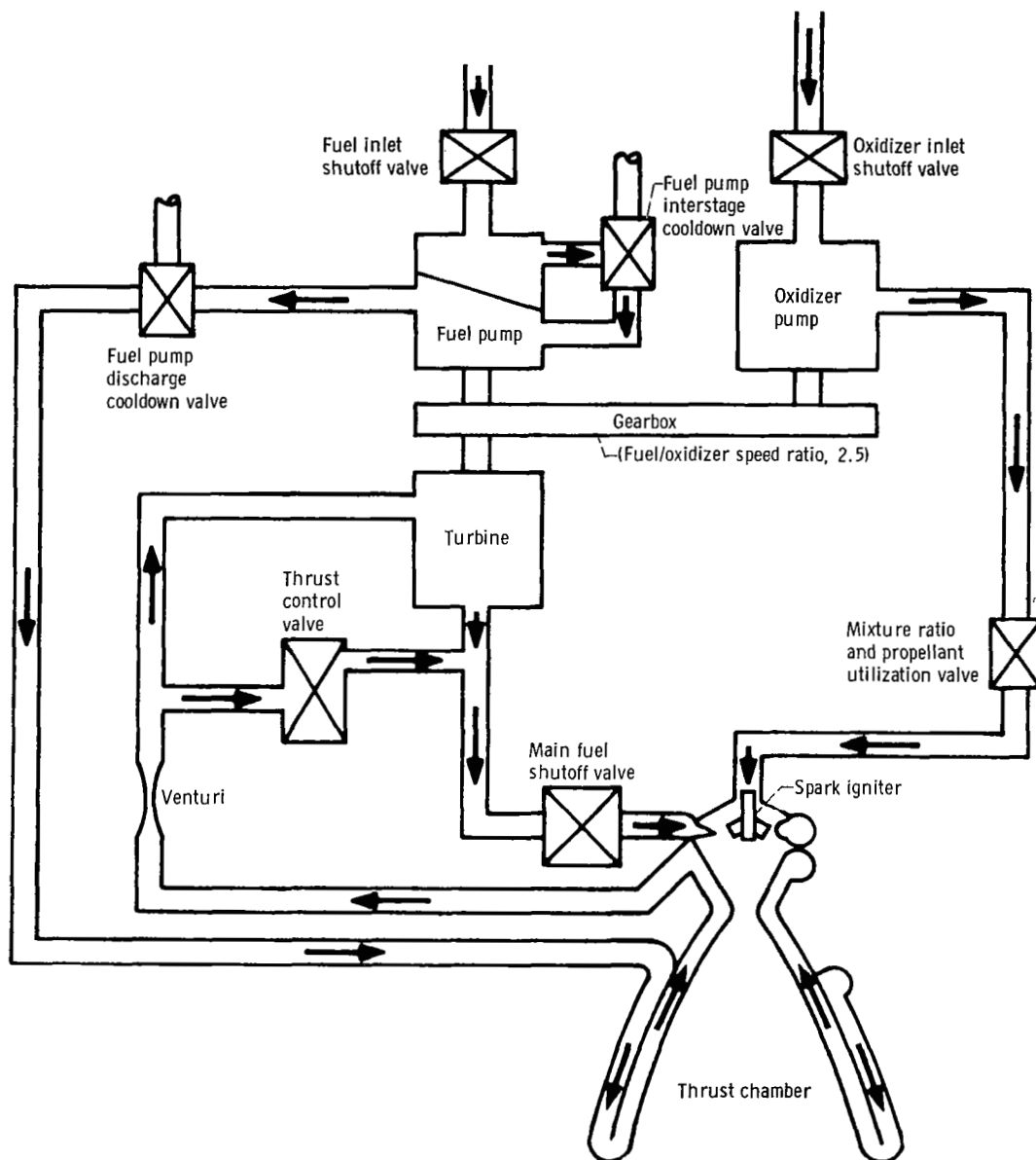
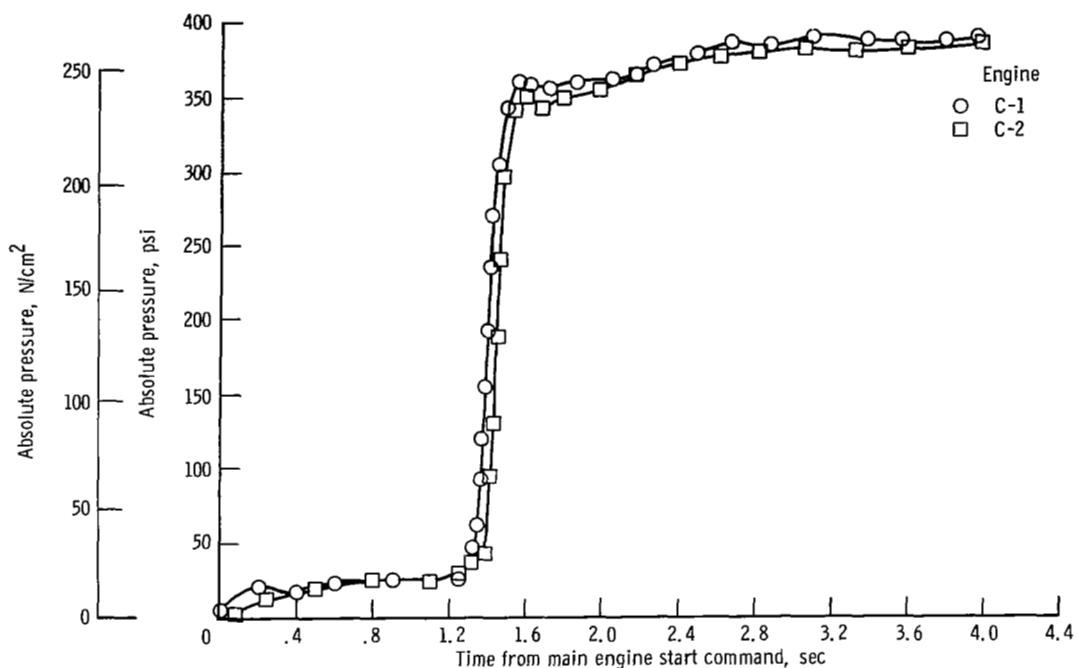Figure V-2. - Centaur main engine schematic drawing, AC-12.

Fuel inlet shutoff valve

Fuel pump interstage cooldown valve

Oxidizer inlet shutoff valve

Fuel pump discharge cooldown valve

Fuel pump

Oxidizer pump

Gearbox

(Fuel/oxidizer speed ratio, 2.5)

Turbine

Thrust control valve

Mixture ratio and propellant utilization valve

Venturi

Main fuel shutoff valve

Spark igniter

Thrust chamber

Figure V-3. - Centaur engine chamber pressure during first start transient, AC-12.
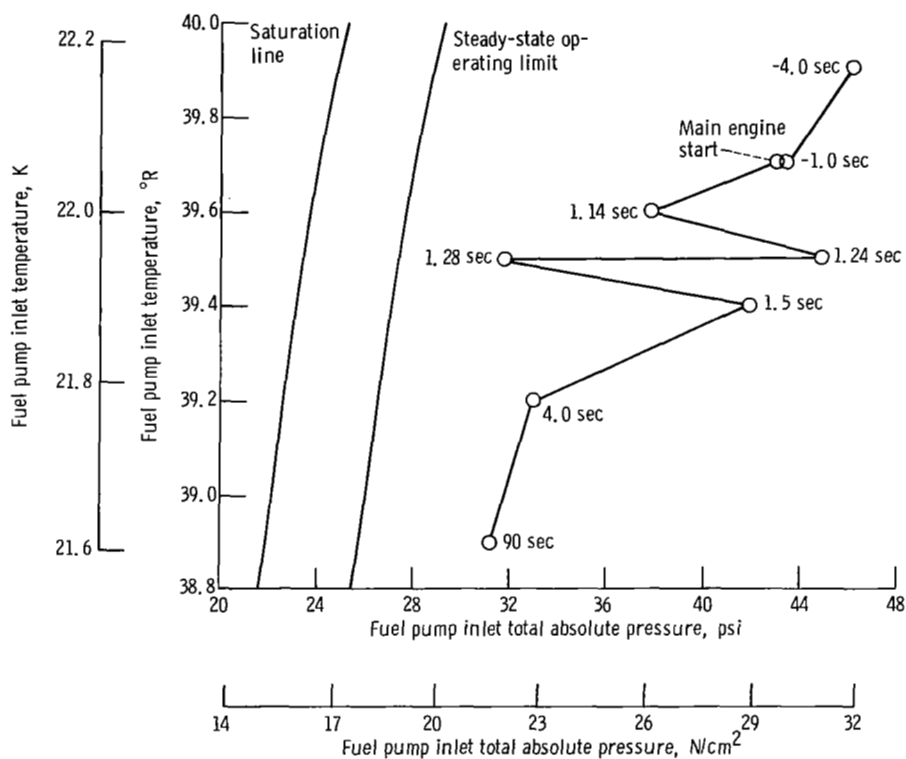
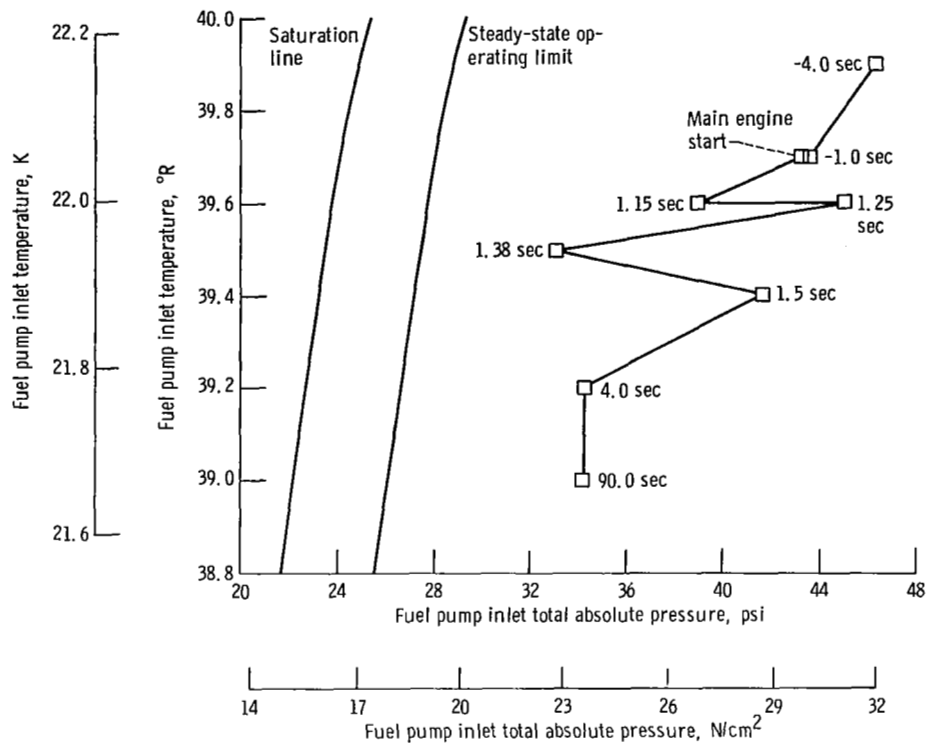Figure V-4. - Centaur C-1 engine fuel pump inlet conditions near engine first start, AC-12.

Figure V-5. - Centaur C-2 engine fuel pump inlet conditions near engine first start, AC-12.
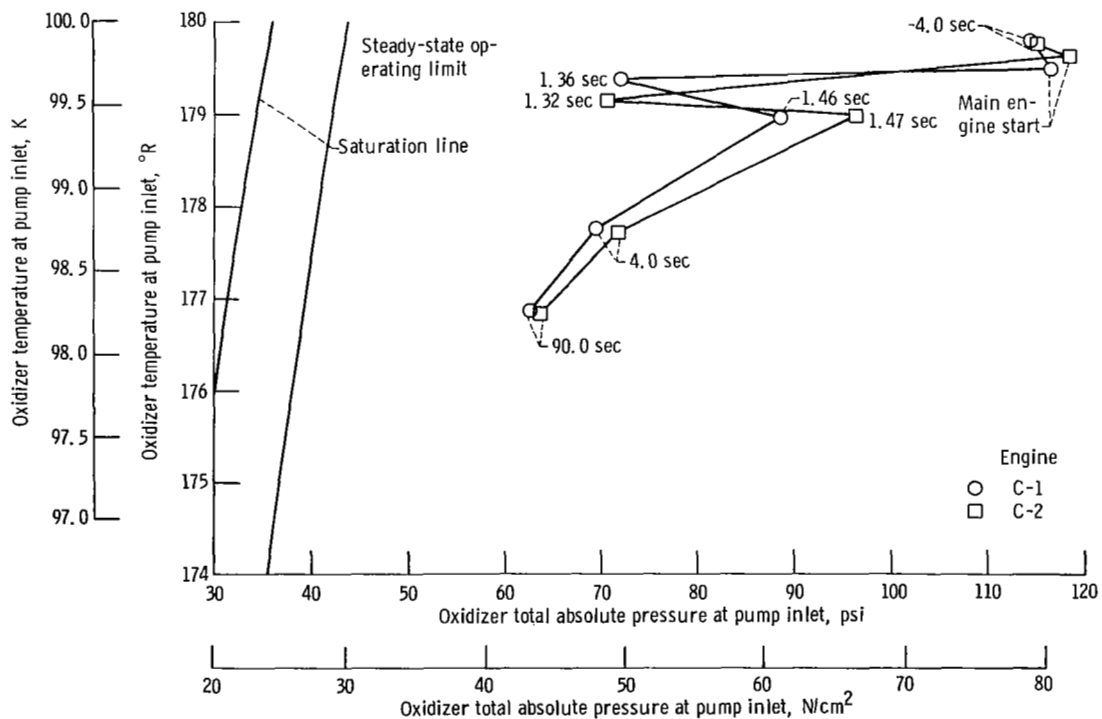

Figure V-6. - Oxidizer pump inlet conditions near main engine first start, AC-12.
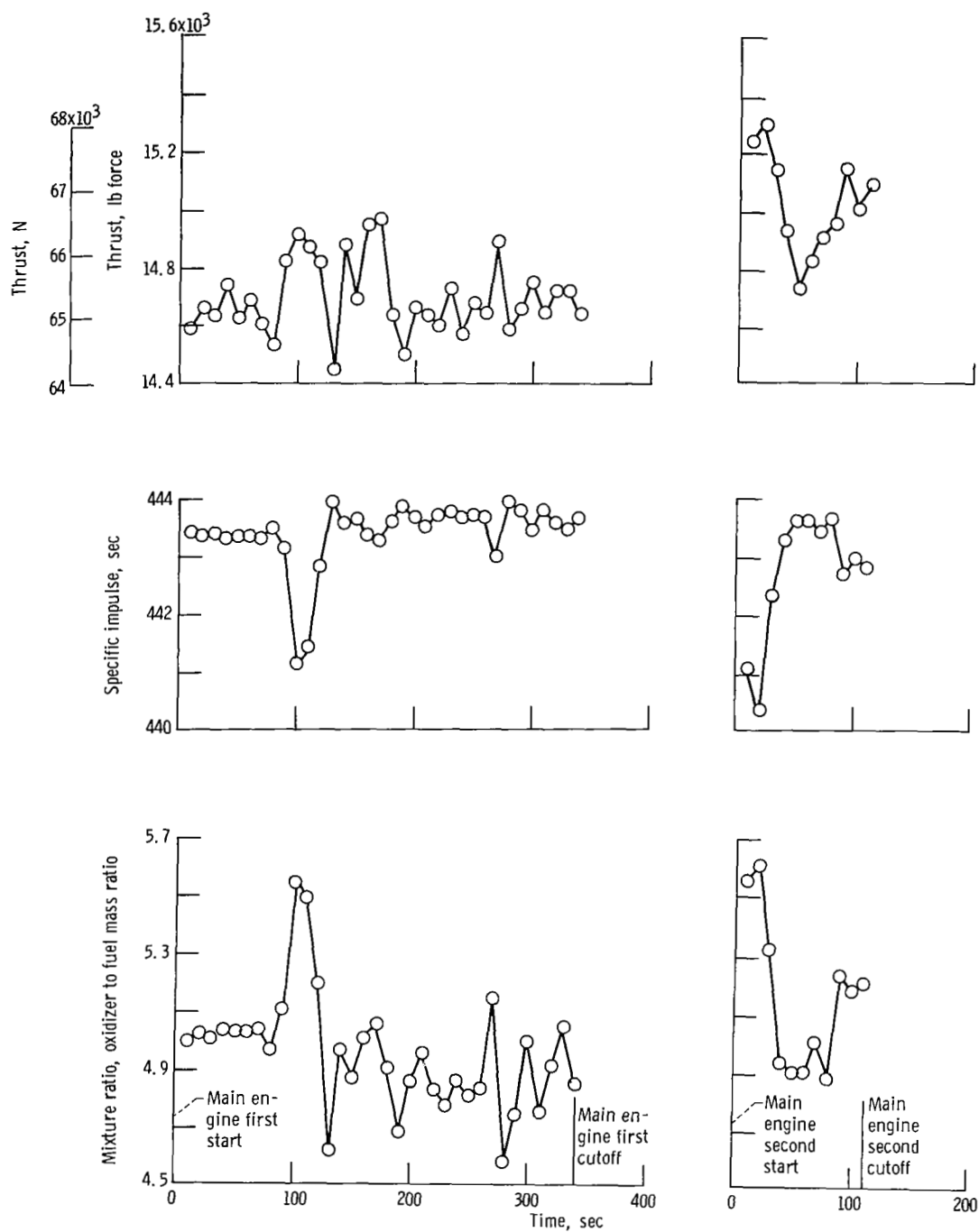
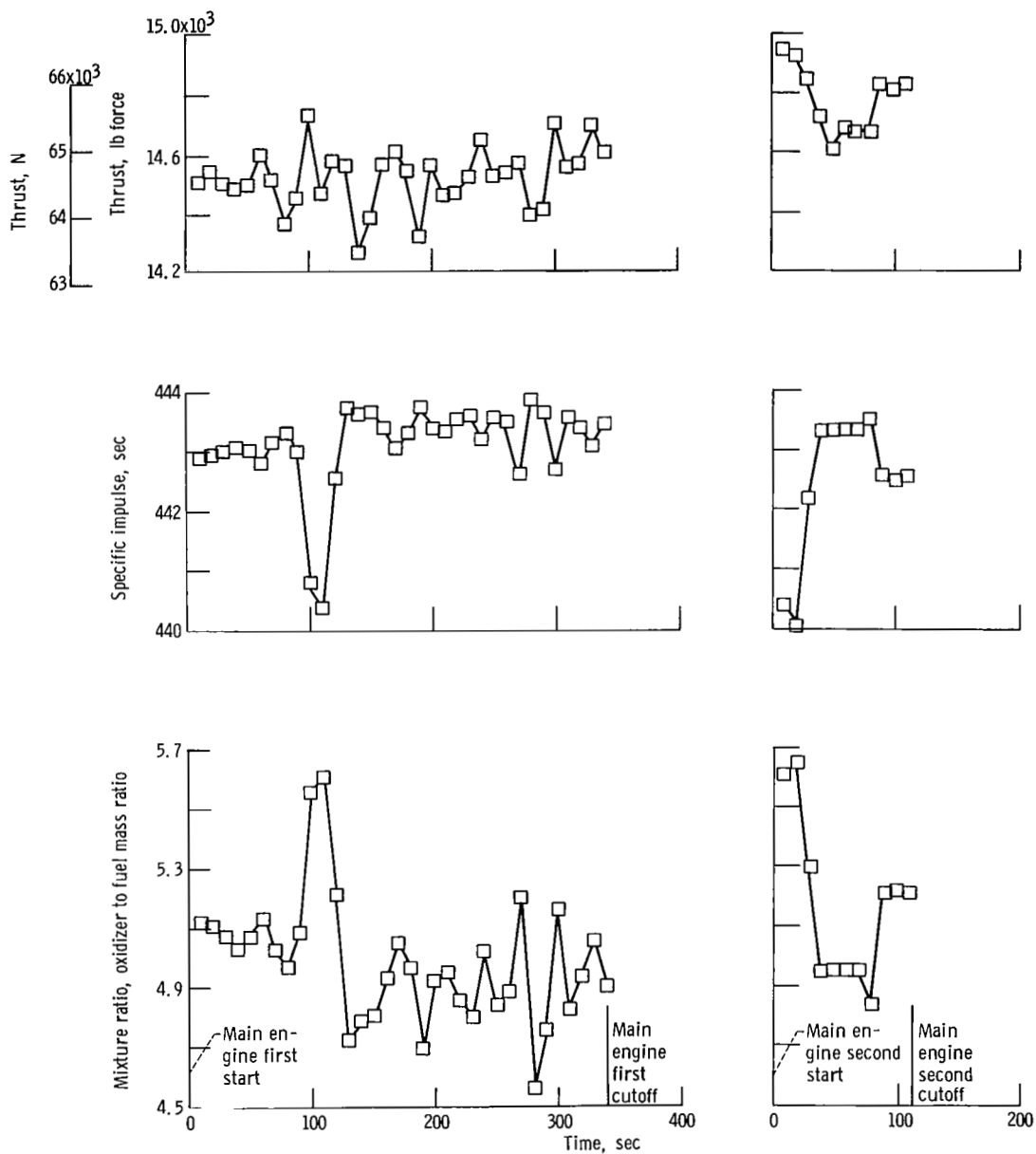Figure V-7. - Centaur C-1 main engine performance by C* method, AC-12.

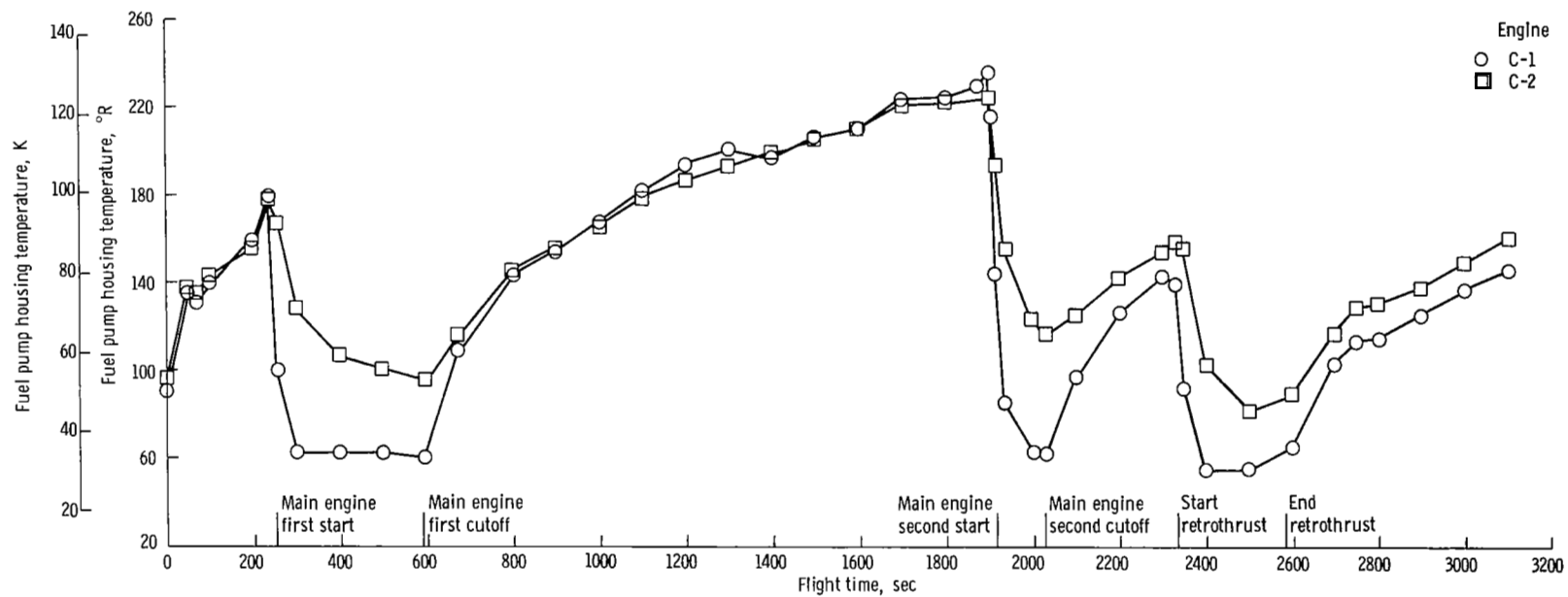Figure V-8. – Centaur C-2 main engine performance by C* method, AC-12.

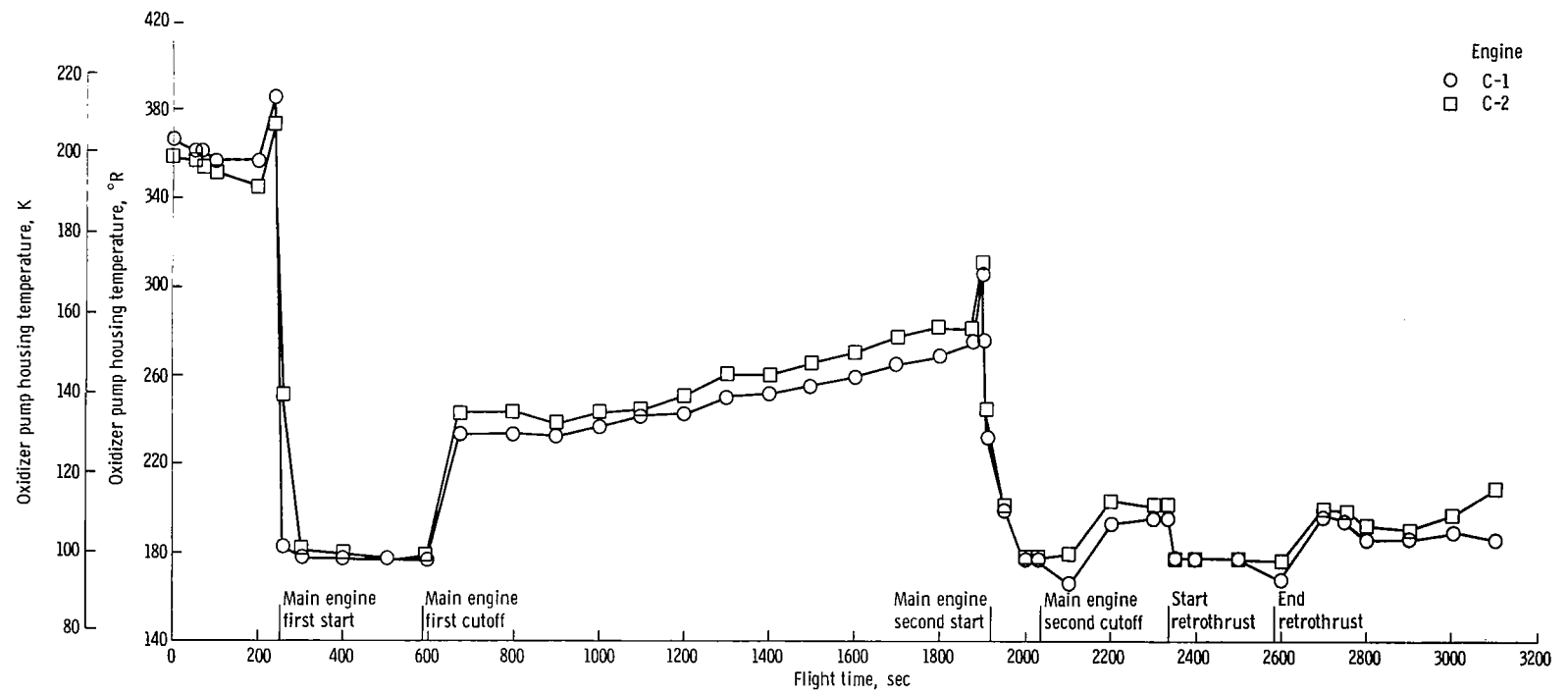Figure V-9. – Centaur fuel pump housing temperatures, AC-12.

Figure V-10. – Centaur oxidizer pump housing temperatures, AC-12.
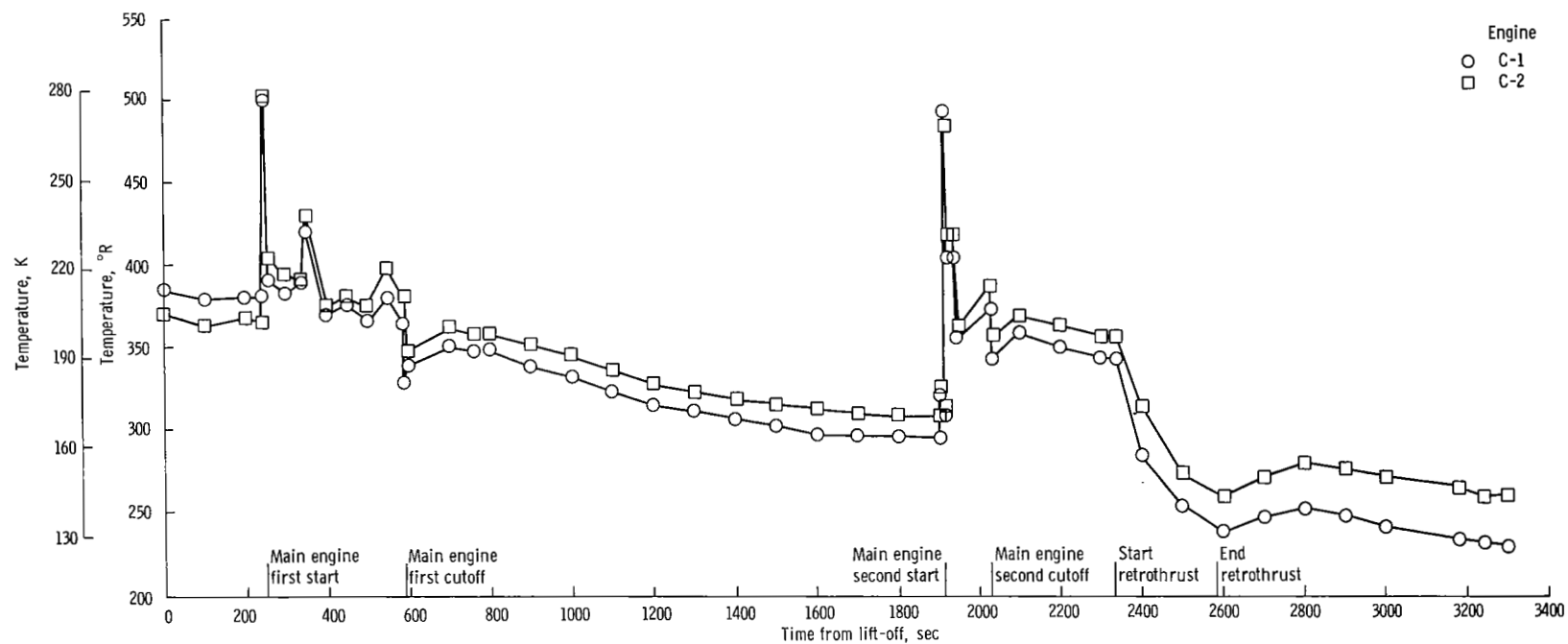
Figure V-11. - Centaur hydrogen turbine inlet temperature, AC-12.
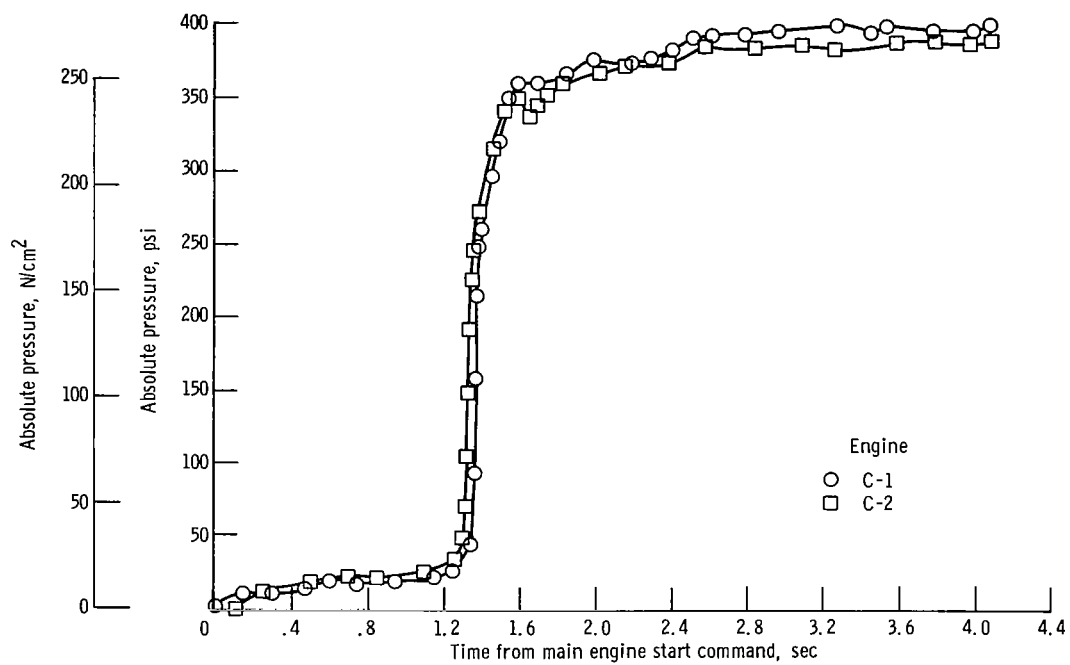
Figure V-12. - Centaur engine chamber absolute pressure during second start transient, AC-12.
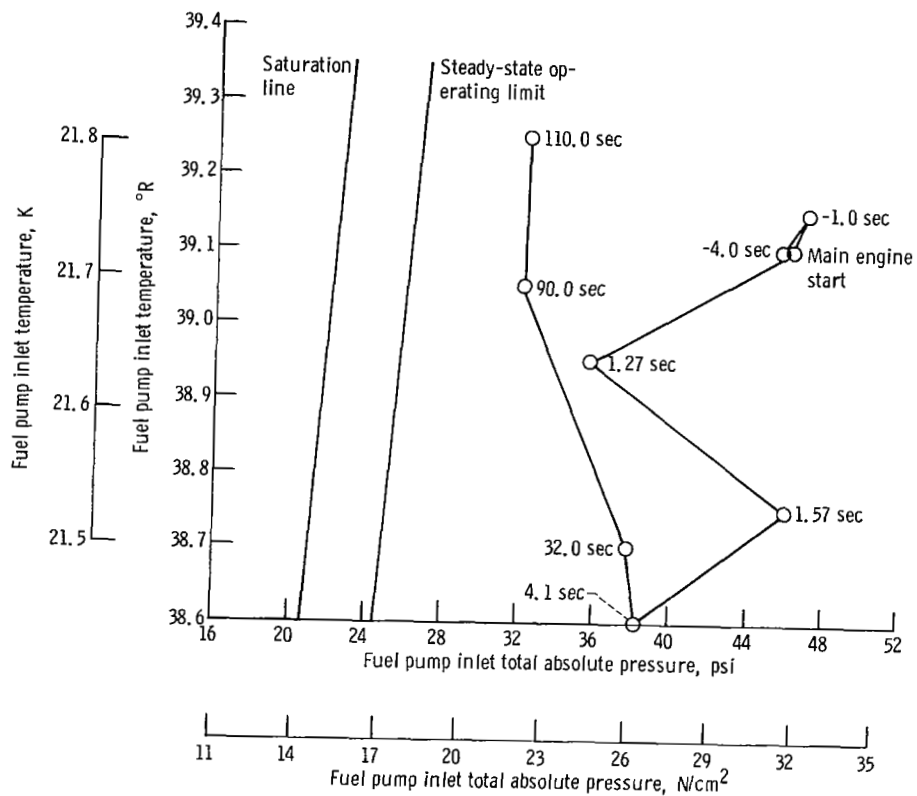
Figure V-13. - Centaur C-1 engine fuel pump inlet conditions near engine second start, AC-12.
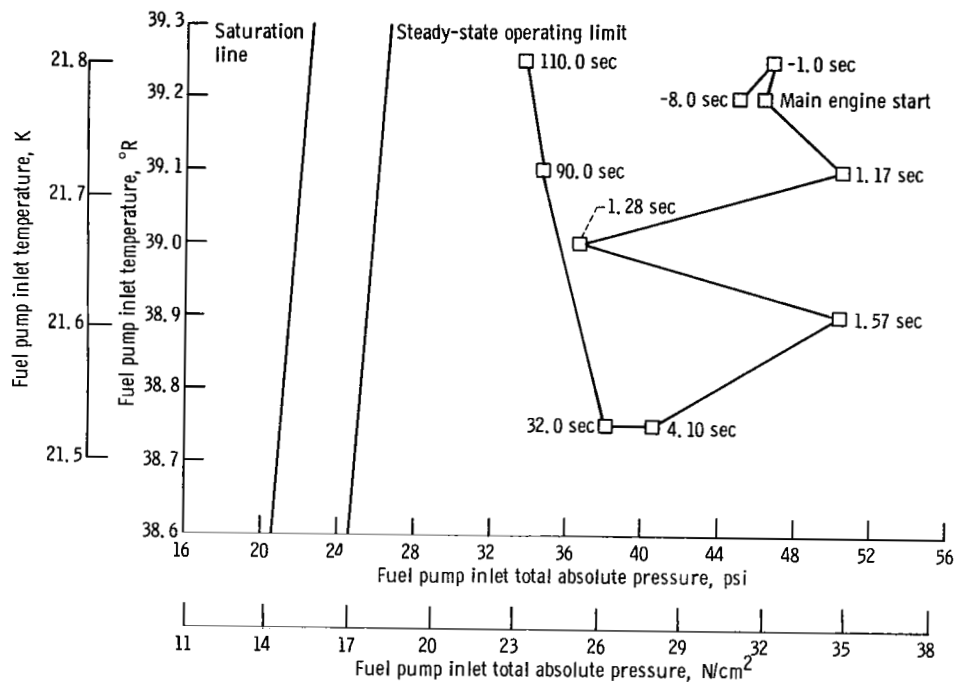
Figure V-14. - Centaur C-2 engine fuel pump inlet conditions near main engine second start, AC-12.
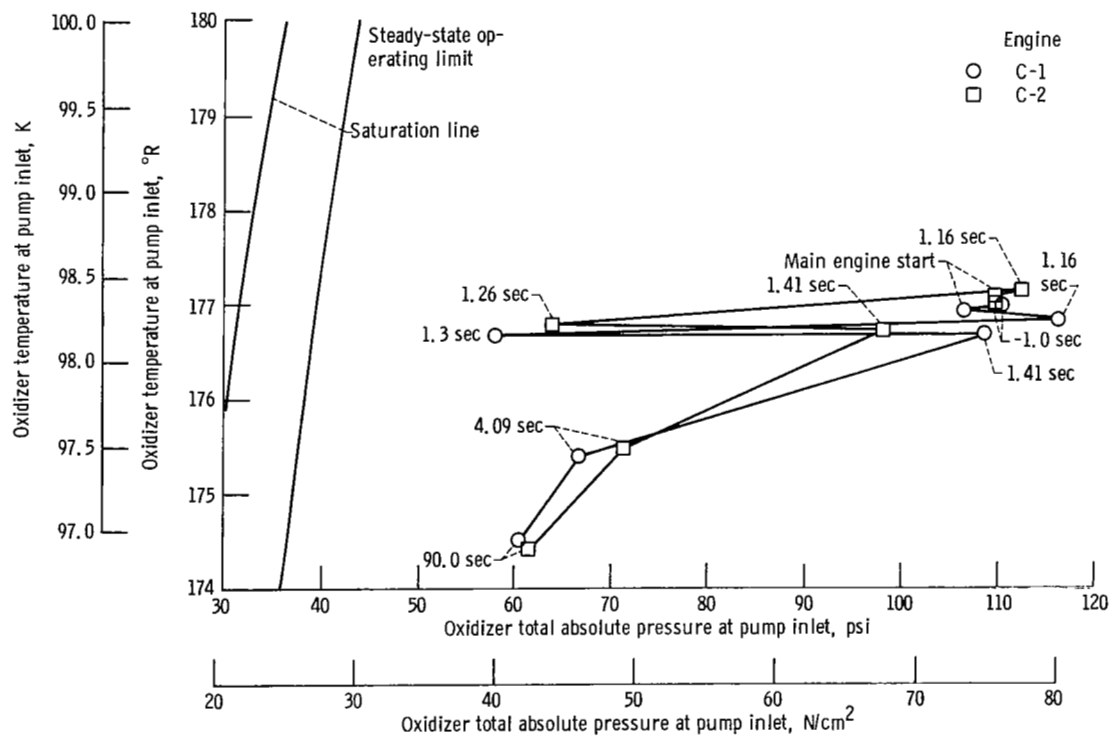
Figure V-15. - Oxidizer pump inlet conditions near main engine second start, AC-12.
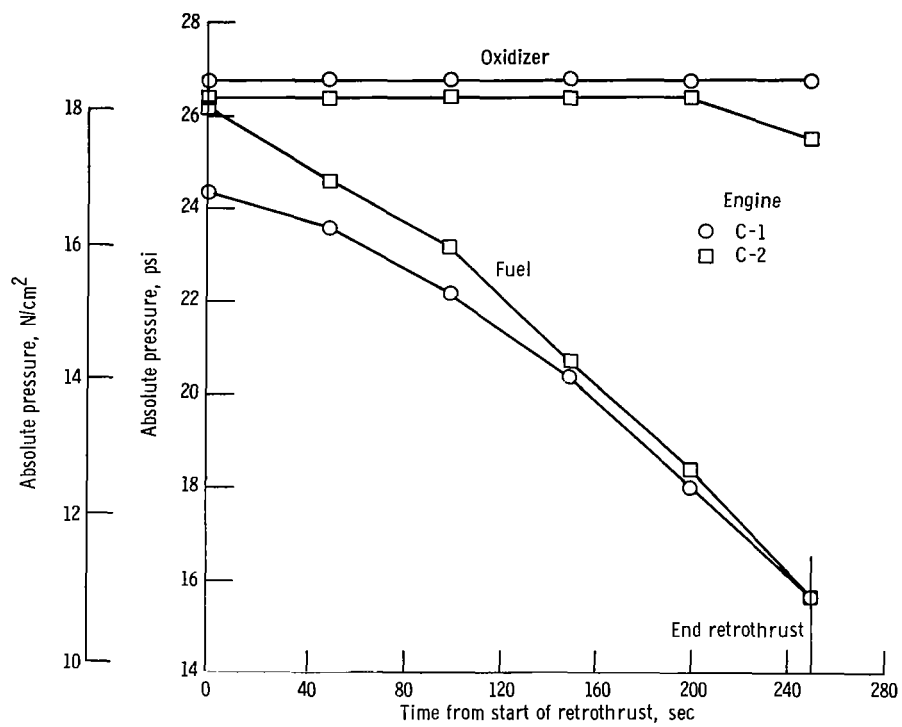
Figure V-16. – Centaur fuel and oxidizer pump inlet absolute pressures during retrothrust, AC-12.
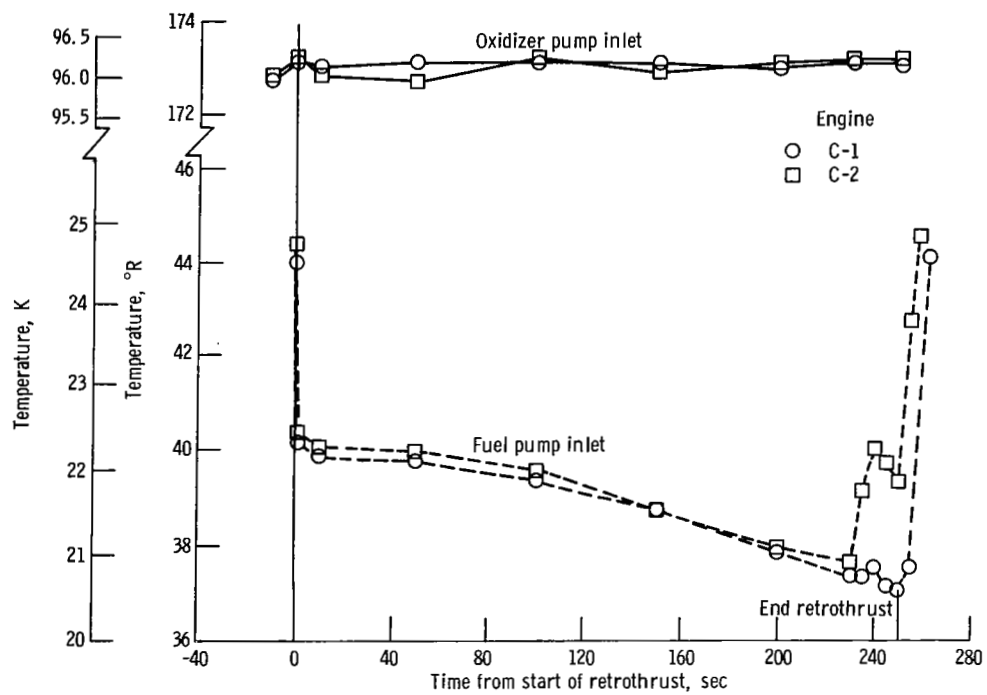
Figure V-17. - Centaur fuel and oxidizer pump temperatures during retrothrust, AC-12.
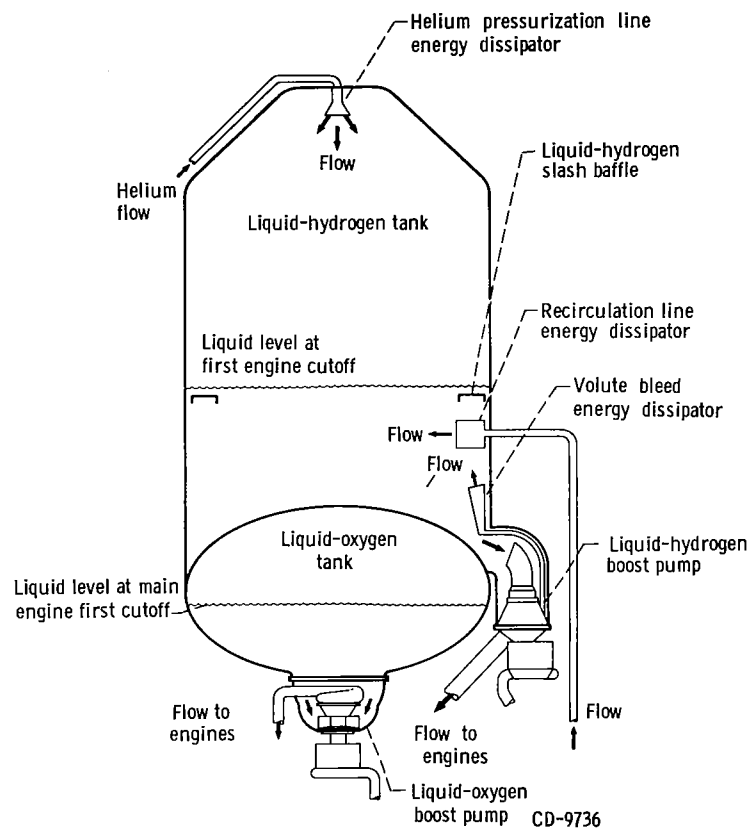
Figure V-18. - Location of Centaur liquid-hydrogen
and liquid-oxygen boost pumps, AC-12.
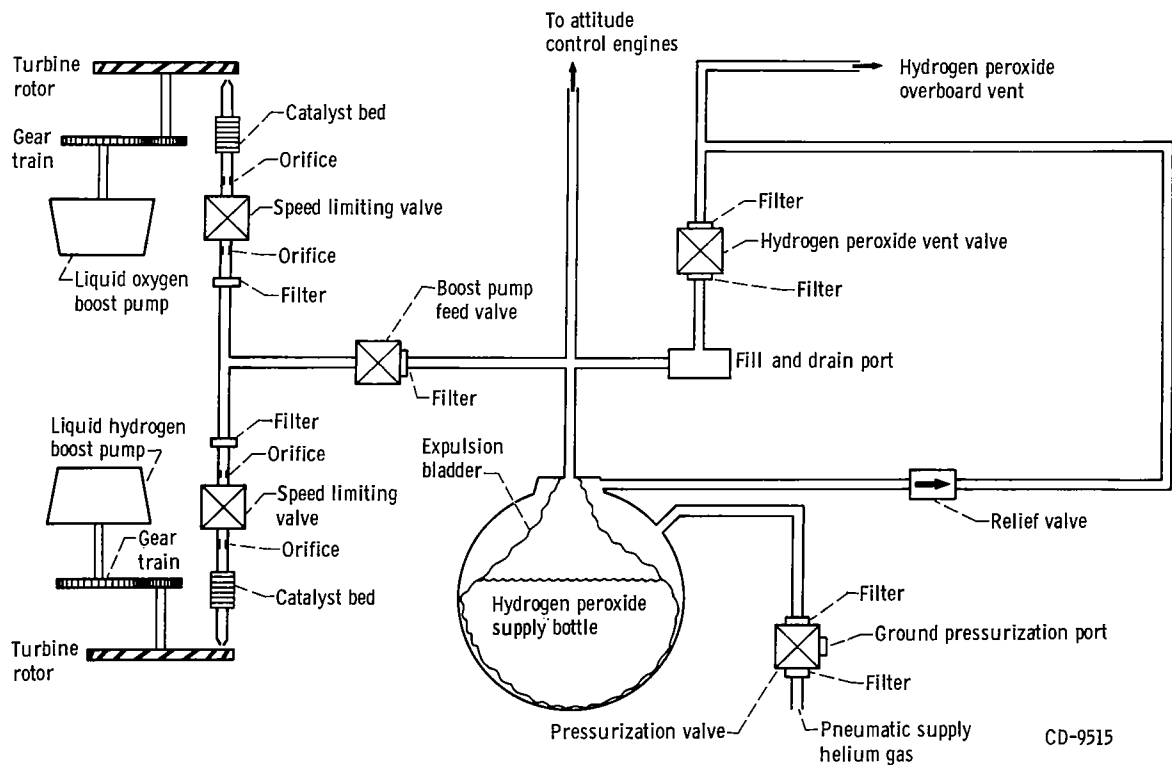
Figure V-19. - Schematic drawing of Centaur boost pump hydrogen peroxide supply, AC-12.

Liquid-oxygen
flow to engines

Volute bleed flow

Pump

Sump

Turbine drive

Turbine exhaust

CD-9513
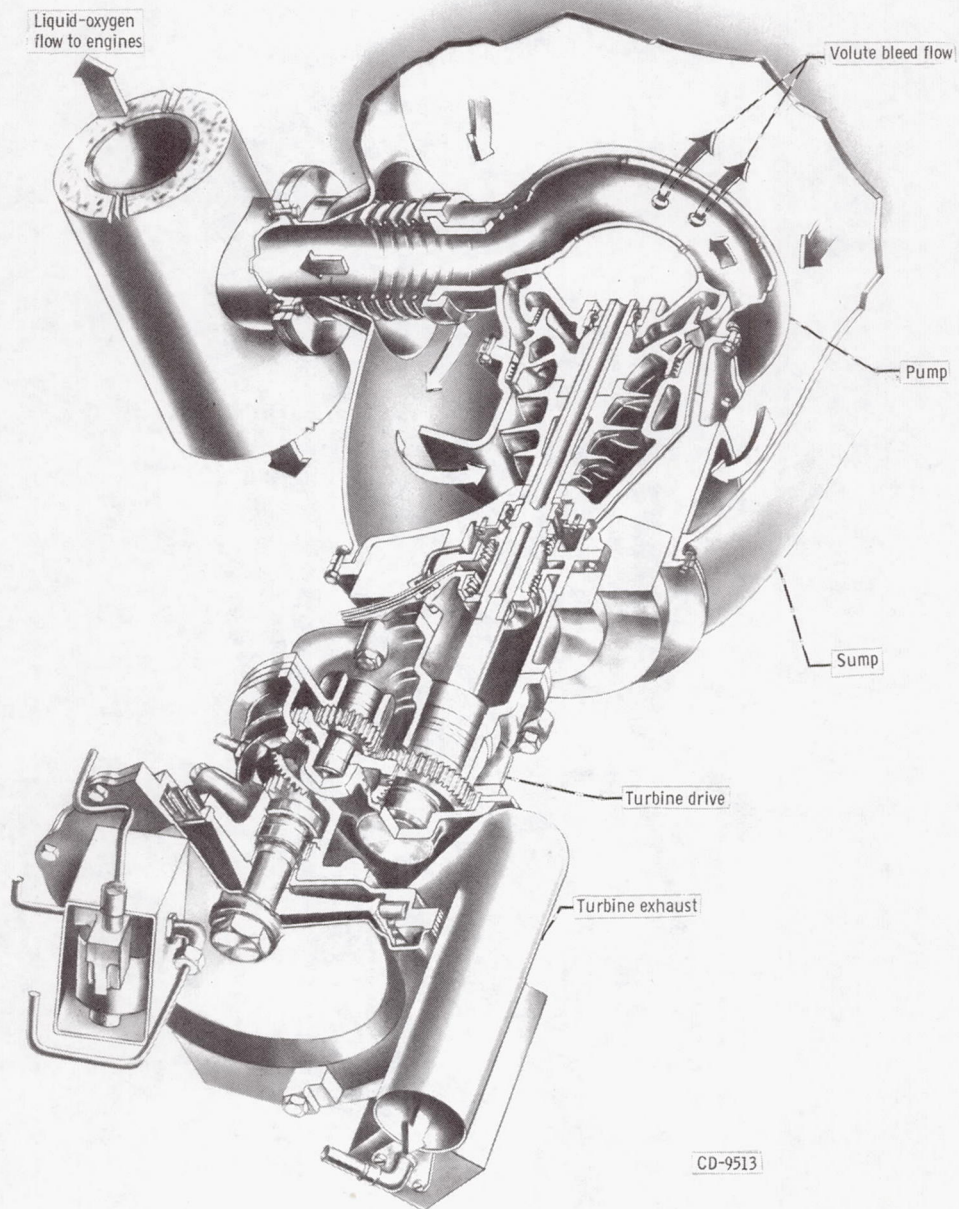
Figure V-20. - Centaur liquid-oxygen boost pump and turbine cutaway, AC-12.

Liquid-hydrogen sump

Volute bleed line

Sump

Pump

Liquid-hydrogen flow to engines

Turbine drive

Turbine exhaust

CD-9512
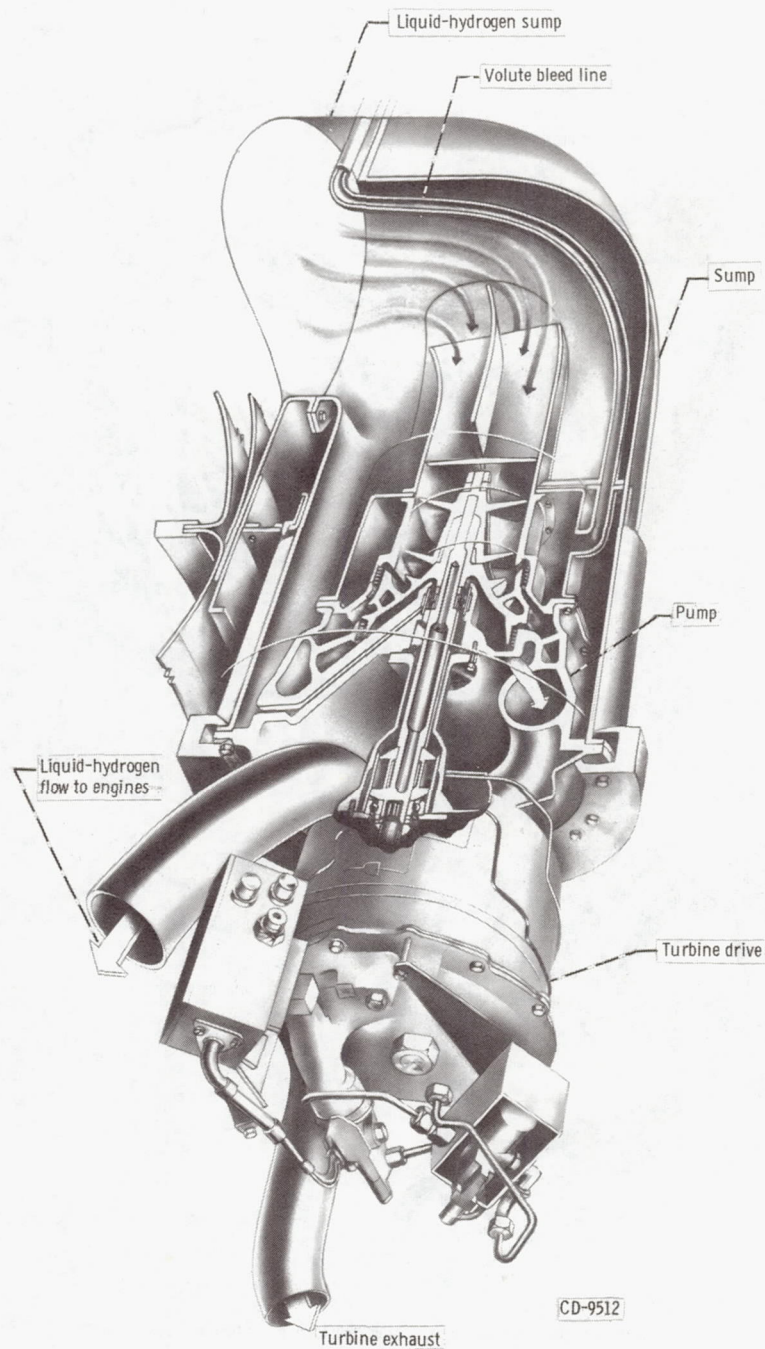
Figure 21. – Centaur liquid-hydrogen boost pump and turbine cutaway, AC-12.

Nozzle

Welded joint

Heat barrier

Catalyst bed

Solenoid control valve

Inlet

Typical A, P, and S engine, except S engine has straight nozzle

A1

A4 ⌐ ⌐P1

V4

S4

V1

S1

Oxidizer boost pump hydrogen peroxide inlet

Fuel boost pump hydrogen peroxide inlet

Hydrogen peroxide tank

Boost pump feed valve

Fill port

Vent valve

Pressur-izing valve

S3

V3

Overboard vent

A3

P2 A2

Pneumatics panel

Relief valve

S2

V2

Helium bottle (reference)

y

IV   I   x

¢ Vehicle

II

III

-x

-y

Hydrogen peroxide control system

Pressure port (helium)

Bladder

Helium

Hydrogen peroxide

Hydrogen peroxide tank

Engine designation	Thrust	
	lb	N
V1, V2, V3, V4	50	222
S1, S2, S3, S4	3	13
A1, A2, A3, A4	3.5	16
P1, P2	6	27

Nozzle

Inlet

Catalyst bed

Solenoid valve

V engine
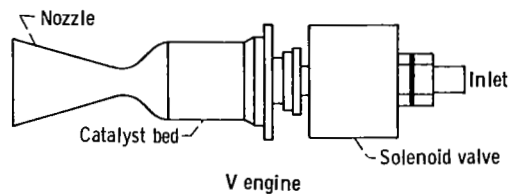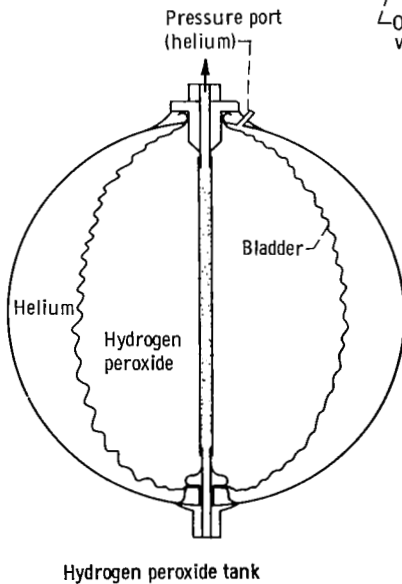
Figure V-22. - Hydrogen peroxide system isometric, AC-12.

53

PROPELLANT LOADING AND PROPELLANT UTILIZATION

by Steven V. Szabo, Jr.

Propellant Level Indicating System for Propellant Loading

System description. - Atlas propellant levels for flight were determined from liquid level sensors located at discrete points in the fuel (RP-1) and liquid-oxygen tanks, as shown in figure V-23. The sensors in the fuel tank were the vibrating piezoelectric crystal type. The sensors in the liquid-oxygen tank were the platinum hot-wire type.

The control circuitry for the fuel level sensors was a piezoelectric oscillator. When in gas, the crystal oscillated. When the sensor was immersed in liquid, the crystal was damped, causing the oscillations to stop. This cessation of oscillations operated a relay and provided a signal for the propellant loading operator.

The control unit for the platinum hot-wire liquid-oxygen sensors was an amplifier that detected a change in voltage level. The amplified signal was applied to an electronic trigger circuit. The liquid-oxygen sensors were supplied with a near-constant current of approximately 200 milliamperes. The voltage drop across a sensor reflected the resistance value of the sensor. The sensing element was a 1-mil (2.54-mm) platinum wire which had a linear resistance temperature coefficient. When dry, the wire has a high resistance and therefore a high voltage drop. When immersed in a cryogenic fluid, it has a low resistance and voltage drop. When the sensor was wetted, a control relay was deenergized, and a signal was sent for the propellant loading operator. The Centaur propellant level indicating system is shown in figure V-24. It utilized hot-wire level sensors in both the liquid-oxygen and liquid-hydrogen tanks. These sensors were similar in operation to the ones used in the Atlas liquid-oxygen tank.

Propellant weights. - Atlas fuel (RP-1) weight at lift-off was calculated to be 77 062 pounds (34 955 kg) based on a density of 49.8 pounds per cubic foot (797 kg/cu m). Atlas liquid oxygen tanked was calculated to be 175 341 pounds (79 535 kg) based on a density of 69.2 pounds per cubic foot (1087 kg/cu m).

Centaur propellant loading was satisfactorily accomplished. Calculated propellant weights at lift-off were 5271 pounds ±3.2 percent (2391 kg ±3.2 percent) of liquid hydrogen and 25 479 pounds ±1.5 percent (11 557 kg ±1.5 percent) of liquid oxygen. Data used to calculate these propellant weights are given in table V-9.

TABLE V-9. – CENTAUR PROPELLANT LOADING DATA, AC-12

(a) U.S. Customary Units

Quantity or event	Propellant tank	
	Hydrogen	Oxygen
Sensor required to be wet at T - 90 sec, percent	99.8	----
Sensor required to be wet at T - 75 sec, percent	----	100.2
Sensor location (vehicle station number)	175	373
Tank volume[a] at sensor, ft^3	1257	371
Ullage volume at sensor, ft^3	11.2	6.6
Liquid hydrogen 99.8 percent sensor dry at -, sec	T - 33	----
Liquid oxygen 100.2 percent sensor dry at -, sec	----	T - 15
Ullage pressure (absolute) at time sensor goes dry, psi	21.4	29.6
Density[b] at time sensor goes dry, lb mass/ft^3	4.2	68.7
Weight in tank at sensor dry, lb mass	5278.0	25 484
Liquid-hydrogen boiloff[c] to vent valve close, lb mass	7.2	---
Liquid-oxygen boiloff[c] to lift-off, lb mass	---	4.5
Ullage volume at lift-off, ft^3	14	6.6
Weight[d] at lift-off, lb mass	5271±3.2%	25 479±1.5%

(b) SI Units

Quantity or event	Propellant tank	
	Hydrogen	Oxygen
Sensor required to be wet at T - 90 sec, percent	99.8	----
Sensor required to be wet at T - 75 sec, percent	----	100.2
Sensor location (vehicle station number)	175	373
Tank volume[a] at sensor, m^3	35.6	10.5
Ullage volume at sensor, m^3	0.32	0.19
Liquid hydrogen 99.8 percent sensor dry at -, sec	T - 33	----
Liquid oxygen 100.2 percent sensor dry at -, sec	----	T - 15
Ullage pressure (absolute) at time sensor goes dry, N/cm^2	14.8	20.4
Density[b] at time sensor goes dry, kg/m^3	67.2	1099
Weight in tank at sensor dry, kg	2394	11 559
Liquid-hydrogen boiloff[c] to vent valve close, kg	3.3	---
Liquid-oxygen boiloff[c] to lift-off, kg	---	2.0
Ullage volume at lift-off, m^3	0.4	0.2
Weight[d] at lift-off, kg	2391±3.2%	11 557±1.5%

[a]Volumes include 1.85 ft^3 (0.05 m^3) liquid oxygen and 2.53 ft^3 (0.72 m^3) liquid hydrogen for lines from boost pumps to engine turbopump inlet valves.

[b]Liquid-hydrogen density taken from ref. 2; liquid-oxygen density taken from ref. 3.

[c]Boiloff rates determined from tanking test to be 0.29 lb mass/sec (0.14 kg/sec) liquid hydrogen and 0.29 lb mass/sec (0.14 kg/sec) liquid oxygen.

[d]Preflight estimates were 5301 lb (2404 kg) of liquid hydrogen and 25 447 lb (11 543 kg) liquid oxygen.

TABLE V-10. – ATLAS PROPELLANT RESIDUAL DATA, AC-12

(a) U.S. Customary Units

Quantity	Propellant	
	Fuel	Oxygen
Density used, lb mass/ft^3	49.83	68.76
Volume[a] below sensing port, ft^3	17.52	27.10
Weight below ports, lb mass	873.0	1863
Gimbal angle correction, lb mass	4	12
Total below ports at port uncovery, lb mass	877	1875
Time from port uncovery to sustainer engine cutoff, sec	6	7
Flow rate[b] used, lb mass/sec	74.6	182.8
Total propellant used from port uncovery to engine cutoff, lb mass	447	1279
Propellant above pump inlet at engine cutoff, lb mass	430	596

(b) SI Units

Quantity	Propellant	
	Fuel	Oxygen
Density used, kg/m^3	797.3	1100
Volume[a] below sensing port, m^3	0.496	0.767
Weight below ports, kg	396	845
Gimbal angle correction, kg	1.8	5.4
Total below ports at port uncovery, kg	397.8	850.4
Time from port uncovery to sustainer engine cutoff, sec	6	7
Flow rate[b] used, kg/sec	33.8	82.9
Total propellant used from port uncovery to engine cutoff, kg	202.8	580.1
Propellant above pump inlet at engine cutoff, kg	195	270.3

[a]Volume includes lines from tank to pump inlet.

[b]Average flow rates between port uncovery and sustainer engine cutoff. Corrected for altitude conditions and flow-rate decay.

Atlas Propellant Utilization System

System description. - The Atlas propellant utilization system (fig. V-25) was used to ensure almost simultaneous depletion of the propellants and minimum propellant residuals at sustainer engine cutoff. This was accomplished by controlling the propellant mixture ratio (ratio of oxidizer flow rate to fuel flow rate) to the sustainer engine. The system consisted of two mercury manometer assemblies, a computer-comparator, a hydraulically actuated propellant utilization (fuel) valve, pressure sensing lines, and associated electrical harnessing. During flight, the manometers sensed propellant head pressures which were indicative of propellant mass. The mass ratio was then compared with a reference ratio in the computer-comparator, and, if needed, a correction signal was sent to the valve controlling the main fuel flow to the sustainer engine (the propellant utilization valve). The oxidizer flow was regulated by the head suppression valve. This valve sensed propellant utilization valve movement and moved in a direction opposite to that of the propellant utilization valve. The opposite movement thus altered propellant mixture ratio but maintained a constant total propellant mass flow to the engine.

System performance. - The Atlas propellant utilization system operation was satisfactory. The propellant utilization system valve angle during flight is shown in figure V-26. The valve was positioned at the liquid-oxygen rich stop until 4.7 seconds after lift-off. The system compensated for an oxygen-rich condition until T + 138 seconds. At T + 138 seconds, the valve was again positioned at the oxygen-rich stop for 30 seconds. After T + 158 seconds, the system compensated for a fuel-rich condition until the fuel head sensing port uncovered at approximately T + 220 seconds. The valve then remained at the oxygen-rich stop until sustainer engine cutoff.

Atlas propellant residuals. - The residuals above the sustainer pump inlets at sustainer engine cutoff were calculated to be 596 pounds (270 kg) of liquid oxygen and 430 pounds (195 kg) of fuel. These residuals were calculated by using the head sensing port uncovery times as reference points. Propellants consumed from port uncovery to sustainer cutoff include the effect of flow-rate decay for a liquid-oxygen depletion. Data used to calculate Atlas residuals is given in table V-10.

Centaur Propellant Utilization System

System description. - The Centaur propellant utilization system was used during flight to control propellant consumption by the main engines and to provide minimum propellant residuals. The system is shown schematically in figure V-27. It was also used during tanking to indicate propellant levels. In flight, the mass of propellant remaining in each tank was sensed by a capacitance probe and compared in a bridge circuit. If the

mass ratio of propellants remaining varied from a predetermined value (5 to 1, oxidizer to fuel), an error signal was sent to the proportional servopositioner which controlled the liquid-oxygen flow-control valve. If the mass ratio was greater than 5 to 1, the liquid-oxygen flow was increased to return the ratio to 5 to 1. If the ratio was less than 5 to 1, the liquid-oxygen flow was decreased. Since the sensing probes do not extend to the top of the tanks, system control was not commanded on until approximately 90 seconds after main engine first start. For this 90 seconds of engine firing, the bridge was nulled, locking the liquid-oxygen flow-control valves at a 5 to 1 propellant mixture ratio.

System performance. - All prelaunch checks and calibrations of the system were within specification.

The in-flight operation of the system was satisfactory during main engine first and second burns. The system liquid-oxygen flow-control valve positions during the engine firings are shown in figure V-28. The system was commanded on by the vehicle programmer at main engine first start plus 88.9 seconds. The valves then moved to the oxygen-rich stop and remained there for approximately 18 seconds. During this time, the system compensated for an excess of 161 pounds (73 kg) of oxygen. This correction resulted from

(1) Engine consumption error during the first 90 seconds of engine firing
(2) Tanking errors
(3) System bias to ensure that liquid oxygen depleted first
(4) System bias to compensate for liquid-hydrogen boiloff during coast. The liquid-oxygen boiloff is zero, and, if this compensation were not made, the mass ratio in the tanks at main engine second start would not be 5 to 1.

The system commanded the valve to control mainly in a hydrogen-rich position during the remainder of the engine first firing period. The maximum valve angle during this time was approximately 35°. At main engine first cutoff, the valves moved to the oxygen-rich stop. Approximately 10 seconds after engine shutdown, the system bias for the coast-phase liquid-hydrogen boiloff was removed from the system. At this time, the valves began to move to the hydrogen-rich stop, in response to the hydrogen-rich propellant ratio in the tanks. After main engine first cutoff, the propellants began to rise in the sensing probes as the result of capillary action. In approximately 100 seconds, the propellants had filled the probes, and the system began to sense a liquid-oxygen-rich propellant ratio in the probes. At this time, the valves moved to the oxygen-rich stop, and remained there for the remainder of the coast period.

The valves were positioned at the oxygen-rich stop at main engine second start (see fig. V-28). Approximately 25 seconds after engine second start, the valves moved from the stop and then controlled at a hydrogen-rich mixture ratio. Approximately 25 seconds prior to main engine second cutoff, the valves were commanded to the 5 to 1 mixture ratio position. This was done because the sensing probes do not extend to the bottoms of the

58

tanks and system control is lost after the liquid level depletes below the probe bottoms.

Propellant residuals. - The propellant residuals were calculated by using data obtained from the propellant utilization system. Liquid propellants remaining at engine first cutoff were calculated by using the times that the propellant levels passed the tops of the sensing probes as reference points. The gaseous hydrogen residual at main engine first cutoff was calculated by using ullage temperature data obtained from flights AC-8 and AC-9. These residual propellant calculations established the liquid-hydrogen level at main engine first cutoff as station 329.5. The gaseous-oxygen residuals were calculated by assuming saturated oxygen gas at the ullage pressure at main engine first cutoff. The liquid-oxygen level was calculated to be at station 424.8 at main engine first cutoff.

The propellants remaining in the tanks at main engine first cutoff are shown in the following table:

Propellant remaining at engine first cutoff	Propellant	
	Hydrogen	Oxygen
Liquid residual, lb; kg	1452; 659	6765; 3068
Gaseous residual, lb; kg	75; 34	130; 59

The liquid-hydrogen level at main engine second cutoff was calculated at station 378.1. The liquid-oxygen level, calculated from propellant utilization system data, was at station 447.1 at main engine second cutoff. The propellant residuals remaining at main engine second cutoff were calculated by using the times that the propellant levels passed the bottoms of the probes as reference points. The residuals are given in the following table:

	Propellant liquid	
	Hydrogen	Oxygen
Total propellants, lb; kg	166; 75	532; 241
Burnable propellants, lb; kg	94; 43	464; 210
Burn time remaining to depletion, sec	8.3	8.3
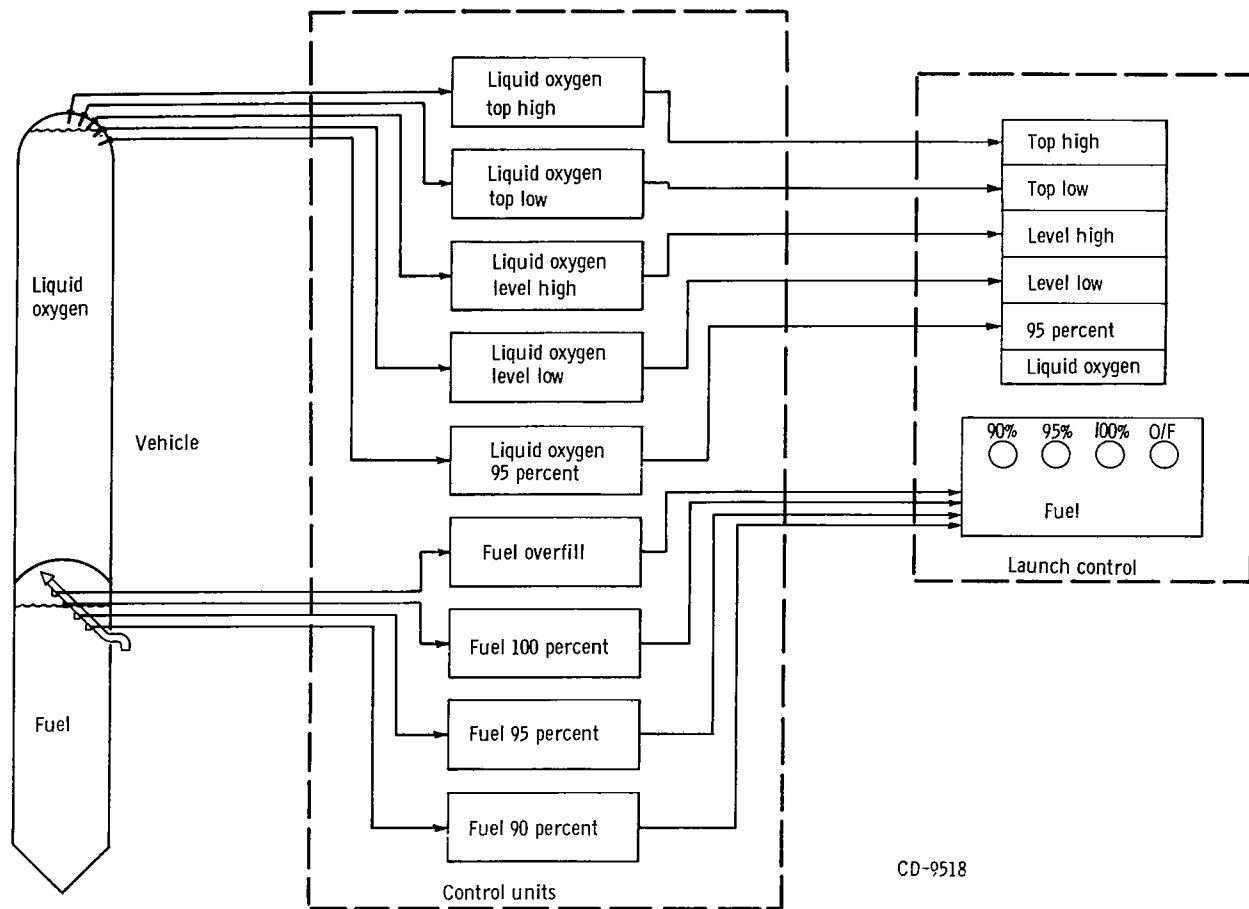
Figure V-23. - Propellant level indicating system for Atlas propellant loading, AC-12. Lights on launch control panel indicate if sensor is wet or dry. (Percent levels are indications of required flights levels and not percent of total tank volume.)
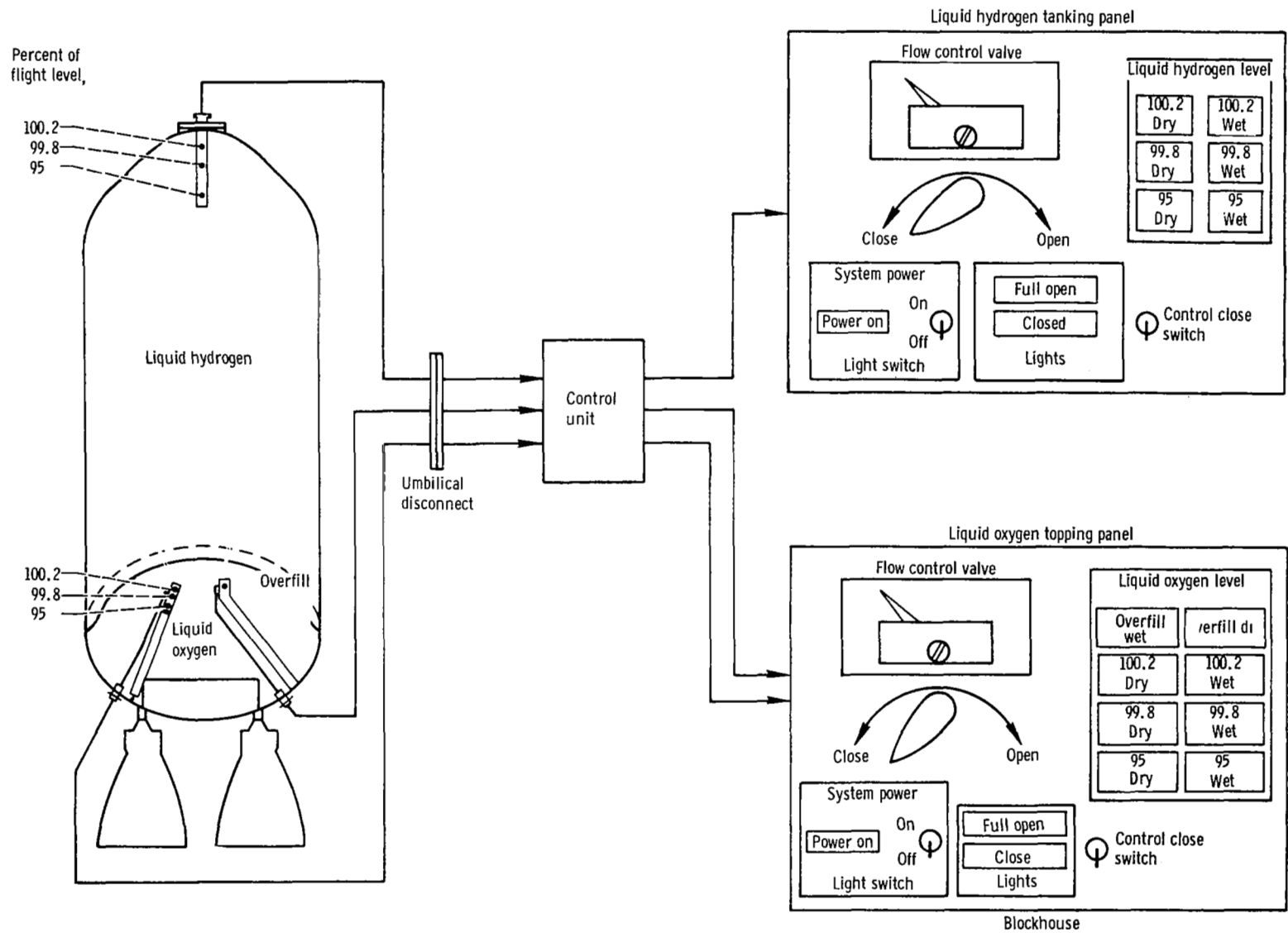
Figure V-24. – Level indicating system for Centaur propellant loading, AC-12.

Figure V-25. – Atlas propellant utilization system, AC-12.

Figure V-26. - Atlas propellant utilization valve angle, AC-12.
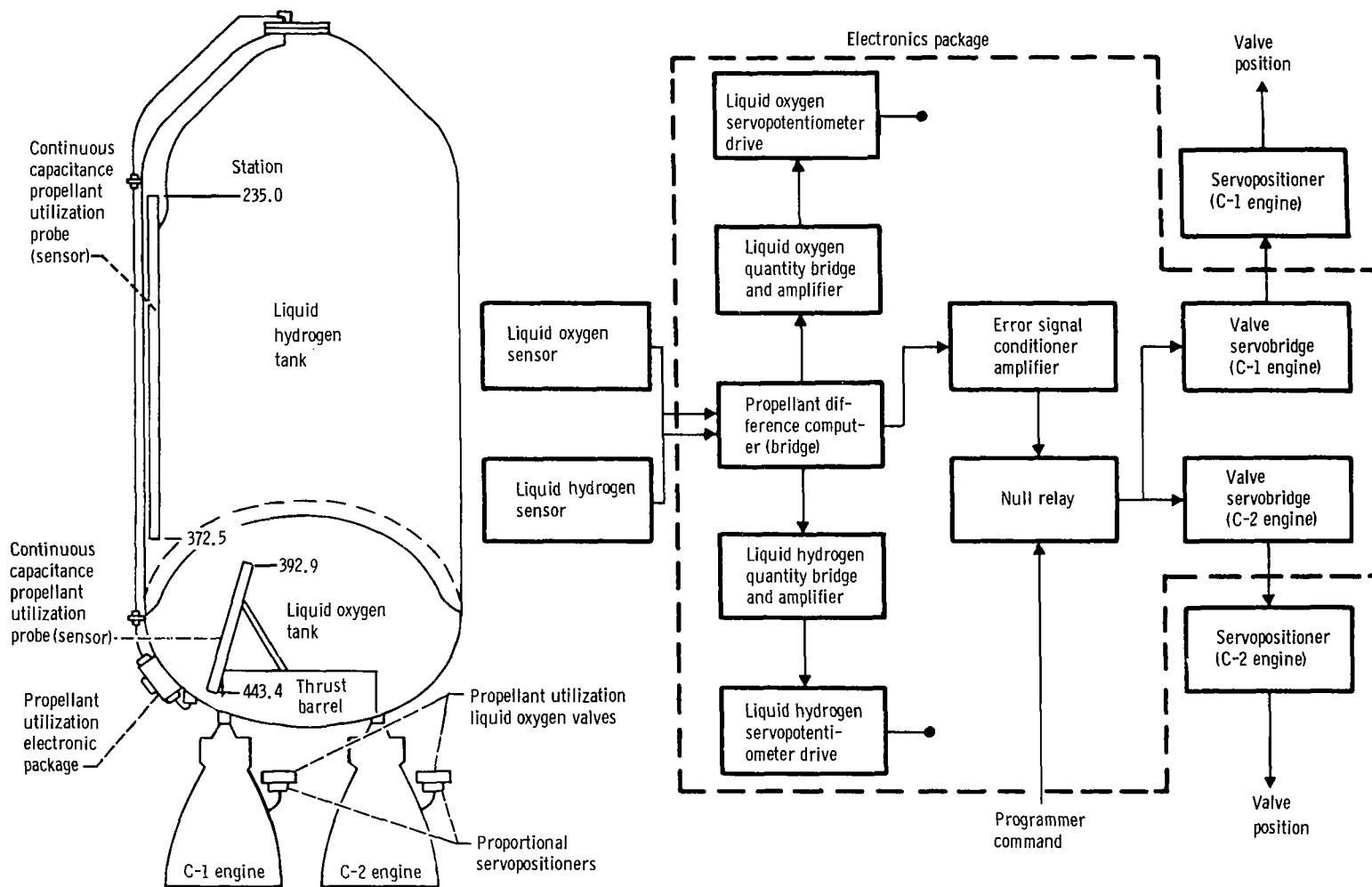
Figure V-27. – Centaur propellant utilization system, AC-12.

(a) Time from main engine first start, 0 to 240 seconds.

(b) Time from main engine first start, 240 to 360 seconds.

(c) Time from main engine second start, 0 to 160 seconds.

Figure V-28. - Centaur propellant utilization valve angles, AC-12.

65

PNEUMATIC SYSTEMS

by William A. Groesbeck and Merle L. Jones

Atlas

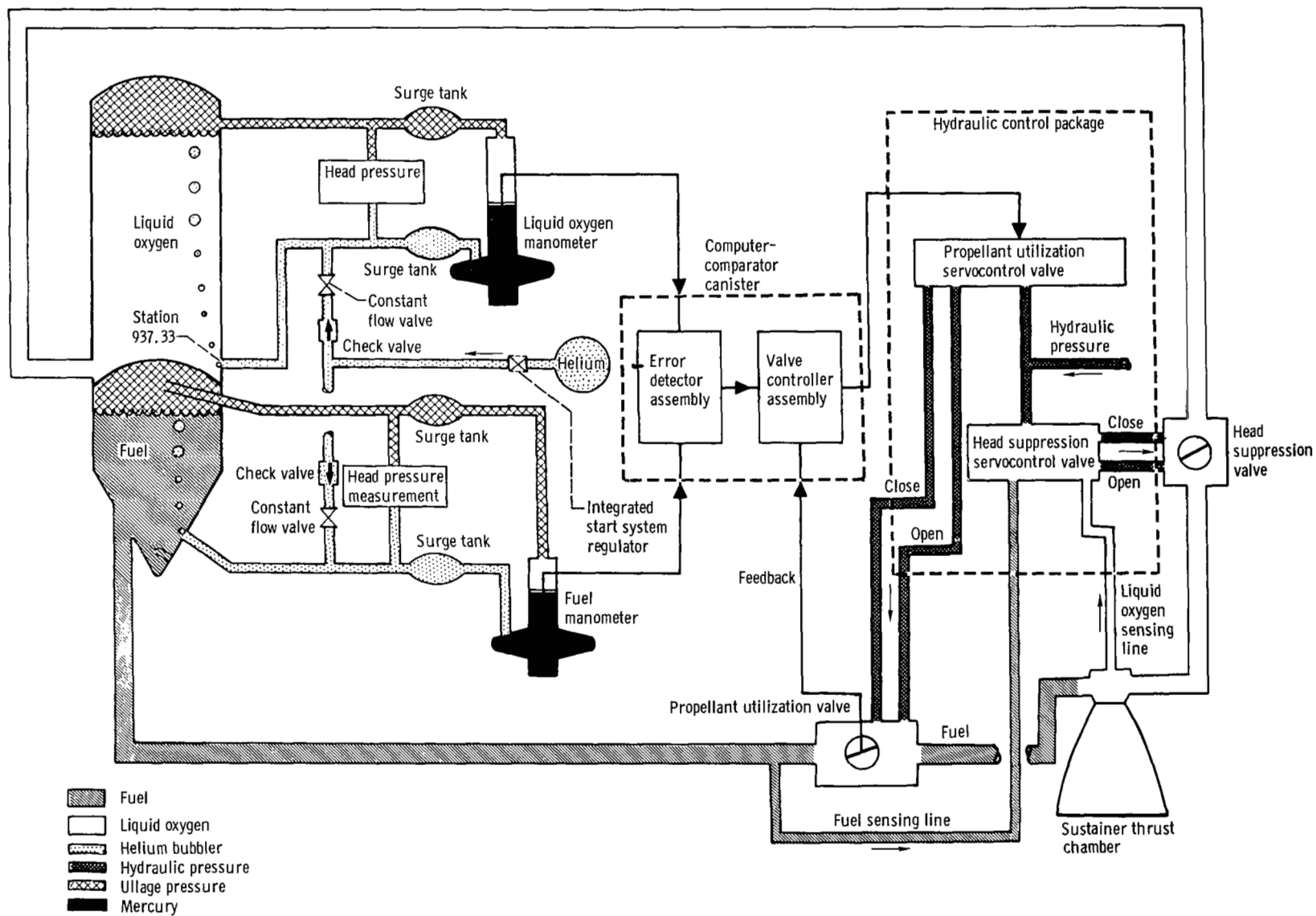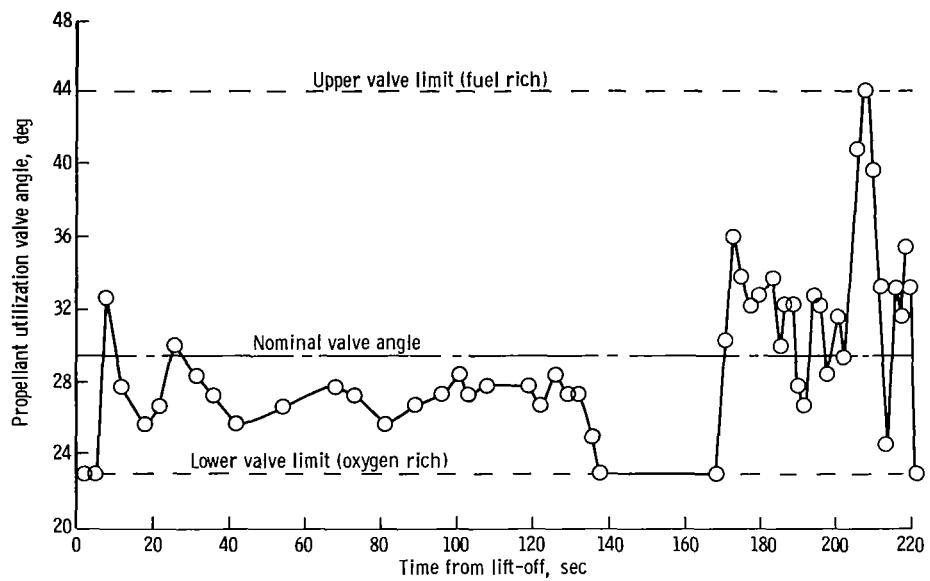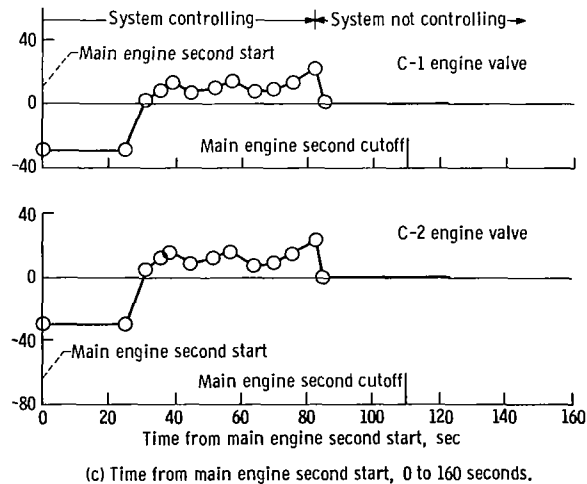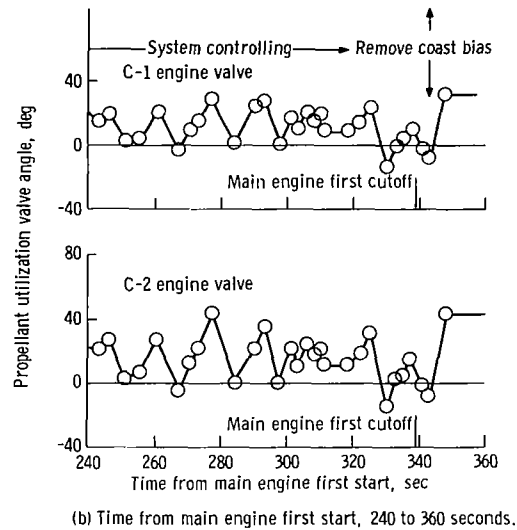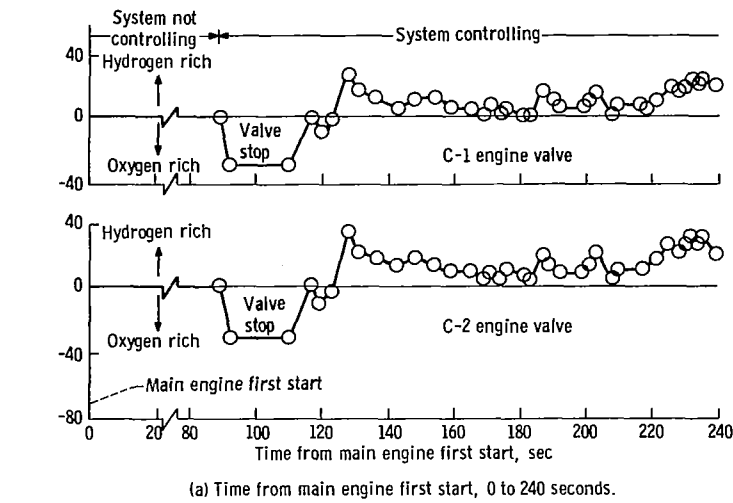System description. - The Atlas penumatic system supplied helium gas for tank pressurization and for various vehicle control functions. The system comprised three independent subsystems; propellant tank pressurization, engine control, and booster section jettison. This system schematic is shown in figure V-29.

Propellant tank pressurization subsystem: This system was used to maintain propellant tank pressures at required levels to (1) support the pressure stabilized tank structure, and (2) satisfy the inlet pressure requirements of the engine turbopumps. In addition, helium was supplied from the fuel tank pressurization line to pressurize the hydraulic reservoirs and turbopump lubricant storage tanks. The system consisted of six shrouded helium storage bottles, a heat exchanger, and fuel and oxidizer tank pressure regulators and relief valves.

The six shrouded helium storage bottles with a total capacity of 44 190 cubic inches (725 000 cm^3) were mounted in the jettisonable booster section. The bottle shrouds were filled with liquid nitrogen during prelaunch operations to chill the helium in order to provide a maximum storage capacity at an absolute pressure of about 3000 psi (2070 N/cm^2). The liquid nitrogen was drained from the shrouds at lift-off. During flight, the cold helium passed through a heat exchanger located in the booster engine turbine exhaust duct before being supplied to the tank pressure regulators.

Tank pressurization control was switched to the airborne systems at about T - 60 seconds. Airborne regulators were set to control fuel tank gage pressure between 57 and 60 psi (39.2 and 41.3 N/cm^2) and the oxidizer tank gage pressure between 28.5 and 31.0 psi (19.6 and 21.4 N/cm^2). However, from about T - 2 minutes to T + 20 seconds the liquid-oxygen regulator was biased by a helium "bleed" flow into the line which sensed ullage pressure. The bias caused the regulator to control tank pressure at a lower level than the normal regulator setting. Depressing the liquid-oxygen-tank pressure increased the differential pressure across the bulkhead between the propellant tanks. The increased differential pressure counteracted the launch transient loads that act in a direction to cause bulkhead reversal. At T + 20 seconds, the bias was removed by closing an explosively actuated valve, and the ullage pressure in the liquid-oxygen tank increased to the normal regulator control range. The increased pressure then provided sufficient vehicle structural stiffness to withstand bending loads during the remainder of the ascent.

Pneumatic regulation of tank pressure is terminated at booster staging. Thereafter,

the fuel tank pressure decayed slowly, but the oxidizer tank pressure was sustained by liquid-oxygen boiloff.

Engine controls subsystem: This system supplied helium pressure for actuation of engine control valves, for pressurization of the engine start tanks, purging booster engine turbopump seals, and for the reference pressure regulators which controlled oxidizer flow to the gas generator. Control pressure in the system was maintained through Atlas-Centaur separation. These pneumatic requirements were supplied from a 4650 cubic inch (76 000 cm^3) storage bottle pressurized to an absolute pressure of about 3000 psi (2070 N/cm^2) at lift-off.

Booster section jettison subsystem: This system supplied pressure for release of the pneumatic staging latches to separate the booster engine package. A command from the Atlas flight control system opened two explosively actuated valves to supply helium pressure to the 10 piston-operated staging latches. Helium for the system was supplied by a single 870-cubic-inch (14 260-cm^3) bottle pressurized to an absolute pressure of about 3000 psi (2070 N/cm^2).

System performance. - The Atlas pneumatic system performance was satisfactory throughout the flight. The individual subsystem performance is discussed in the following sections.

Propellant tank pressurization: Control of propellant tank pressures was switched from ground to airborne subsystems at T - 47.5 seconds. Ullage pressures were properly controlled throughout the flight. Tank pressurization data for the flight are shown in figure V-30 and table V-11.

The fuel tank pressure regulator controlled at gage pressures between 57.8 and 58.5 psi (39.8 and 40.3 N/cm^2) until termination of pneumatic control at booster staging. During sustainer engine firing, the fuel-tank pressure decreased normally and was 48.1 psi (33.1 N/cm^2) at engine shutdown.

Oxidizer tank gage pressure on switching to airborne regulation was steady at 26.5 psi (18.2 N/cm^2). The pressure dropped to 24.5 psi (16.9 N/cm^2) at engine start and then showed a gradual increase during the vehicle ascent due to reduction in atmospheric pressure. When the regulator bias was terminated at T + 20 seconds, pneumatic regulation increased the ullage gage pressure abruptly from 26.1 to 29.2 psi (18.0 to 20.1 N/cm^2). At T + 89 seconds the ullage pressure increased above the regulator control range as a result of liquid-oxygen boiloff. The regulator then closed down, stopping any further helium flow into the tank. At booster engine shutdown, the ullage pressure increased rather abruptly as the result of the sudden decrease in propellant outflow and an increase in liquid-oxygen boiloff rate. The boiloff rate increased because of the abrupt reduction in hydrostatic pressure caused by the decrease in vehicle acceleration from 5.62 to about 1.1 g's. After booster staging, the ullage pressure was maintained at about 31 psi (21 N/cm^2).

TABLE V-11. – ATLAS PNEUMATICS SYSTEM DATA SUMMARY, AC-12

Pneumatic subsystem	Measurement		Units	Time from lift-off, sec			
				Requirement at T - 0	Lift off, T - 0	Booster engine cutoff, T + 142.3 sec	Sustainer engine cutoff, T + 237.7 sec
Propellant tank pressurization	Liquid-oxygen-tank ullage (gage) pressure		psi N/cm^2	23.3 to 28.5 16.1 to 19.7	26.4 18.2	30.0 20.7	31.0 21.4
	Liquid-oxygen-tank regulator sensing line (gage) pressure		psi N/cm^2	----------- -----------	30.3 20.8	---- ----	---- ----
	Fuel-tank ullage (gage) pressure		psi N/cm^2	57.8 to 61.5 39.9 to 42.4	58.5 40.3	58.0 39.9	48.0 33.1
	Pressurization bottles helium storage	Pressure (gage)	psi N/cm^2	3100 to 3400 2137 to 2344	3262 2248	929 640	---- ----
		Temperature	$^\circ$F K	-308 max. 85 max.	-324 75.5	-369 50.5	---- ----
		Mass	lb kg	----------- -----------	165.5 75	80.2 36.3	---- ----
Engine controls	Booster engine pneumatic regulator outlet (gage) pressure		psi N/cm^2	715 to 785 493 to 541	744 512	749 516	---- ----
	Sustainer engine pneumatic regulator outlet (gage) pressure		psi N/cm^2	565 to 635 390 to 438	599 413	598 412	606 417
	Controls bottle helium storage (gage) pressure		psi N/cm^2	2900 to 3400 2000 to 2344	3265 2250	2740 1888	2575 1775
Booster jettison	Staging bottle helium storage (gage) pressure		psi N/cm^2	2900 to 3400 2000 to 2344	3250 2240	---- ----	---- ----

Engine control regulators: The booster and sustainer pneumatic regulators provided the required helium pressures for engine control throughout the flight. Significant performance values are shown in table V-11.

Booster section jettison system: System performance was satisfactory. The explosive actuated valves were opened on command at T + 145.3 seconds allowing high-pressure helium to actuate the 10 booster staging latches.

Centaur

System description. - The Centaur pneumatic system, which is shown schematically

in figure V-31, consisted of five subsystems; propellant tank venting, propellant tank pressurization, propulsion pneumatics, helium purge, and nose fairing pneumatics.

The structural stability of the propellant tanks was maintained throughout the flight by the propellant boiloff gas pressures. These pressures were controlled by a vent system on each propellant tank. Two pilot-controlled, pressure-actuated vent valves and ducting comprised the hydrogen tank vent system. The primary vent valve was fitted with a continuous-duty solenoid valve which, when energized, locked the vent valve preventing operation. The secondary hydrogen vent valve did not have the control solenoid and was always in the enabled-to-relieve mode. The relief range of the secondary valve was above that of the primary valve and prevented overpressurization of the hydrogen tank when the primary vent valve was locked. Until nose fairing jettison, the vent gases were ducted overboard through a single vent. After jettison, venting occurred through diametrically opposed nozzles which balanced the vent thrust forces. The oxygen tank vent system used a single vent valve which was fitted with the control solenoid valve. The vented gases were ducted overboard through the interstage adapter. The duct was oriented to aline the venting thrust vector with the vehicle center of gravity.

The vent valves were commanded to the locked mode at specific times to (1) permit the hydrogen tank pressure to increase during the atmospheric ascent to satisfy the structural requirements of the pressure-stabilized tank, (2) permit controlled pressure increases in the tanks to satisfy the boost pump pressure requirements, (3) restrict venting during nonpowered flight to avoid vehicle disturbing torques, and (4) restrict hydrogen venting to nonhazardous times.[1]

The propellant tank pressurization subsystem supplied helium gas in controlled quantities for in-flight pressurization in addition to that provided by the propellant boiloff gases. It consisted of two normally closed solenoid valves and orifices and a pressure switch assembly which sensed oxygen tank pressure. The solenoid valves and orifices provided metered flow of helium to the propellant tanks for step pressurization during both main engine start sequences. The pressure sensing switch controlled the pressure in the oxygen tank from boost pump first start to main engine first start.

The propulsion pneumatics subsystem supplied helium gas at regulated pressures for actuation of main engine control valves and pressurization of the hydrogen peroxide storage bottle. It consisted of two pressure regulators, which were referenced to ambient pressure, and two relief valves. Pneumatic pressure supplied through the engine controls regulator was used for actuation of the engine inlet valves, the engine chilldown

---

[1]A fire might occur during the early part of the atmospheric ascent if a plume of vented hydrogen washed back over the vehicle and was exposed to an ignition source. A similar hazard could occur at Atlas booster engine staging when residual oxygen envelops a large portion of the vehicle.

valves, and the main fuel shutoff valve. The second regulator, located downstream of the engine controls regulator, further reduced the pressure to provide expulsion pressurization for the hydrogen peroxide storage bottle. A relief valve downstream of each regulator prevented overpressurization.

A ground-airborne helium purge subsystem was used to prevent air ingestion under the insulation panels and cryopumping into various propulsion system areas. A common airborne distribution system was used for prelaunch purging from a ground helium source and postlaunch purging from an airborne helium storage bottle. This subsystem distributed helium gas for purging the cavity between the hydrogen tank and the insulation panels, the seal between the nose fairing and the forward bulkhead, the propellant feed lines, the boost pumps, the engine chilldown vent ducts, the engine thrust chambers, and the hydraulic power packages. The umbilical charging connection for the airborne bottle could also be used to supply the purge from the ground source should an abort occur after ejection of the ground purge supply line.

The nose fairing pneumatic subsystem provided the required thrust for nose fairing jettisoning. It consisted of a nitrogen storage bottle and an explosive actuated valve with an integral thruster nozzle in each fairing half. Release of the gas through the nozzles provided the necessary thrust to propel the fairing halves away from each other and from the vehicle.

Propellant tank pressurization and venting. - The ullage pressures for the hydrogen and oxygen tanks during the flight are shown in figure V-32. The hydrogen tank absolute pressure was 21.1 psi (14.5 N/cm^2) at T - 7.9 seconds when the primary hydrogen vent valve was locked. After vent valve lockup, the tank absolute pressure increased, at an average rate of 4.22 psi per minute (2.91 $(N/cm^2)/min$), to 26.3 psi (18.1 N/cm^2) at T + 66 seconds. At this time, the secondary vent valve relieved and regulated tank pressure until T + 68.9 seconds when the primary vent valve was enabled. The tank pressure was then reduced and was regulated by the primary vent valve.

At T + 142.3 seconds, the primary hydrogen vent valve was locked and remained locked for 7.7 seconds during Atlas booster engine staging. During this period of nonventing, the hydrogen ullage absolute pressure increased to 22.9 psi (15.8 N/cm^2). Following booster engine staging, the primary vent valve was enabled and allowed to regulate tank pressure. At T + 237.7 seconds, the primary hydrogen vent valve was again locked, and the tank was pressurized with helium for 1 second. The tank absolute pressure increased from 20.8 to 22.2 psi (14.3 to 15.3 N/cm^2). As the warm helium in the tank cooled, the absolute pressure decreased to 20.8 psi (14.3 N/cm^2) at T + 249.2 seconds (Centaur main engine first start). The absolute pressure at engine prestart (T + 241.2 sec) was 21.1 psi (14.8 N/cm^2).

The ullage absolute pressure in the oxygen tank was 29.8 psi (20.5 N/cm^2) at lift-off. After lift-off, the increasing vehicle acceleration suppressed the propellant boiling and

caused the pressure to decrease. At T + 85 seconds, the vent valve reseated and venting ceased. The pressure then began to increase gradually until Atlas booster engine cutoff. At this time, the sudden reduction in the acceleration caused an increase in the liquid-oxygen boiloff and an ullage absolute pressure rise to 32.4 psi (22.3 N/cm^2). As thermal equilibrium was reestablished in the tank, the ullage absolute pressure decreased to 29.1 psi (20.1 N/cm^2).

At T + 204.3 seconds, the oxygen tank vent valve was locked, and the helium pressurization of the tank began. The tank absolute pressure increased to 39.8 psi (27.4 N/cm^2) which was the upper limit of the pressure switch. As the warm helium gas cooled in the tank, the absolute pressure decreased to 38.4 psi (26.5 N/cm^2), when the pressure switch closed, and additional helium was injected into the tank. After the second cycle, the heat input from the boost pump recirculation flow increased the boiloff and caused the pressure to increase before it reached the lower limit of the pressure switch. At engine prestart, the absolute pressure was 40.2 psi (27.7 N/cm^2). After engine prestart, the absolute pressure decreased to 39.3 psi (27.1 N/cm^2) at main engine first start and decreased thereafter to its saturation value of approximately 29.6 psi (20.4 N/cm^2).

The ullage pressures in both propellant tanks decreased normally during main engine first firing. At engine cutoff, the ullage absolute pressures in the hydrogen and oxygen tanks were 15.9 psi (11.0 N/cm^2) and 26.6 psi (18.3 N/cm^2), respectively. The primary hydrogen vent valve was enabled after main engine cutoff, while the oxygen tank vent valve remained locked.

During the coast period following main engine first cutoff, the hydrogen tank pressure increased at a rate of 0.53 psi per minute (0.36 (N/cm^2)/min). At T + 1108 seconds, the tank pressure reached the regulating range of the primary vent valve and was regulated by that valve for the duration of the coast period. The oxygen tank ullage pressure increased gradually throughout the coast period and remained well within the allowable limits.

At T + 1877 seconds, the primary hydrogen vent valve was locked, and at the same time helium was injected into both propellant tanks. The step pressurization of the oxygen tank was timed to last 18 seconds. The pressure sensing switch, used prior to the main engine first start, was electrically by-passed. During this 18-second period, the oxygen tank ullage absolute pressure rose from 28.0 psi (19.3 N/cm^2) to 30.0 psi (20.7 N/cm^2). After engine prestart, the pressure decreased slightly until main engine second start and decreased more rapidly thereafter. The helium step pressurization of the hydrogen tank was also a timed function, lasting 40 seconds until main engine second start. The absolute pressure increased to 26.3 psi (18.1 N/cm^2), when the relief setting of the secondary vent valve was reached. Tank pressure was then regulated by that valve until main engine second start. During the engine firing, the oxygen tank ullage absolute pressure decreased to 25.0 psi (17.2 N/cm^2) at main engine cutoff, while the hydrogen tank

ullage absolute pressure decreased to 21.6 psi (14.9 N/cm^2).

Following main engine second cutoff, the hydrogen tank ullage pressure increased at a rate of 0.76 psi per minute (0.52 (N/cm^2)/min). A sudden pressure decrease at T + 2138.4 seconds coincided with the start of lateral thrust in the Centaur turnaround maneuver, indicating the splashing of liquid hydrogen into the ullage. The pressure then increased at approximately the same rate until the start of retrothrust at T + 2333.7 seconds. During this period following main engine second cutoff, the oxygen tank ullage pressure increased at a much lower rate than the hydrogen tank ullage pressure. At T + 2333.7 seconds, the differential pressure across the bulkhead between the two tanks had diminished to 0.5 psi (0.3 N/cm^2).

After the start of retrothrust, the hydrogen tank pressure decreased for approximately 40 seconds, indicating either gaseous or two-phase outflow. The pressure then remained constant for approximately 40 seconds, indicating liquid outflow. After that the pressure began to decrease, indicating the resumption of gaseous or two-phase outflow. During the period of retrothrust, the oxygen tank pressure remained relatively constant, indicating liquid outflow. At T + 2583 seconds, the engine valves were closed terminating the retrothrust maneuver. The primary hydrogen and the oxygen vent valves were enabled to prevent ultimate rupture of the tanks in space.

Propulsion pneumatics. - The engine controls regulator output absolute pressure was 478 psi (330 N/cm^2) at T - 0, but shortly after lift-off the output absolute pressure began to increase until it reached 502 psi (346 N/cm^2) at T + 50 seconds. The absolute pressure then remained constant, indicating the possibility of relief valve actuation, until T + 85 seconds when it decreased slightly to 496 psi (342 N/cm^2). At booster engine cutoff the output absolute pressure dropped abruptly to 472 psi (325 N/cm^2) and then increased to 484 psi (334 N/cm^2). At T + 177 seconds, the absolute pressure again decreased abruptly to 460 psi (317 N/cm^2) and remained relatively constant after that. These variable output pressures did not affect engine operation.

The hydrogen peroxide bottle pressure regulator maintained a proper system level throughout the flight. The regulator output absolute pressure was 322 psi (222 N/cm^2) at T - 0. After lift-off, the absolute pressure decreased with a corresponding decrease in ambient pressure to 308 psi (212 N/cm^2) and then remained relatively constant.

Helium purge subsystem. - The ground purge system operated normally throughout the countdown. The total helium flow rate to the vehicle at T - 0 was 182 pounds per hour (82.6 kg/hr). The differential pressure across the insulation panels after hydrogen tanking was 0.24 psi (0.16 N/cm^2). The minimum allowable differential pressure to prevent air ingestion is 0.03 psi (0.02 N/cm^2). At T - 10.2 seconds, the airborne purge system was activated, and at T - 4 seconds, the ground purge was terminated. The supply of helium in the airborne purge bottle lasted through most of the atmospheric ascent.

Nose fairing pneumatics. - There is no airborne instrumentation in this system, but proper jettisoning of the nose fairing indicated proper functioning of the nose fairing pneumatics subsystem.
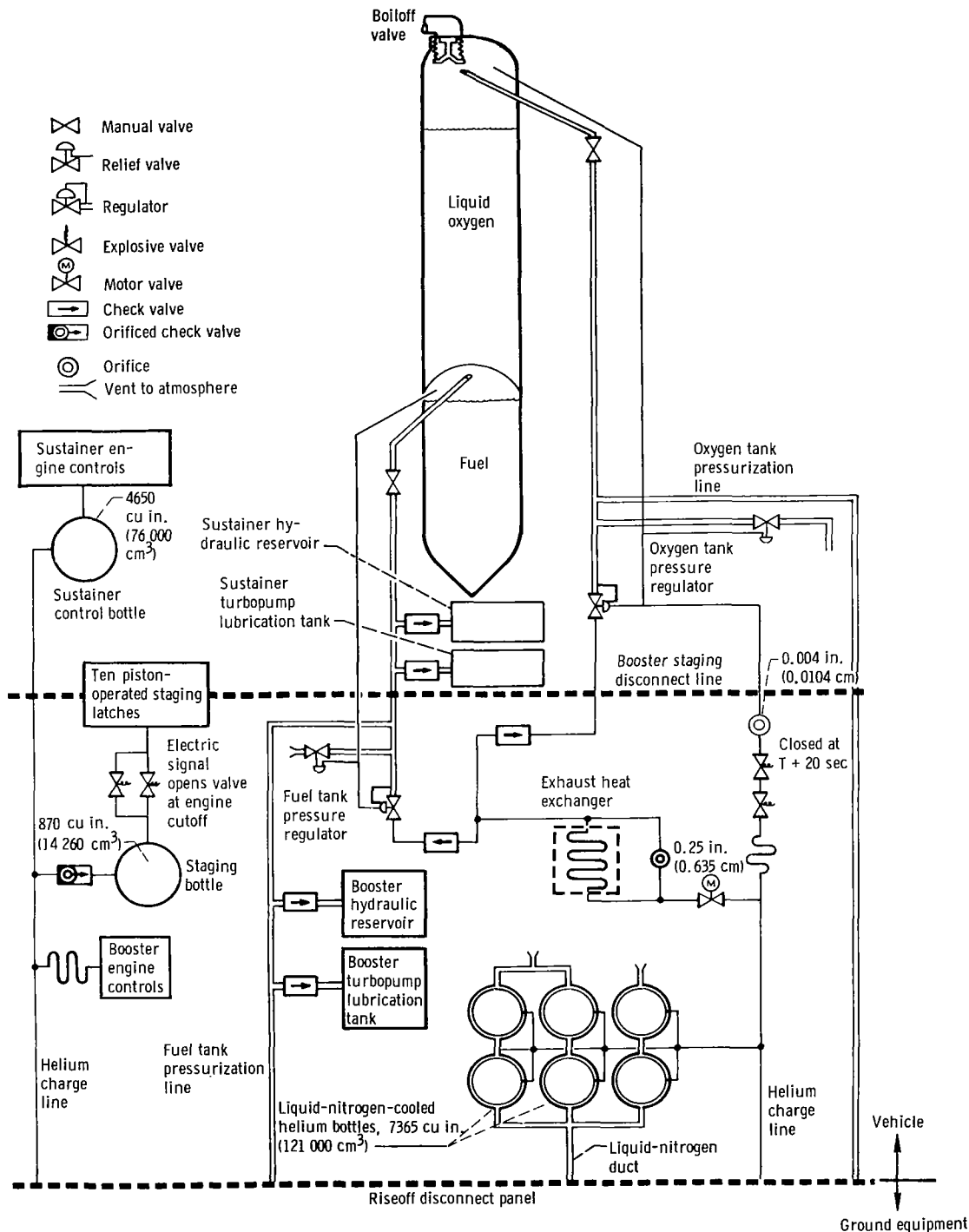
Figure V-29. - Atlas vehicle pneumatic system, AC-12.
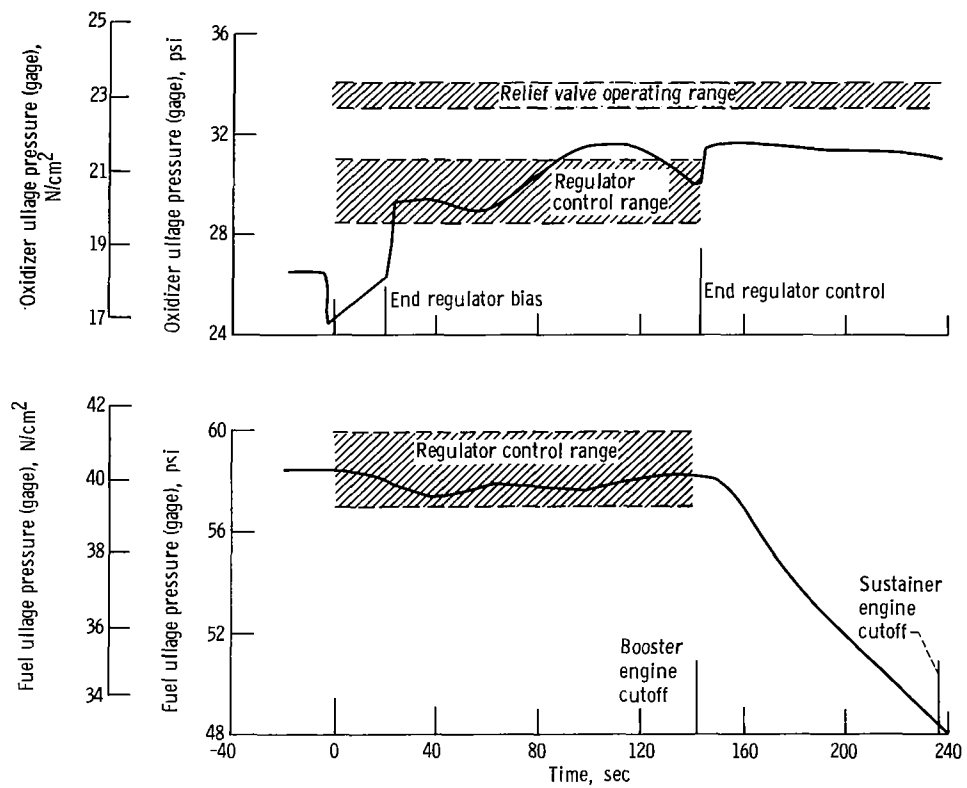
Figure V-30. – Atlas fuel and oxidizer tank ullage pressures, AC-12.

Engine controls
    Regulator pressure (gage), 440 to 475 psi (303 to 327 N/cm^2)
    Relief valve pressure (gage), 475 to 525 psi (327 to 362 N/cm^2)
Hydrogen peroxide bottle
    Pressure regulator (gage), 297 to 315 psi (205 to 217 N/cm^2)
    Relief valve pressure (gage), 320 to 354 psi (221 to 244 N/cm^2)
Orifice-tank pressurization
    Oxygen tank, 0.043-in. (0.109-cm) diameter
    Hydrogen tank, 0.089-in. (0.226-cm) diameter
Constant bleed orifice, 135 standard cu in./min (2211 standard cm^3/min)
Pressure switch (oxygen tank), 38 to 40 psia (26 to 28 N/cm^2 abs)
Helium bottle
    Volume, 7365 cu in. (120 639 cm^3)
    Initial pressure, 3200 psia (2206 N/cm^2 abs)

CD-9843-31

(a) Tank pressurization and propulsion pneumatics subsystems.

Figure V-31. - Centaur pneumatics system, AC-12.

To nose fairing seal

Hydrogen tank

To automatic
launch sequencer

Helium
storage
bottle

Oxygen
tank

To insulation panel
panel purge ring

Pressure switch

S

To engine
chilldown
vent ducts

Solenoid valve
(normally open)

To engines
and boost
pumps

To
hydraulic
system

Helium bottle
    Volume, 4650 cu in. (76 167 cm^3)
    Initial pressure, 2380 psia (1641 N/cm^2 abs)
Pressure switch, 2000 psia (1379 N/cm^2 abs)

T - 4 sec disconnect

T - 0 disconnect

CD-9844-31

(b) Helium purge subsystem.

Figure V-31. - Continued.

Vent valves
Primary hydrogen, 19.0 to 21.5 psia (13.1 to 14.8 N/cm^2 abs)
Secondary hydrogen, 24.8 to 26.8 psia (17.1 to 18.5 N/cm^2 abs)
Oxygen, 29.0 to 32.0 psia (20.0 to 22.1 N/cm^2 abs)

Thruster bottles
Volume, 870 cu in.
(14 251 cm^3)
Initial pressure (gage)
2500 psi (1724 N/cm^2)

Nose fairing
pneumatic subsystem

Tank venting subsystem

CD-9845-31
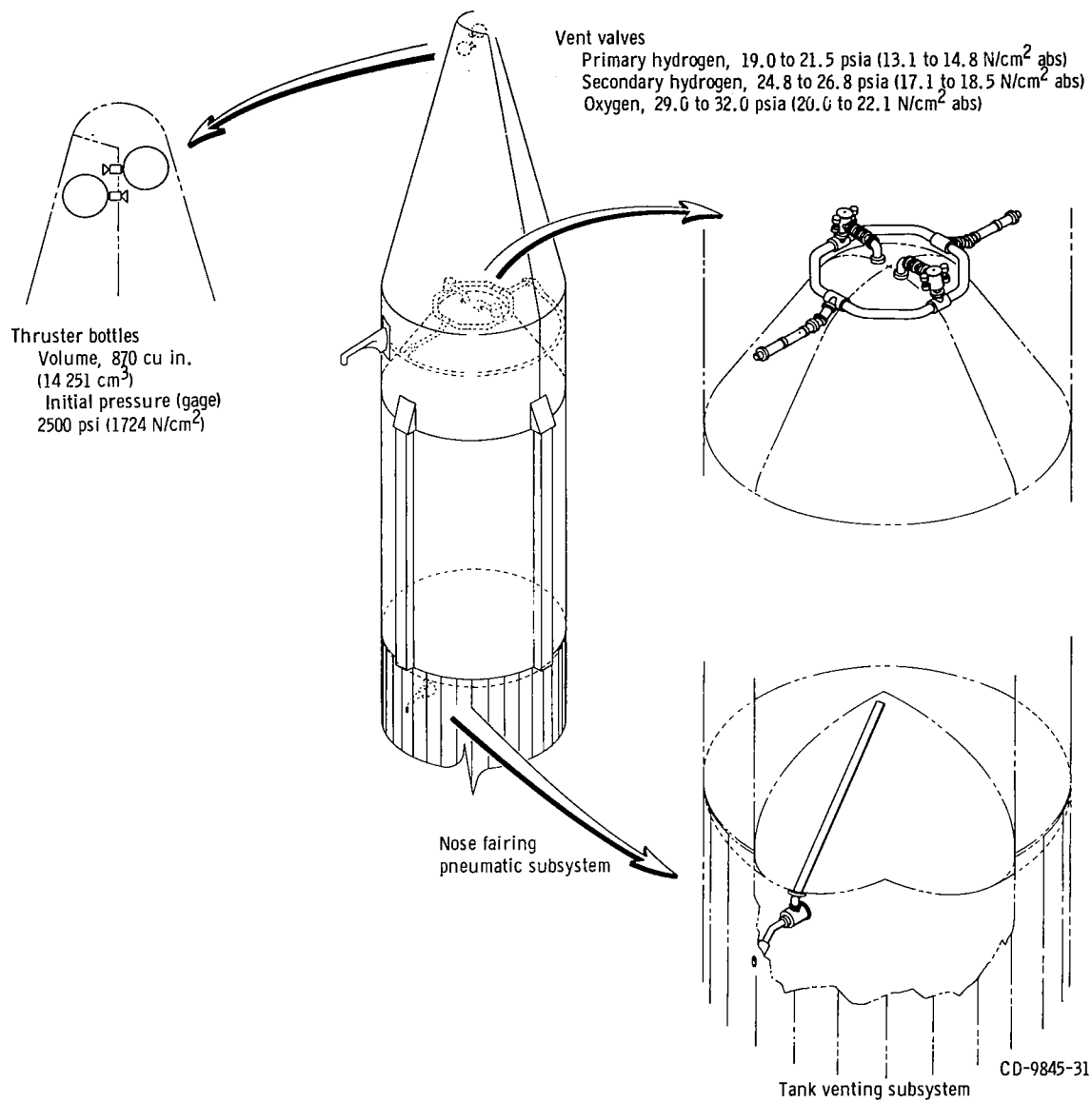
(c) Tank venting and nose fairing pneumatics subsystems.

Figure V-31. – Concluded.

(a) Time, -20 to 200 seconds.

(b) Time, 200 to 400 seconds.

(c) Time, 400 to 800 seconds.
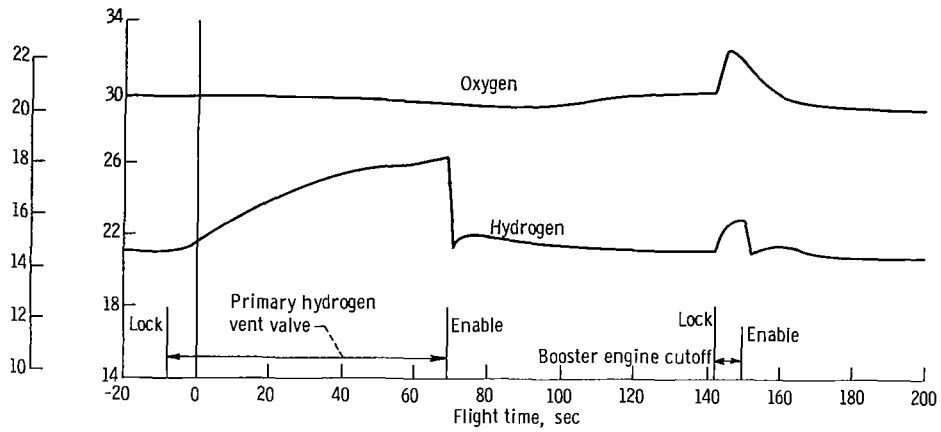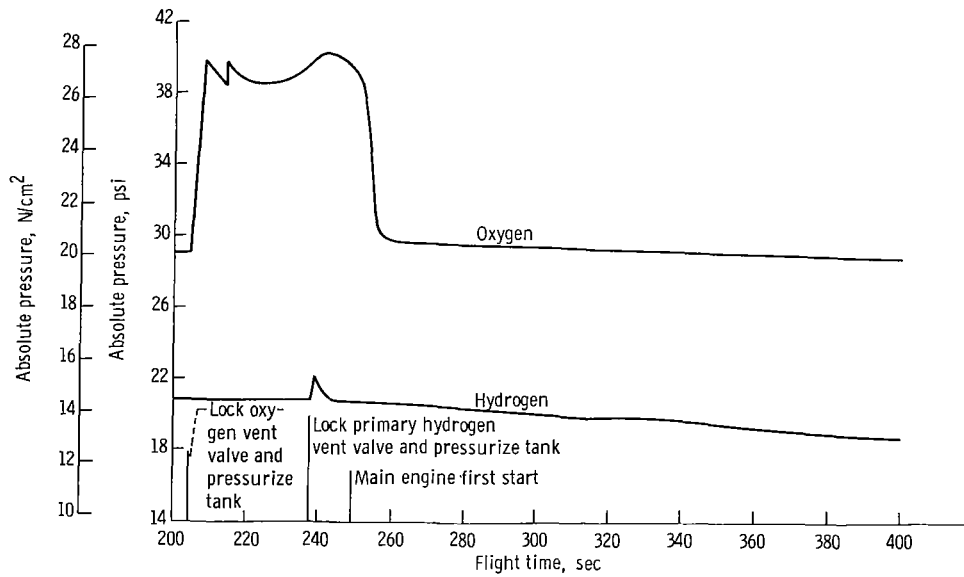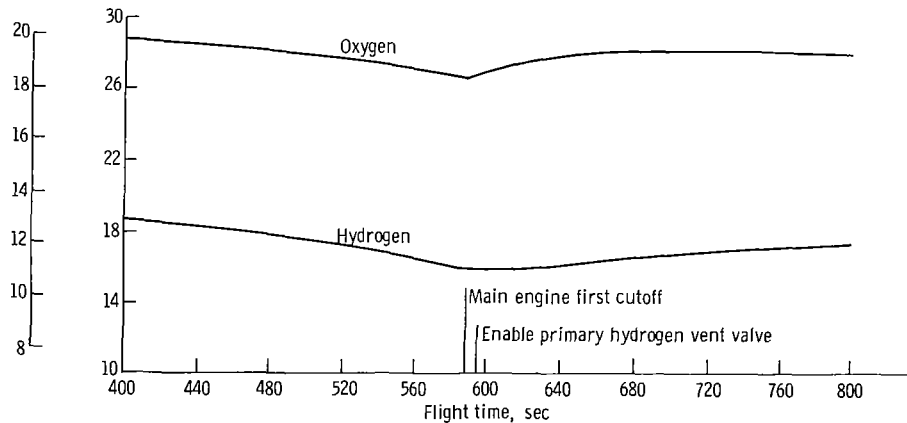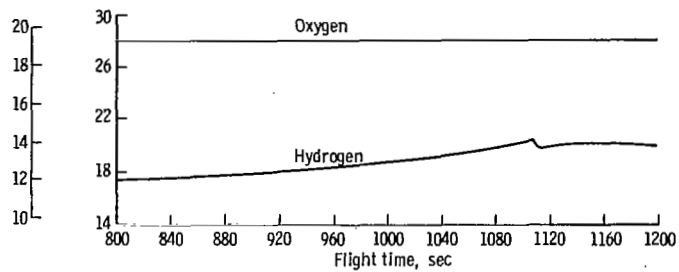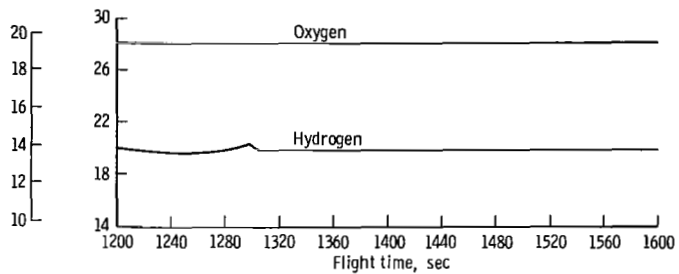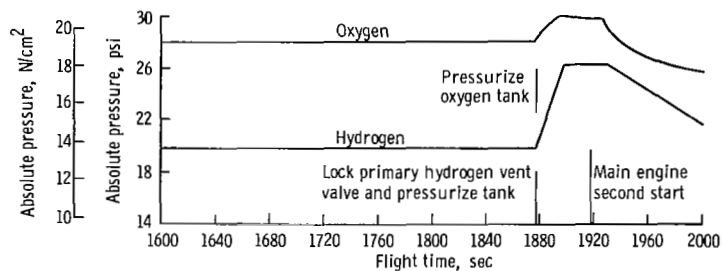
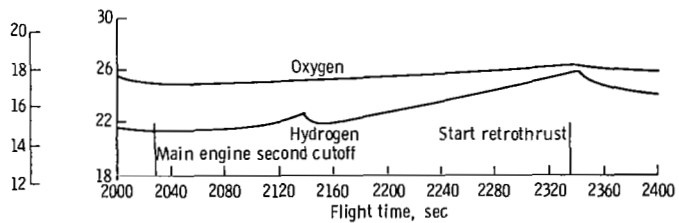Figure V-32. – Centaur tank pressure history, AC-12.

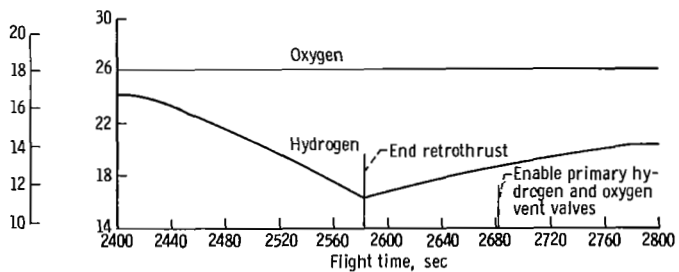(d) Time, 800 to 1200 seconds.

(e) Time, 1200 to 1600 seconds.

(f) Time, 1600 to 2000 seconds.

(g) Time, 2000 to 2400 seconds.

(h) Time, 2400 to 2800 seconds.

Figure V-32. - Concluded.

HYDRAULIC SYSTEMS

by Eugene J. Cieslewicz

Atlas

System description. - Two hydraulic systems, shown in figures V-33 and V-34, were used on the Atlas stage to supply fluid power for operation of sustainer engine control valves and for thrust vector control of all engines. One system was used for the booster engines and the other for the sustainer engine.

The booster hydraulic system provided power solely for gimbaling the two thrust chambers of the booster engine system. System pressure was supplied by a single, pressure-compensated, variable-displacement pump driven by the engine turbopump accessory drive. Additional components of the system included four servocylinders, a high-pressure relief valve, two accumulators, and a reservoir. Engine gimbaling in response to flight control commands was accomplished by the servocylinders which provided separate pitch, yaw, and roll control during the booster phase of flight. The maximum booster engine gimbal angle capability was $\pm 5^{\circ}$ in the pitch and yaw planes.

The sustainer stage used a system similar to that of the booster, but, in addition, provided hydraulic power for sustainer engine control valves and gimbaling of the two vernier engines.

The sustainer engine was held in the centered position until booster engine cutoff. At this time, disturbances created by booster differential cutoff impulse were damped by gimbaling the sustainer and vernier engines. The sustainer engine was centered a second time for 0.7 second during booster stage jettison. Vehicle engine roll control was maintained throughout the sustainer phase by differential gimbaling of the vernier engines. The actuator limit travel of the vernier engines was $\pm 70^{\circ}$, $\pm 3^{\circ}$ for the sustainer engine.

System performance. - Hydraulic system pressure data for both the booster and sustainer circuits are shown in figure V-35. Pressures were stable throughout the boost flight phase. The transfer of fluid power from ground to airborne hydraulics systems was normal. Hydraulic pump discharge pressures increased at T - 2 seconds up to flight levels in less than 2 seconds. Starting transients produced a normal overshoot of about 10 percent in the hydraulic pump discharge pressure. Absolute pressure in the booster hydraulic circuit stabilized at 3140 psi (2165 N/cm^2) and in the sustainer circuit at 3060 psi (2110 N/cm^2).

Engine gimbaling during the flight was generally less than $1\frac{1}{2}^{\circ}$ in the pitch and yaw planes. However, a 2° gimbal angle was required in pitch during the period of maximum dynamic pressure. As expected, the gimbal angles were well within the engine gimbal limits.

Centaur

System description. - Two separate but identical hydraulic systems, shown in figure V-36, were used on the Centaur stage. Each system gimbaled one engine for pitch, yaw, and roll control. Each system consisted of two servocylinders and an engine-coupled power package containing high and low pressure pumps, reservoir, accumulator, pressure intensifying bootstrap piston, and relief valves for pressure regulation. Hydraulic pressure and flow were provided by a constant-displacement vane-type pump driven by the liquid-oxygen turbopump accessory drive shaft. An electrically powered recirculation pump was also used to provide low pressure for engine gimbaling requirements during prelaunch checkout, to aline the engines prior to main engine start, and for limited thrust vector control during the propellant tank discharge for the Centaur retrothrust operation. Maximum engine gimbal capability was $\pm 3^\circ$.

System performance. - The hydraulic system properly performed all guidance and flight control commands throughout the flight. System pressures and temperatures as a function of the flight time are shown in figures V-37 and V-38.

Activation of the low pressure recirculation pumps provided absolute hydraulic pressures of 127 psi (88 N/cm^2) for the C-1 engine system and 123 psi (85 N/cm^2) for the C-2 engine system. These pumps provide pressure and flow for centering the engines prior to main engine first and second starts.

Main system absolute pressure in the C-1 and C-2 systems reached 1132 psi (781 N/cm^2) and 1130 psi (779 N/cm^2), respectively, for the Centaur main engine first and second firings. Manifold temperature rose from 58. 6° F (288 K) and 60. 2° F (289 K), respectively, for C-1 and C-2 at main engine first start to 155. 1° F (341 K) and 159. 2° F (344 K) at main engine cutoff. After cutoff, the temperature at the C-1 manifold dropped to a low of 104. 8° F (313 K) before main engine second start. The C-2 manifold temperature also dropped to a low of 113. 2° F (318 K) before main engine second start. The manifold temperature at main engine second cutoff was 155. 1° F (341 K) for C-1 and 160° F (344 K) for C-2.
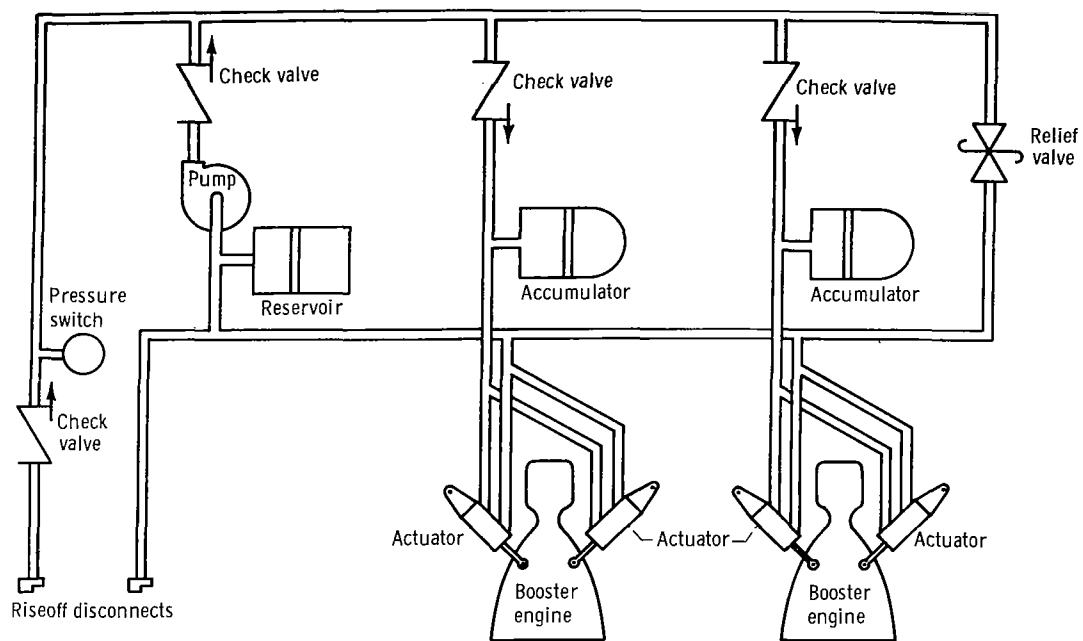
Figure V-33. - Atlas booster hydraulic system, AC-12.
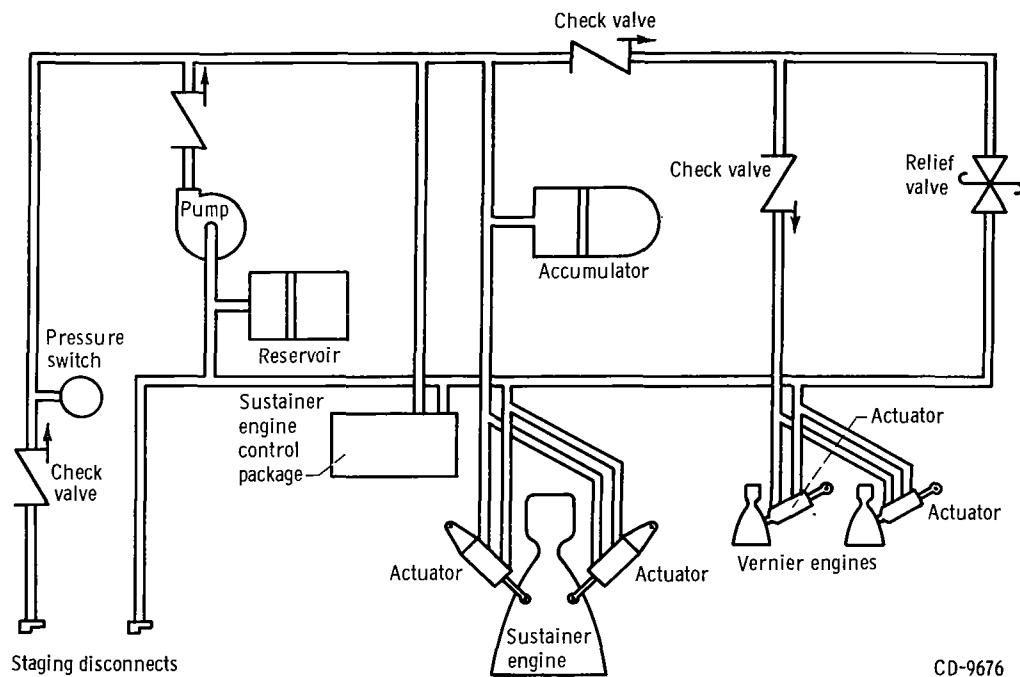
CD-9676

Figure V-34. - Atlas sustainer hydraulic system, AC-12.
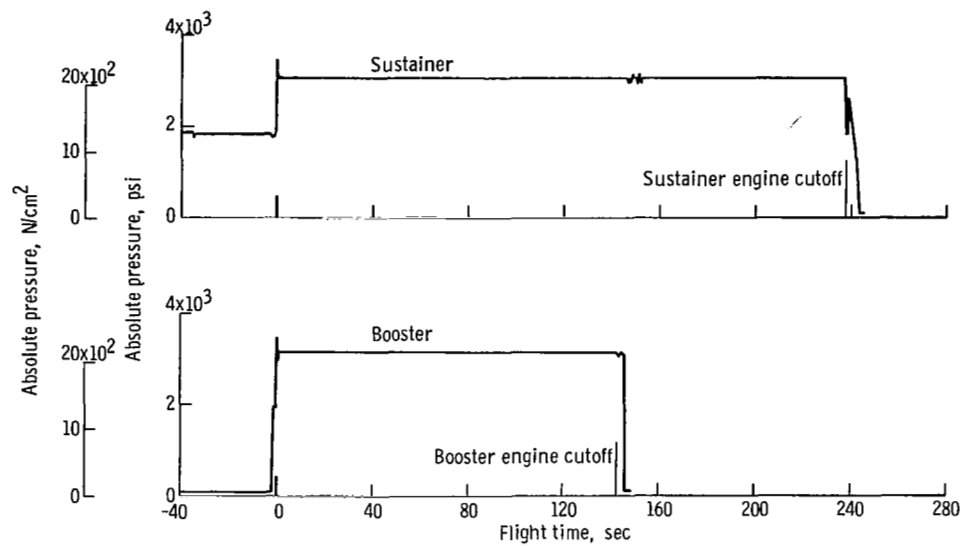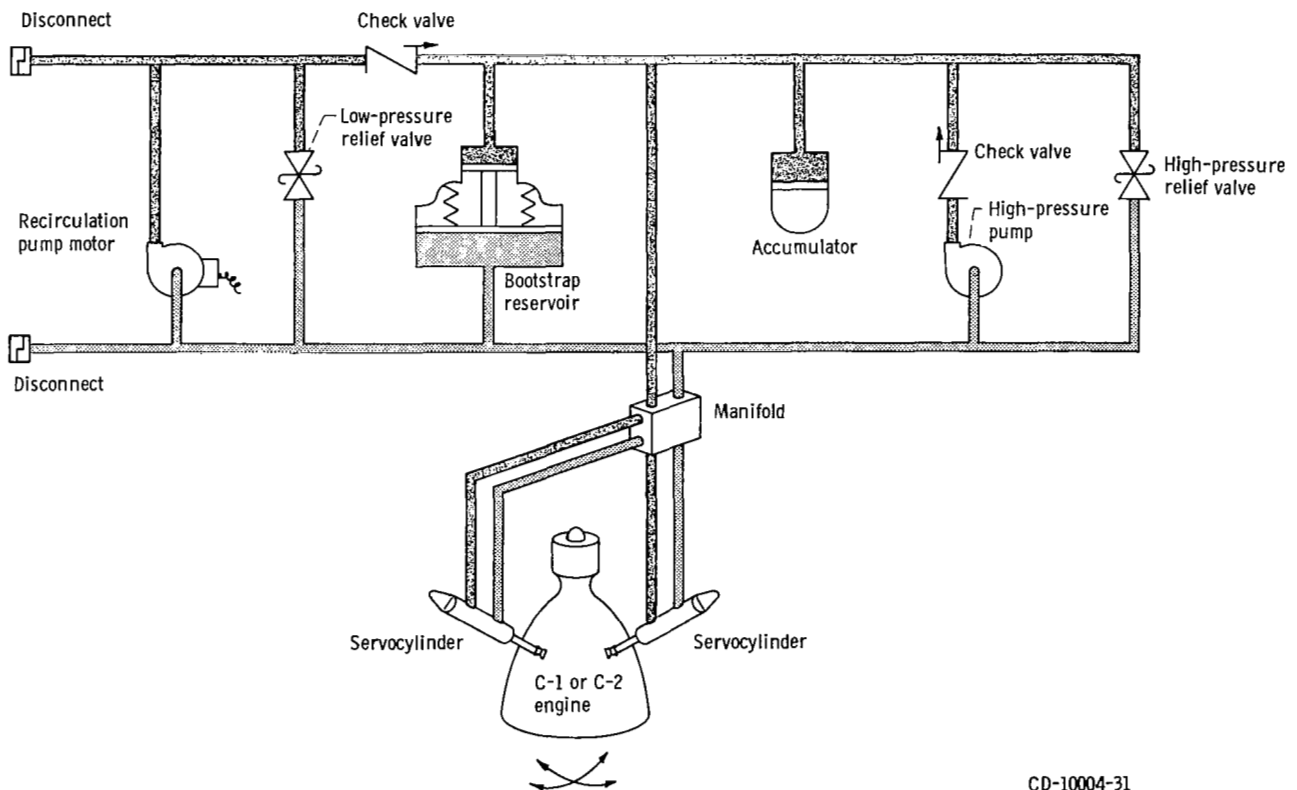
CD-9676

Figure V-35. – Atlas booster and sustainer hydraulic pump line pressure, AC-12.

CD-10004-31

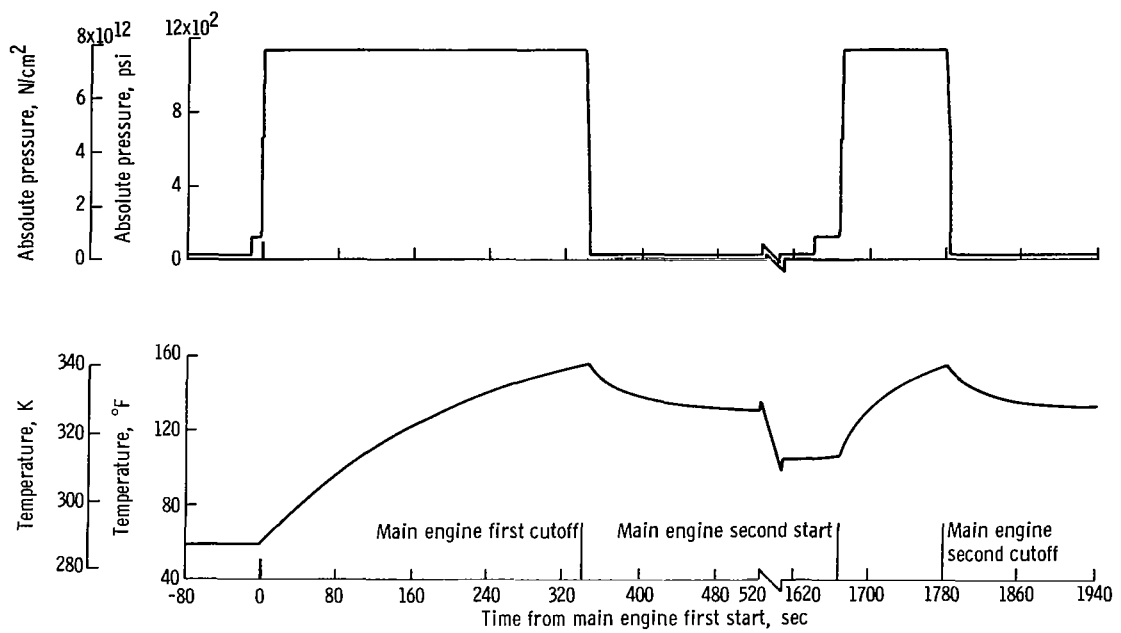Figure V-36. – Centaur hydraulic system, AC-12.

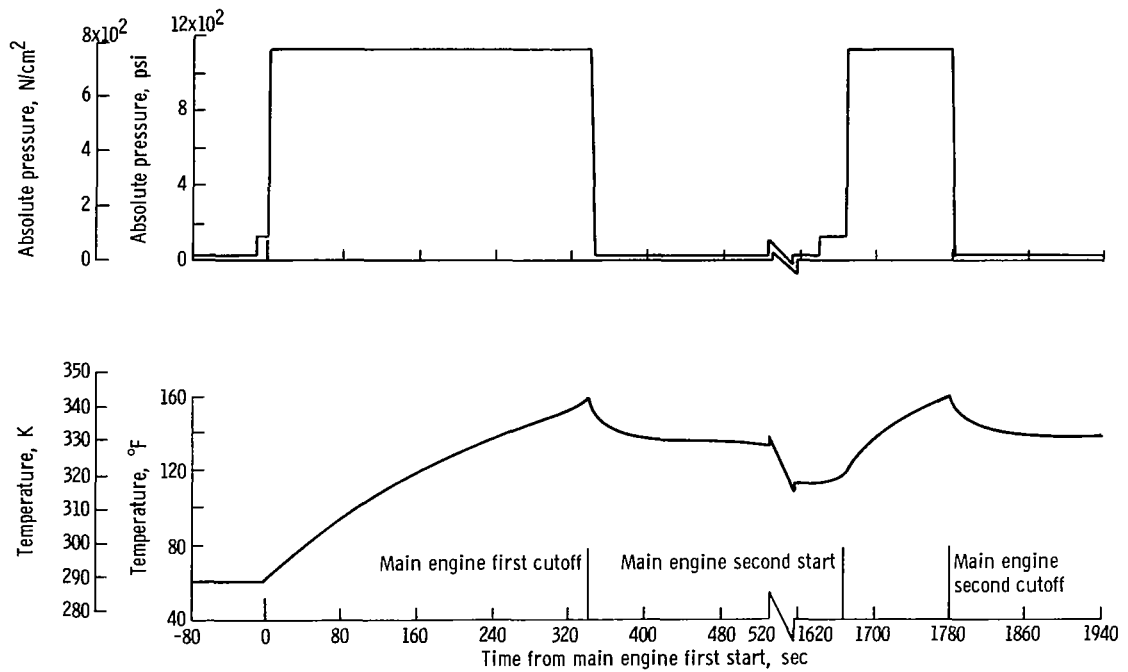Figure V-37. - C-1 engine hydraulic system pressure and temperature, AC-12.

Figure V-38. - C-2 engine hydraulic system pressure and temperature, AC-12.

84

VEHICLE STRUCTURES

by Robert C. Edwards, Charles W. Eastwood, Jack Humphrey, and Dana H. Benjamin

Atlas Structures

Atlas system description. - The Atlas vehicle structure included the basic tank and all bolt-on hardware. The propellant tanks provided the primary vehicle structure. These tanks were thin-walled pressure-stabilized sections of monocoque construction (see fig. V-39). They required a minimum pressure for various periods of flight in order to maintain structural stability. The structural strength of the tank, as a pressure vessel, determined the maximum allowable pressure in the propellant tanks.

The Atlas launcher assembly supported and balanced the vehicle in the vertical position prior to launch. This was accomplished by two holddown and release arms and by two auxiliary supports. (Fig. V-40 shows the launcher assembly.) At launch, the assembly restrained the vehicle to prevent release during Atlas engine thrust buildup. Pneumatic holddown cylinders applied the restraining force. This force prevented rotation of the release arms and rise of the vehicle. Bleed valves on the cylinders were opened at launch and caused the pneumatic pressure to decay thereby reducing the holddown force. When the restraining force decreased to a lower value than the net upward force, the vehicle began to rise. The movement of the vehicle initiated rotation of the holddown and release arms. A kick strut link on each arm engaged a fitting on the vehicle and transmitted force from the vehicle to the support pin retraction mechanism. After approximately 8.7 inches (22.1 cm) of vehicle rise, the pins were fully retracted and the mechanisms locked. The forces supplied by the vehicle through the kick struts were then applied directly to the arms to rotate them clear of the vehicle.

Atlas launcher transients. - The vehicle and its components experienced transient longitudinal and lateral oscillating loads transmitted through the kick struts by launcher mechanism forces at lift-off. Various components of the launcher were instrumented to monitor these loads.

The maximum kick strut loads and the maximum longitudinal oscillatory acceleration were measured and these data are compared with data from previous flights in table V-12. The maximum longitudinal oscillatory acceleration of the vehicle was 0.64 g's peak to peak. This value is about average for all recorded accelerations and is within the design allowable limit for the vehicle. The actual loads seen by the kick struts were slightly larger than loads recorded on previous flights.

Atlas tank pressure criteria. - The Atlas oxidizer tank structure was subjected to the highest bending loads between T + 60 and T + 90 seconds. Ullage pressure during that time was above the minimum required for resisting the maximum design loads (see

TABLE V-12. - LOADS ON LAUNCHER KICK STRUTS AT LIFT-OFF, AC-12

Flight	Maximum kick strut loads,				Loads determined by -	Longitudinal oscillatory acceleration (peak to peak), g's	Accelerometer location vehicle station
	B-1 strut		B-2 strut				
	lb	N	lb	N			
AC-12	32 600	144 900	30 980	137 800	Measure of kick strut spring deflection	0.64	1043
AC-9	27 850	123 800	27 250	121 000	Strain gages on kick struts	0.94	173
	30 100	133 800	30 100	133 800	Measure of kick strut spring deflection		
AC-7	31 200	138 800	29 600	131 600	Measure of kick strut spring deflection	0.56	1043
AC-8	29 000	128 900	30 000	133 400	Strain gages on kick struts	0.58	173
AC-10	28 000	124 400	25 600	113 800	Strain gages on kick struts	0.81	1043

fig. V-41). The least differential between minimum required and actual pressures occurred at T + 60 seconds. At that time, the oxidizer tank absolute pressure was 35.0 psi (24.1 N/cm^2). The minimum required tank absolute pressure, which includes design margins, was 34.5 psi (23.8 N/cm^2). The maximum allowable oxidizer tank pressure was most closely approached at T + 100 seconds. At this time, the absolute pressure was 33.0 psi (22.8 N/cm^2); the allowable maximum absolute pressure was 36.7 psi (25.3 N/cm^2).

The Atlas fuel tank pressure did not approach the maximum allowable or minimum required pressure during the booster and sustainer phase of flight (see fig. V-42).

Quasi-steady-state load factors. - A maximum acceleration of 5.62 g's was reached at booster engine cutoff which was within the ±3 sigma range (5.62 to 5.78 g's; see the appendix). Thus, the longitudinal or axial load factor was within the design limits.

Centaur Structures

Centaur system description. - The Centaur vehicle structure included the basic tank and all bolt-on hardware. The propellant tanks provided the primary vehicle structure. These tanks were thin-walled pressure-stabilized sections of monocoque construction (see fig. V-43). They required a minimum pressure for various periods of flight in order to maintain structural stability. The structural strength of the tank, as a pressure vessel, determined the maximum allowable pressure in the propellant tanks. The propellant tanks were vented as required during the flight to prevent excessive ullage pressures. (See the section PNEUMATIC SYSTEMS, Centaur.)

Centaur tank pressure criteria. - Maximum design loads were used to compute maximum allowable and minimum required tank pressures. Appropriate factors of safety were also included. The AC-12 flight pressure profile is compared with the design pressure profile in figure V-44. These pressure profiles are identical to the ones shown in the Centaur PNEUMATIC SYSTEMS section with pressure limits added. The tank locations and criteria which determined the maximum allowable and minimum required tank pressures during different phases of the flight are described in figure V-45.

The liquid-oxygen tank pressure was of concern only at booster engine cutoff (T + 142.3 sec) when the maximum allowable absolute pressure was at a minimum of 33.0 psi (22.7 N/cm^2). At this time, the actual absolute pressure, as shown in figure V-44(a), was 29.9 psi (20.6 N/cm^2). The liquid-oxygen tank pressure did not approach the minimum required during any period of the flight.

The strength of the liquid-hydrogen tank was governed by the capability of the conical section of the forward bulkhead to resist hoop stress. Thus, the differential pressure across the forward bulkhead determined the maximum allowable liquid-hydrogen-tank pressure. This allowable differential pressure was 26.8 psi (18.5 N/cm^2). The liquid-hydrogen-tank pressure reached a value near the allowable design maximum just prior to opening of the primary hydrogen vent valve at T + 68.9 seconds (see fig. V-44(a)). The maximum allowable absolute pressure was 26.8 psi (18.5 N/cm^2) plus the nose fairing internal absolute pressure of 2.4 psi (1.7 N/cm^2). Thus, the maximum allowable liquid-hydrogen-tank absolute pressure was 29.2 psi (20.1 N/cm^2). The actual liquid-hydrogen-tank absolute pressure at this time was 26.1 psi (18.0 N/cm^2).

The liquid-hydrogen-tank pressure also reached a value near the allowable design maximum prior to main engine second start at T + 1910 seconds and during the turn-around maneuver at T + 2335 seconds (see fig. V-44(d)). The liquid-hydrogen-tank absolute pressure at both these times was 26.2 psi (18.1 N/cm^2). Since the pressure on the exterior of the forward bulkhead was zero at these times, the maximum allowable tank absolute pressure was 26.8 psi (18.5 N/cm^2).

The liquid-hydrogen-tank pressure approached the minimum required pressure at the following times: prelaunch, launch, primary hydrogen vent valve opening, and nose fairing jettison.

(1) Prior to launch, the insulation panel pretensioning imposed local bending stresses on the liquid-hydrogen-tank cylindrical skin. The minimum required liquid-hydrogen-tank absolute pressure at this time was 19.0 psi (13.1 N/cm^2); the actual tank absolute pressure was 21.4 psi (14.8 N/cm^2) (see fig. V-44(a)).

(2) During the launch phase (T + 0 to T + 10 sec), the payload imposed compression loads on the forward bulkhead due to inertia and lateral vibration. The minimum required liquid-hydrogen-tank absolute pressure was 20.5 psi (14.2 N/cm^2) at T + 10 sec-

onds; at this time the actual tank absolute pressure was 22.9 psi (15.8 N/cm^2) (see fig. V-44(a)).

(3) Just after the primary hydrogen vent valve was opened at T + 68.9 seconds, the inertia and bending compression loads were critical at station 409.6 on the cylindrical skin. The minimum required liquid-hydrogen-tank absolute pressure was 20.5 psi (14.1 N/cm^2). The tank absolute pressure at this time was 21.4 psi (14.8 N/cm^2) (see fig. V-44(a)).

(4) At nose fairing jettison, the nose fairing exerted inboard radial loads at station 219. The minimum required tank absolute pressure at this time was 18.5 psi (12.8 N/cm^2); the tank absolute pressure was 20.3 psi (14.0 N/cm^2) (see fig. V-44(b)).

The maximum allowable differential pressure between the liquid-oxygen and liquid-hydrogen tanks was limited by the strength of the Centaur intermediate bulkhead. The liquid-oxygen-tank pressure must always be greater than the liquid-hydrogen-tank pressure to stabilize the bulkhead (prevent bulkhead reversal).

The maximum design allowable differential pressure across the intermediate bulkhead was 23.0 psi (15.9 N/cm^2). During pressurization of the liquid-oxygen tank, the actual differential was 19.9 psi (13.7 N/cm^2) at T + 214 seconds (see fig. V-44(b)).

The desirable minimum differential pressure across the intermediate bulkhead was 2.0 psi (1.4 N/cm^2). Before the primary hydrogen vent valve was opened at T + 68.9 seconds, the actual differential pressure across the intermediate bulkhead was 2.6 psi (1.8 N/cm^2) less a hydrostatic head pressure of 1.0 psi (0.7 N/cm^2), for a net differential pressure of 1.6 psi (1.1 N/cm^2) (see fig. V-44(a)). During main engine second burn at T + 1950 seconds, the differential pressure across the intermediate bulkhead was 2.9 psi (2.0 N/cm^2) (see fig. V-44(d)). During the turnaround maneuver at T + 2335 seconds, the differential pressure across the intermediate bulkhead was indicated to be only 0.2 psi (0.1 N/cm^2) (see fig. V-44(d)). It was anticipated that the differential pressure might be below the minimum design allowable during the turnaround maneuver. However, it was felt that the possibility of bulkhead reversal was slight, and if the bulkhead did reverse, there was little likelihood that the spacecraft would be subjected to a hazardous condition.

Vehicle Dynamic Loads

The Atlas-Centaur launch vehicle receives dynamic loading from several sources. The loads fall into three major categories: (1) external loads from aerodynamic and acoustic sources, (2) transients from engines starting and stopping and from the separation systems, (3) loads due to dynamic coupling between major systems.

Previous flights of the Atlas-Centaur have shown that these loads were within the structural limits established by ground test and model analysis. For this flight, there-

fore, only a limited number of dynamic flight measurements was made. With this amount of flight instrumentation, only a limited check of significant launch vehicle dynamic loads and local vibrations could be made. The instruments used and the parameters measured are tabulated as follows:

Instruments	Corresponding parameters
Low-frequency range accelerometer	Launch vehicle longitudinal vibration
Centaur pitch rate gyro	Launch vehicle pitch plane vibration
Centaur yaw rate gyro	Launch vehicle yaw plane vibration
Angle-of-attack sensor	Vehicle aerodynamic loads
High-frequency accelerometers	Local spacecraft vibration

Launch vehicle longitudinal vibrations as measured on the Centaur forward bulkhead are shown in figure V-46. The frequency and amplitude of the vibrations measured on this flight are compared with four other representative flights.

During launcher release, longitudinal vibrations were excited. (See the previous discussion of Atlas launcher transients, p. 85.) The amplitude and frequency of these vibrations were similar to those seen during other launches. Atlas intermediate bulkhead pressure fluctuations were the most significant effects produced by the launcher-induced longitudinal vibrations. The peak pressure fluctuations computed from these vibrations were 4.9 psi (3.4 N/cm^2). Since the bulkhead static differential pressure measured at this time was 9.0 psi (6.2 N/cm^2), the calculated minimum differential pressure was 4.1 psi (2.8 N/cm^2). The minimum design allowable differential pressure across the bulkhead was 2.0 psi (1.4 N/cm^2).

During Atlas flight between T + 69 and T + 142 seconds, intermittent longitudinal vibrations of 0.11 g's, at a frequency of 11 hertz were observed on the forward bulkhead. These vibrations are believed to be caused by dynamic coupling between structure, engines, and propellant lines (commonly referred to as "POGO"). The amplitude and frequency of the vibrations were similar for the five vehicles, shown in figure V-46, because the controlling parameters have not changed from flight to flight. These vibrations at the measured amplitudes did not produce significant vehicle loads (see ref. 4).

During booster engine thrust decay, short duration transient longitudinal vibrations of 0.48 g's at a frequency of 13 hertz were observed. The analytical models did not indicate significant structural loading due to these vibrations.

During the boost phase of flight, the vehicle vibrates in the pitch and yaw axis as an integral unit at all its natural frequencies. Previous analyses and tests have defined these natural frequencies or modes and the shapes which the vehicle assumes when the

modes are excited. The rate gyros on the Centaur provide data for determining the deflection of these modes. The maximum first mode deflection was seen in the pitch plane at T + 136 seconds (fig. V-47). The deflection was less than 3 percent of the allowable deflection. The maximum second mode deflection was seen in the yaw plane at T + 40 seconds (fig. V-48). The yaw deflection was less than 12 percent of the allowable deflection.

Predicted angles of attack were based on upper wind data obtained from a balloon released near the time of launch. Vehicle bending moments were calculated by using predicted angles of attack, engine gimbal angle data, vehicle weights, and vehicle stiffnesses. These moments were added to axial load equivalent moments and to moments resulting from random dispersions. The most significant dispersions considered were uncertainties in launch vehicle performance, vehicle center-of-gravity offset, and upper atmosphere wind. The total equivalent predicted bending moment (based on wind data) was divided by the design bending moment allowable to obtain the predicted structural capability ratio, as shown in figure V-49. This ratio is expected to be greatest between T + 52 and T + 80 seconds due to high aerodynamic loads during this period. The maximum structural capability ratio predicted for this period was 0.80.

Differential pressures were measured on the nose fairing cap in the pitch plane and the yaw plane. Total pressure was computed from a trajectory reconstruction. Angles of attack were computed from these data and are compared with predicted angles of attack in figures V-50 and V-51. Since the actual angles of attack were within the expected dispersion values, it follows that the predicted structural capability ratio of 0.80 was not exceeded.

Local shock and vibration were measured by four spacecraft accelerometers. Three of these accelerometers were time shared with each other. Since most of the transients occurring in flight were missed by these time-shared accelerometers, they were not included as part of the data presented.

A summary of the most significant shock and vibration levels measured by the continuous accelerometer is shown in table V-13. The steady-state vibration levels were highest near lift-off, as expected. The maximum level of the shock loads (13 g's) occurred at Atlas-Centaur separation. These shock levels are of short duration (0.15 sec) and do not provide significant loads. An analysis of the data indicates that the levels were well within spacecraft qualification levels.

TABLE V-13. – COMPARISON OF AC-12 AND AC-10 MAXIMUM

SHOCK AND VIBRATION LEVELS

[Spacecraft accelerometer location: retromotor attachment 1; z-axis
sensitivity; 790-Hz analysis band.]

Flight event	AC-12		AC-10	
	Maximum g's single amplitude	Predominant frequency, Hz	Maximum g's single amplitude	Predominant frequency, Hz
Launch	2.2	150 to 450	0.456	140
Booster engine cutoff	1.2	17	0.8	11
Booster jettison	0.46	16	0.5	16
Insulation panel jettison	10.1	600 to 700	10	700
Nose fairing jettison	0.49	20	1.4	32
Atlas-Centaur separation	13	600 to 700	12	600
Main engine first start	0.5	20 to 21	0.38	20
Main engine first cutoff	0.95	22	1.14	33
Main engine second start	0.66	20 to 22	-----	---
Main engine second cutoff	0.97	24	-----	---
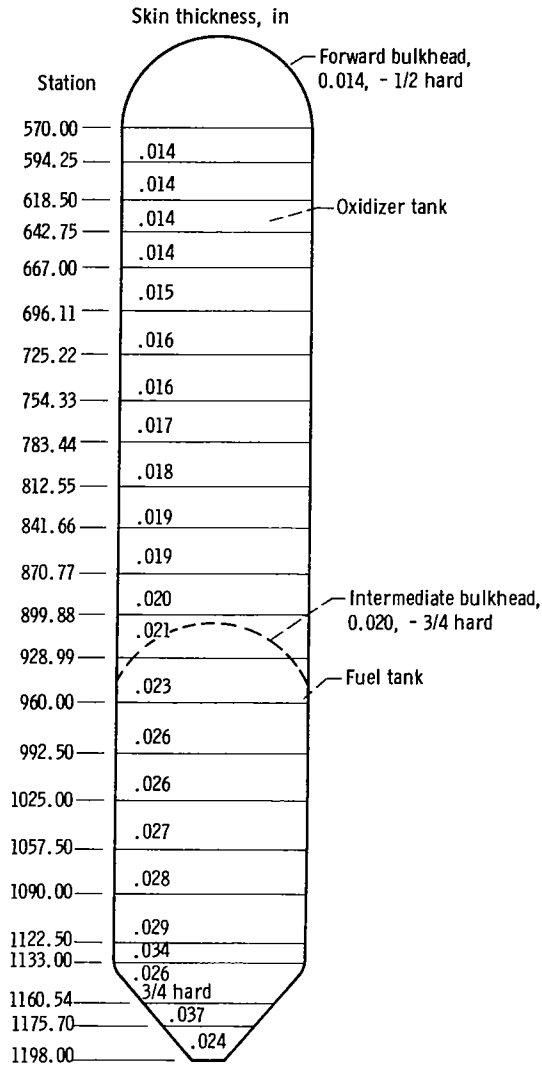
Figure V-39. - Atlas propellant tanks, AC-12. (Unless noted otherwise, all material is 301 extra-full-hard stainless steel.)
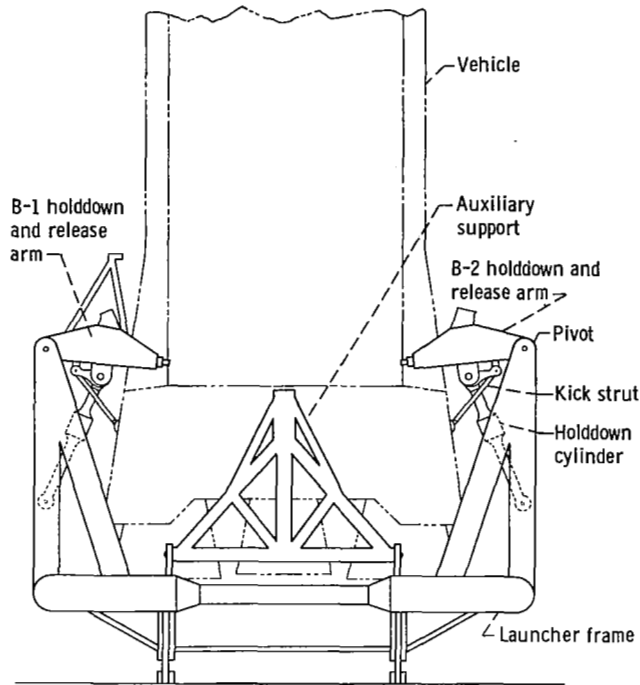
Figure V-40. - Atlas launcher assembly, AC-12.
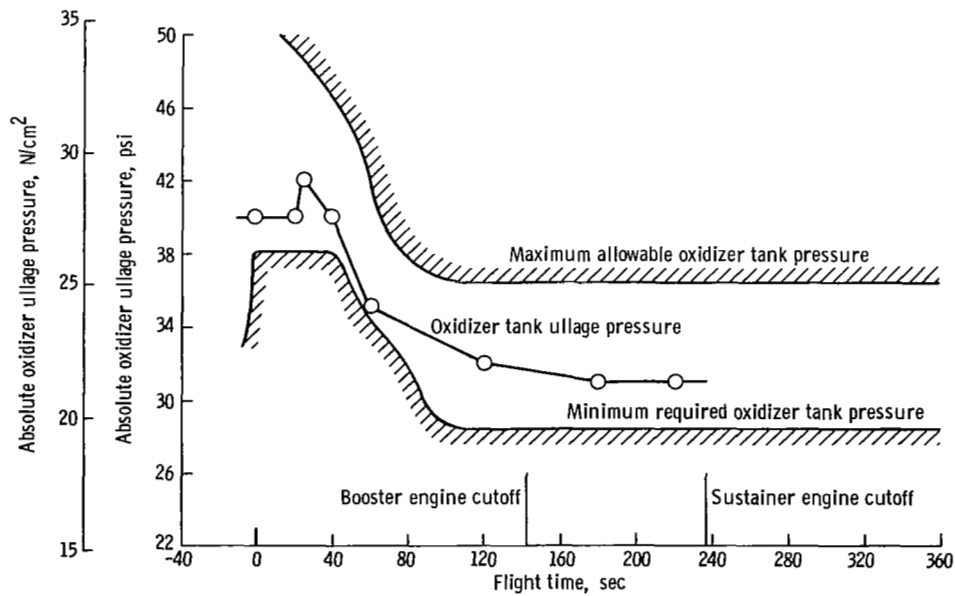
Figure V-41. - Atlas oxidizer tank pressure, AC-12.
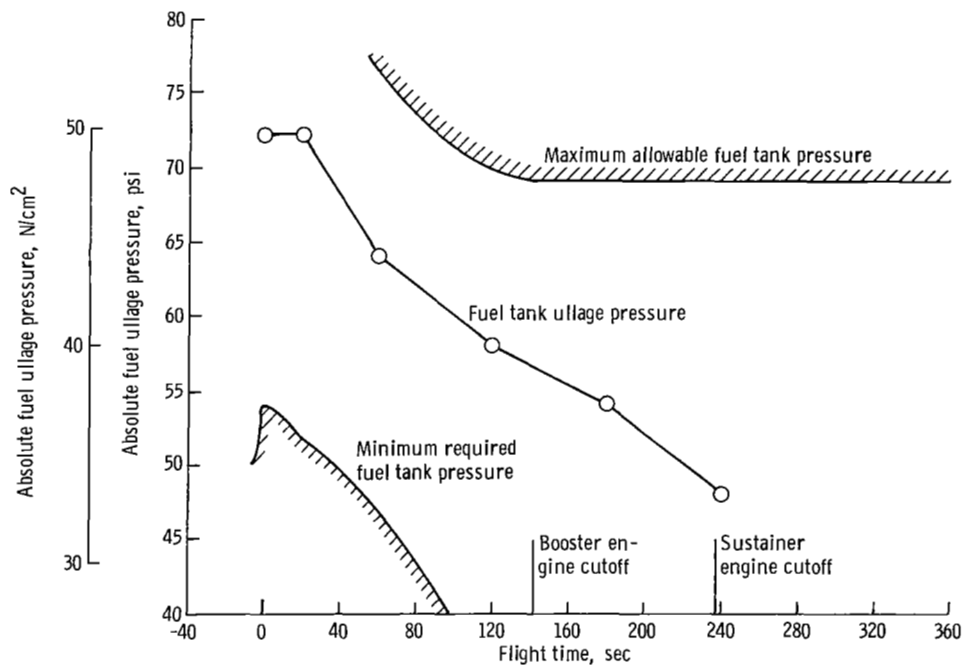
Figure V-42. - Atlas fuel tank pressure, AC-12.

Skin thickness, in.
Forward bulkhead

—0.016 to 0.010, 1/2 hard
—0.016 to 0.012, extra hard
—0.016 to 0.010, 1/2 hard

Station 218.90 —

Fuel tank

—0.014, extra hard

Intermediate bulkhead
—0.026 to 0.013, 1/2 hard

Station 412.72 —

Oxidizer tank

—0.018, 3/4 hard

—0.020, 3/4 hard

CD-9782-31
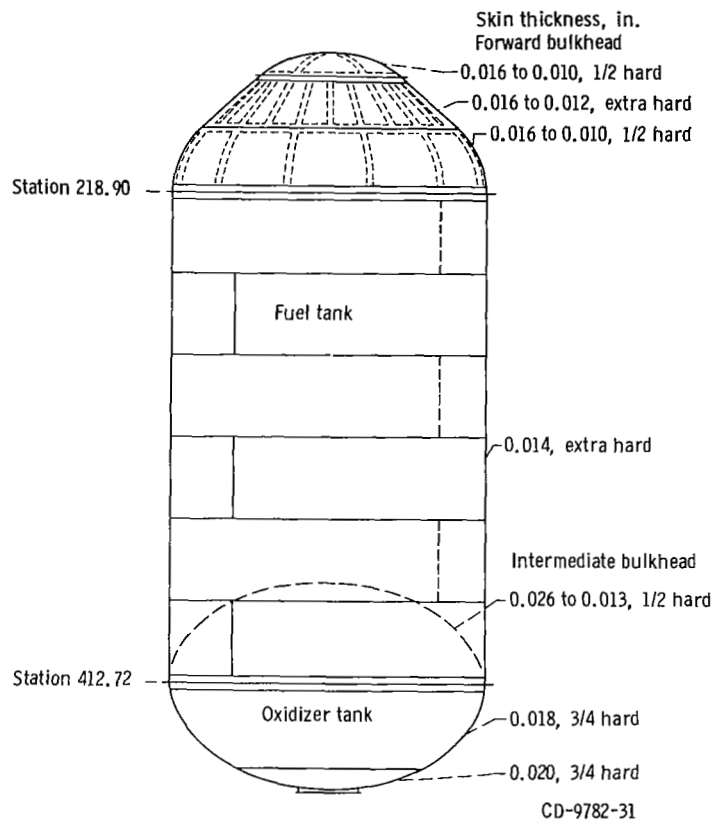
Figure V-43. – Centaur propellant tanks, AC-12. (All material 301 stainless steel of hardness indicated.)
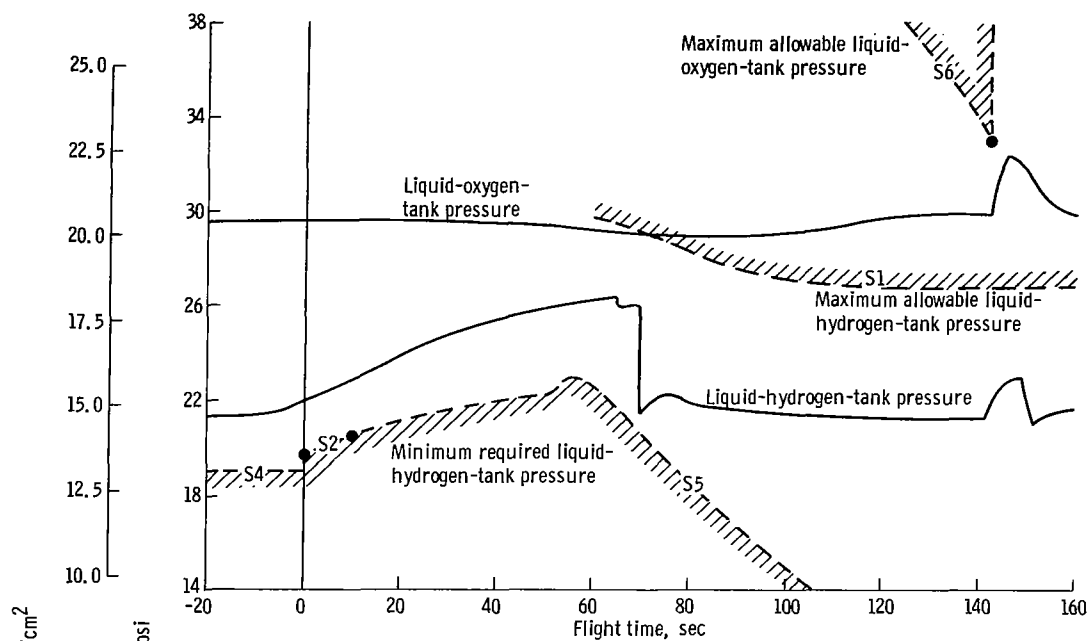
(a) Time, -20 to 160 seconds.
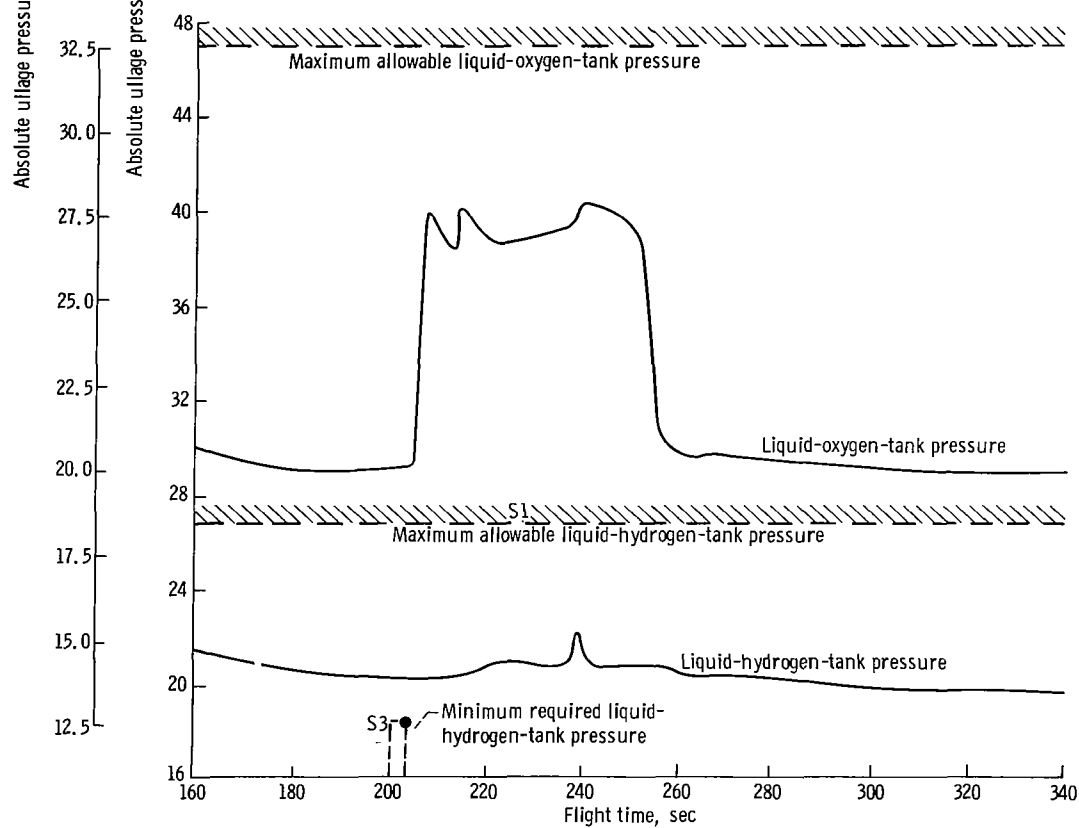
(b) Time, 160 to 340 seconds.

Figure V-44. - Centaur tank pressure profiles, AC-12. (S1, S2, etc. indicate tank locations and criteria which determine allowable pressure (see fig. V-45).

96
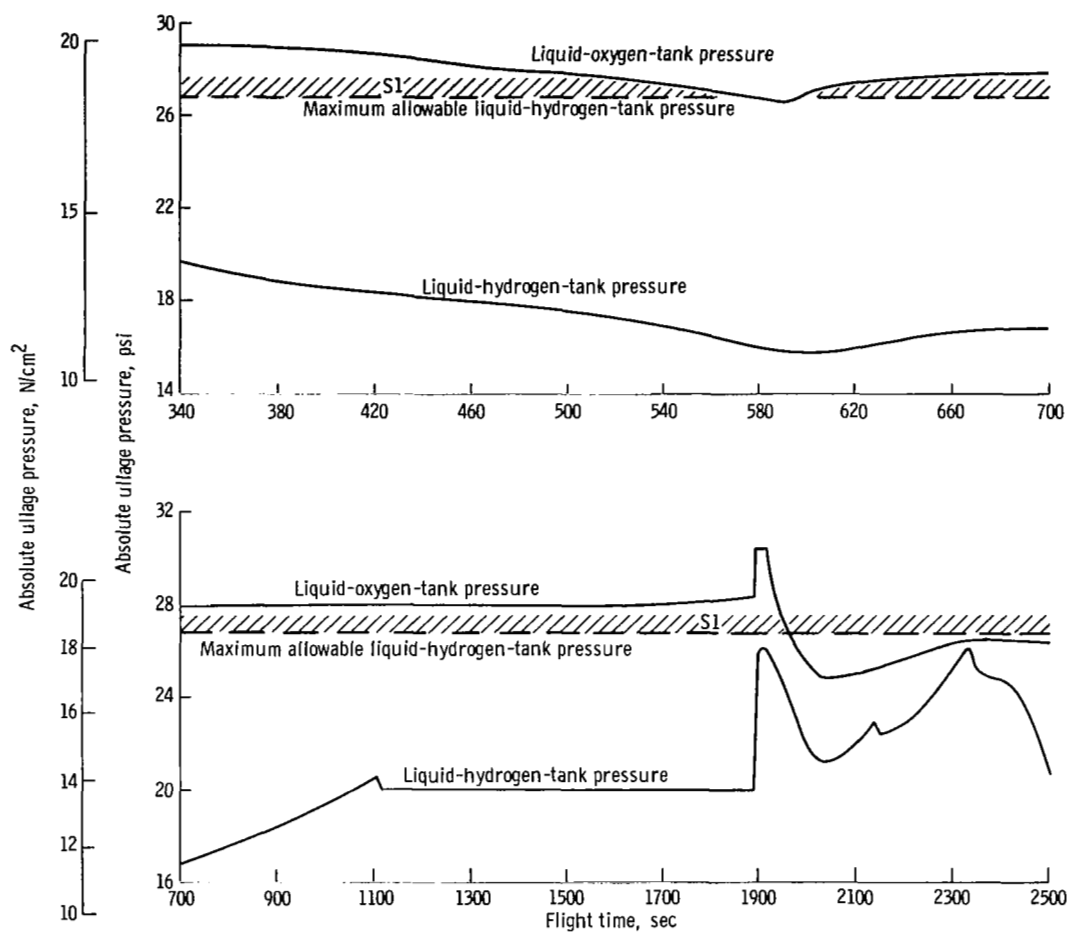
(d) Time, 700 to 2500 seconds.

Figure V-44. - Concluded.
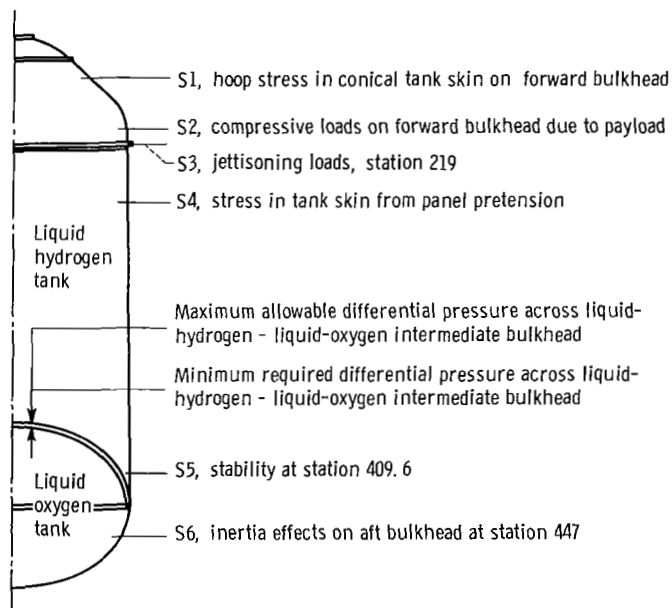
Figure V-45. - Tank locations and criteria which determine allowable pressures, AC-12.

S1, hoop stress in conical tank skin on forward bulkhead

S2, compressive loads on forward bulkhead due to payload

S3, jettisoning loads, station 219

S4, stress in tank skin from panel pretension

Liquid hydrogen tank

Maximum allowable differential pressure across liquid-hydrogen – liquid-oxygen intermediate bulkhead

Minimum required differential pressure across liquid-hydrogen – liquid-oxygen intermediate bulkhead

S5, stability at station 409. 6

Liquid oxygen tank

S6, inertia effects on aft bulkhead at station 447

Figure V-46. - Comparison of longitudinal vibrations for Atlas-Centaur flights. Length of bars indicates duration of vibration.
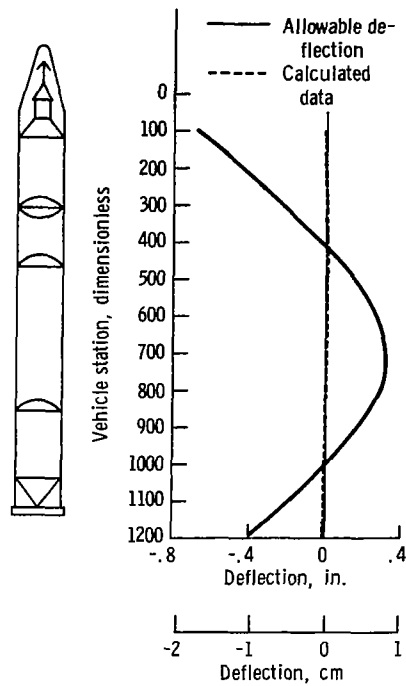
Figure V-47. - Maximum pitch plane first bending mode amplitudes at T + 136 seconds, AC-12.
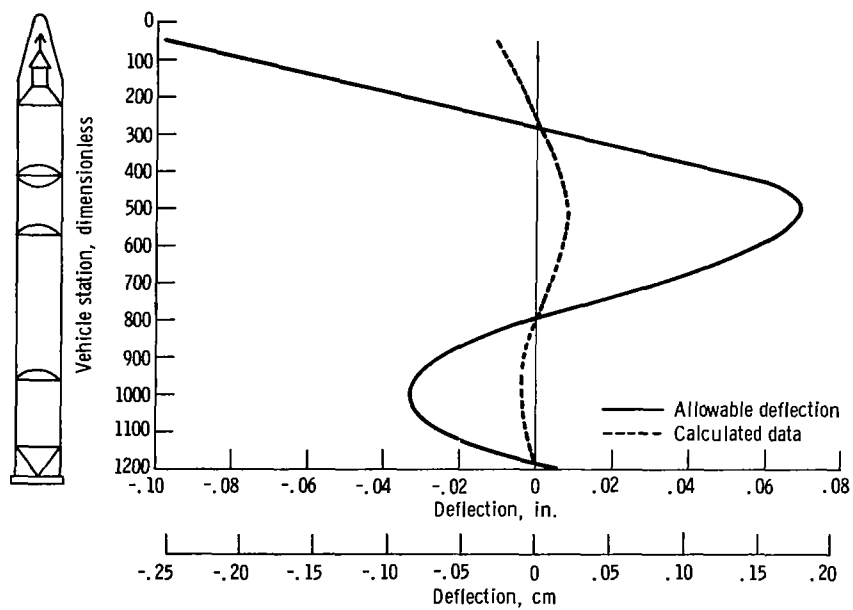
Figure V-48. - Maximum yaw plane second bending mode amplitudes at T + 40 seconds, AC-12.

(a) Most sensitive stations.
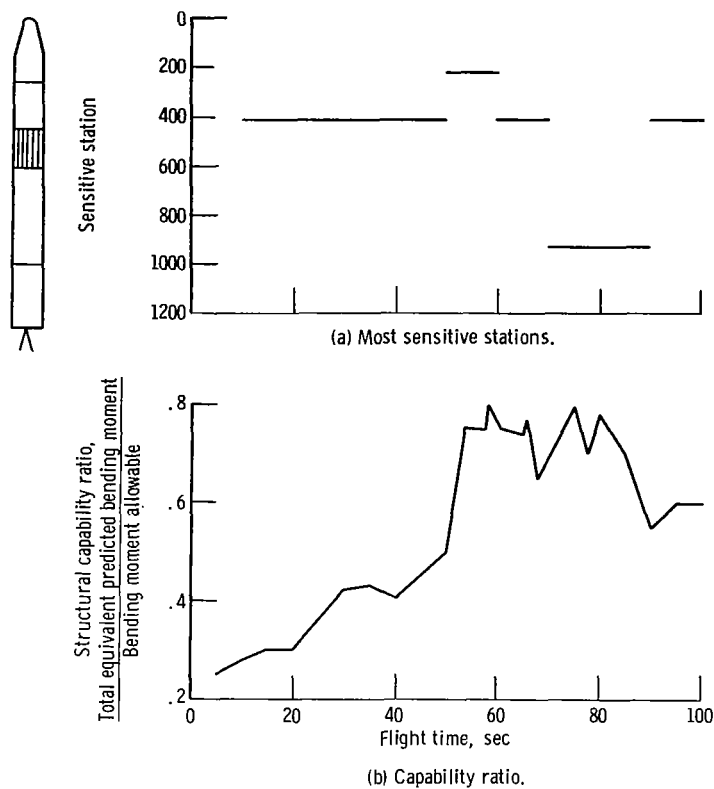
(b) Capability ratio.

Figure V-49. - Maximum predicted structural capability ratio during aerodynamic loading, AC-12.
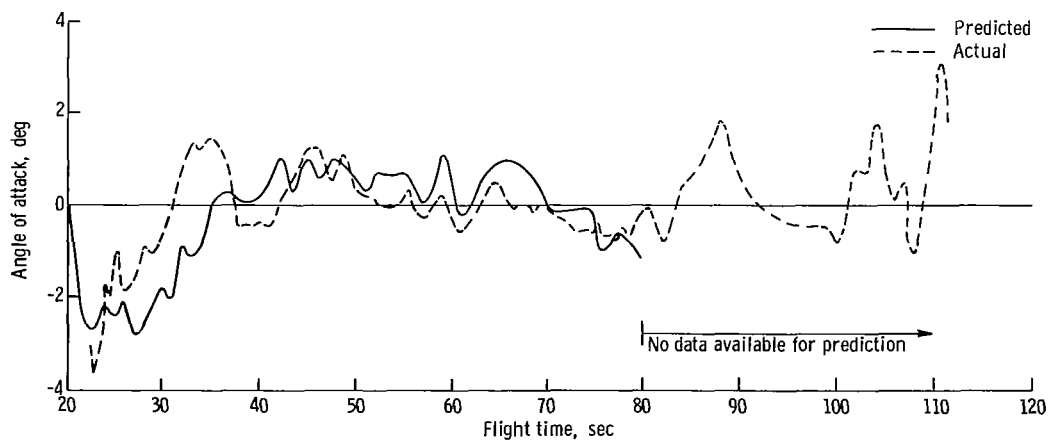
Figure V-50. - Predicted and actual pitch angles of attack, AC-12.
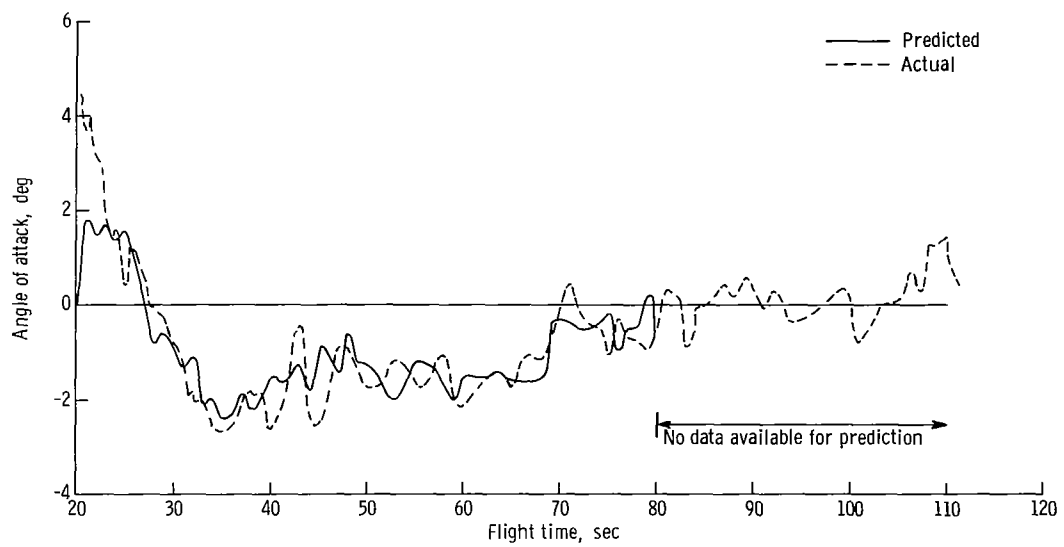
Figure V-51. - Predicted and actual yaw angles of attack, AC-12.

SEPARATION SYSTEMS

by Thomas L. Seeholzer

Stage Separation

System description. - The Atlas-Centaur flights required systems for the staging of (1) Atlas and Centaur and (2) Centaur and the Surveyor spacecraft.

Atlas-Centaur staging, as shown in figure V-52, was accomplished by a flexible, linear, shaped charge which cut the interstage adapter circumferentially near its forward end. The Atlas and interstage adapter were then separated from Centaur by firing the retrorockets on the Atlas approximately 0.1 second after shaped-charge firing.

The Surveyor spacecraft was separated from Centaur by actuation of three pyro-technically operated pin-puller latches mounted on the forward payload adapter, as shown in figure V-53. Separation force was provided by three mechanical spring assemblies, each having a 1-inch (2.54-cm) stroke, mounted adjacent to each separation latch on the forward adapter.

Atlas-Centaur separation system performance. - Vehicle staging was initiated by the firing of the shaped charge at T + 239.6 seconds which severed the interstage adapter at station 413. The eight retrorockets mounted around the aft end of the Atlas fired 0.1 second later to decelerate the Atlas and provide separation from the Centaur. Accelerometer and other recorded data indicated that all eight retrorockets ignited.

The displacement gyros indicated that the Atlas rotated 0.41° about the yaw axis at the time it cleared the Centaur. The resulting horizontal motion at the forward end of the interstage adapter was 4.1 inches (10.4 cm) along the x-x axis. The total clearance available along this axis was about 31 inches (78.7 cm).

The pitch rate gyros indicated 0.18° rotation about the pitch axis by the time Atlas cleared the Centaur. The resulting vertical motion at the forward end of the interstage adapter was approximately 1.8 inches (4.57 cm). Motion in the pitch plane was more critical than in the yaw plane. Only 11 inches (28.0 cm) clearance were available along the y-y axis.

Spacecraft separation system performance. - The Surveyor III was separated from Centaur at T + 2093.3 seconds. This event was verified by the Pretoria tracking station. Data from the extensometers located on the separation spring assemblies indicated all three separation latches actuated within 2 milliseconds of each other. The three jettison spring assemblies were calibrated, as shown in figure V-54. These springs yielded approximately identical data for stroke against time, as shown in figure V-55. Separation was successful and the separation springs produced forward motion with no significant spacecraft rotation.

103

Jettisonable Structures

System description. - The Atlas-Centaur vehicle also used jettisonable structures consisting of hydrogen tank insulation panels, a nose fairing, and related separation systems.

The hydrogen tank insulation was made up of four fiberglass honeycomb panels bolted together along the longitudinal axis to form a cylindrical cover over the Centaur tank. The panels were tied circumferentially, at their aft end by a metal ring to the Centaur vehicle. At the forward end a circumferential Teflon and fiberglass cloth seal connected the panels to the base of the nose fairing at station 219.

The four insulation panels were separated by firing flexible, linear, shaped charges located at the forward, aft, and longitudinal seams. After shaped-charge firing, the panels were forced to rotate about hinge points by (1) center-of-gravity offset, (2) in-flight purge pressure, and (3) elasticity of the panels due to preload hoop tension. Each panel was hinged about two points located on the interstage adapter (figs. V-56 and V-57). After approximately 45° of rotation, the panels were freed from the Centaur vehicle.

The nose fairing was a fiberglass honeycomb structure consisting of a cylindrical section approximately 6 feet (1.83 m) long bolted to a conical section approximately 16 feet (4.87 m) long. It was assembled in two jettisonable halves with the split line along the x-x axis, as shown in figure V-58. During the boost phase of flight (0 to T + 143 sec), the nose fairing was subjected to bending loads, axial loads, and high temperatures, as the vehicle passed through the atmosphere. Thermal protection, in the form of a subliming agent called Thermolag, was applied to both cone and cylindrical sections of the nose fairing in order to maintain necessary strength at high temperatures. The aft circumferential connection to the Centaur tank was severed by firing of a flexible, linear, shaped charge, and the nose fairing split line was opened by release of eight pyrotechnically operated pin-puller latches (fig. V-58). The nose fairing was then jettisoned by nitrogen gas thrusters located in the forward end, one in each fairing cone half. The thrusters, when fired, forced the fairing halves to pivot outboard around their respective hinge points. After approximately 35° rotation, the fairings separated from the Centaur vehicle.

Insulation panel separation system performance. - Flight data indicated that the four insulation panels were jettisoned satisfactorily. The flexible, linear, shaped charge severed the forward, aft, and longitudinal seams of these panels. Firing of the shaped charge occurred at T + 176.156 seconds. At 35° of panel rotation, breakwire transducers attached to one hinge arm of each panel provided event time data (see fig. V-57). Since these data were monitored on a commutated channel, the panel 35° position event times in the following table are mean times:

Panel 35° rotation position event time		
Panel location, quadrant	Instrumented hinge arm, quadrant	Event mean time, sec
I - II	I	T + 176. 57
II - III	III	T + 176. 64
III - IV	III	T + 176. 59
IV - I	I	T + 176. 62

Panel rotation average velocities, as determined from the data, were approximately 73 to 85 degrees per second compared with 85 degrees per second on AC-9 and 79 to 81 degrees per second on the AC-7 flight.

Nose fairing separation system performance. - The nose fairing pyrotechnically operated unlatching mechanisms fired at T + 202. 49 seconds. At T + 202. 9 seconds, the thruster bottle discharge valves fired and nose fairing separation from the Center vehicle started. Disconnect pins in the electrical connectors, which separate at fairing jettison, provided data indicating approximately 3° of fairing rotation. The mean time of this event for each fairing half as determined from the commutated data was T + 203. 01 seconds.

Spacecraft compartment pressure decayed in a normal manner from sea level value at launch to approximately zero by T + 120 seconds. The data indicated that the compartment pressure remained at zero throughout nose fairing separation with no pressure surge at thruster bottle discharge.
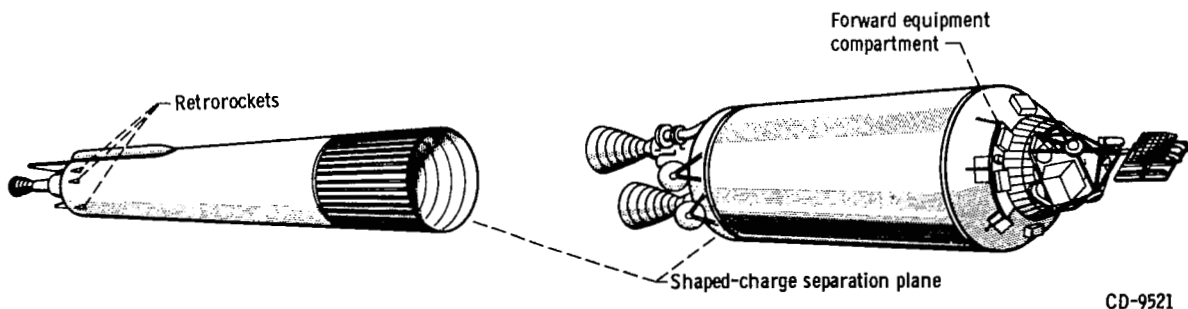
Figure V-52. - Atlas-Centaur separation system, AC-12.

Adapter forward
plane station 128

Spacecraft
electrical
disconnect

+x

+y

Mast

I

II   III

IV

Spacecraft
adapter

-y   -x

Ballast

Separation latch
(three places)

Separation springs
(three places)

Retractable
pin

Clevis

Spacecraft
attachment
fitting

Direction of
spacecraft
separation

Adapter
flange

Pyrotechnic pin
retraction unit
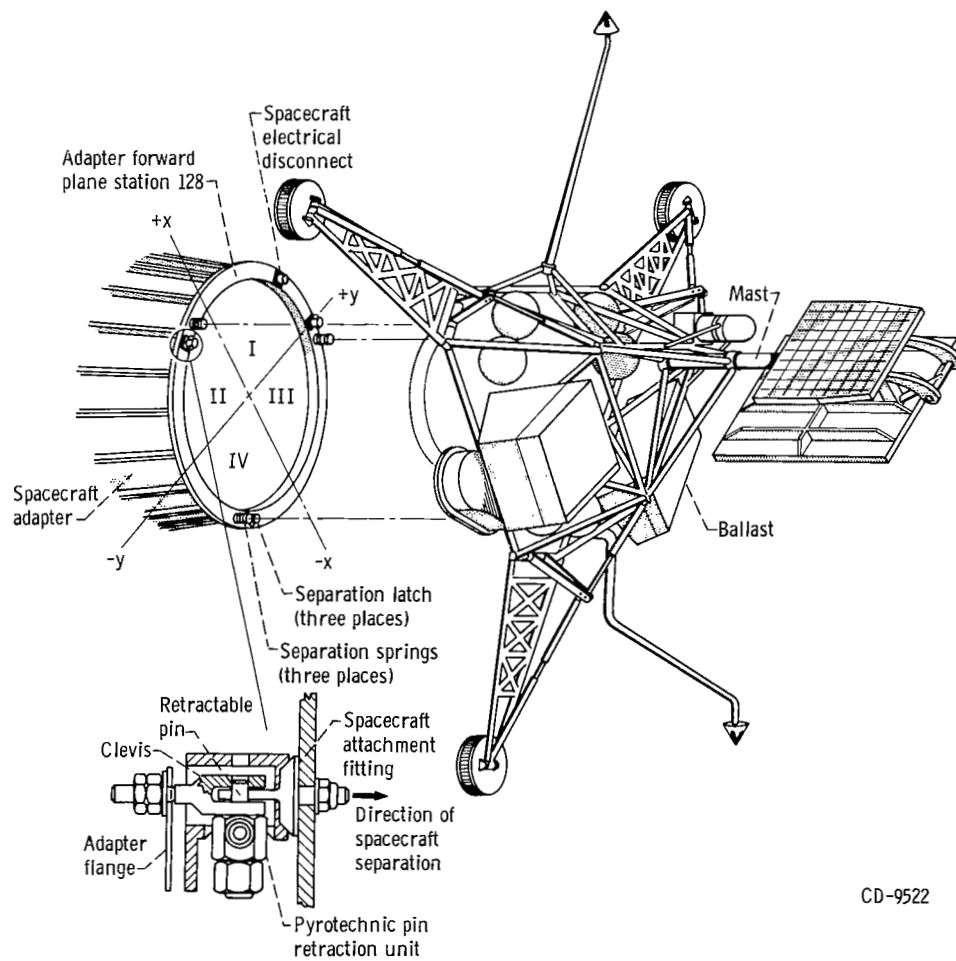
CD-9522

Figure V-53. – Centaur-Surveyor separation system, AC-12.
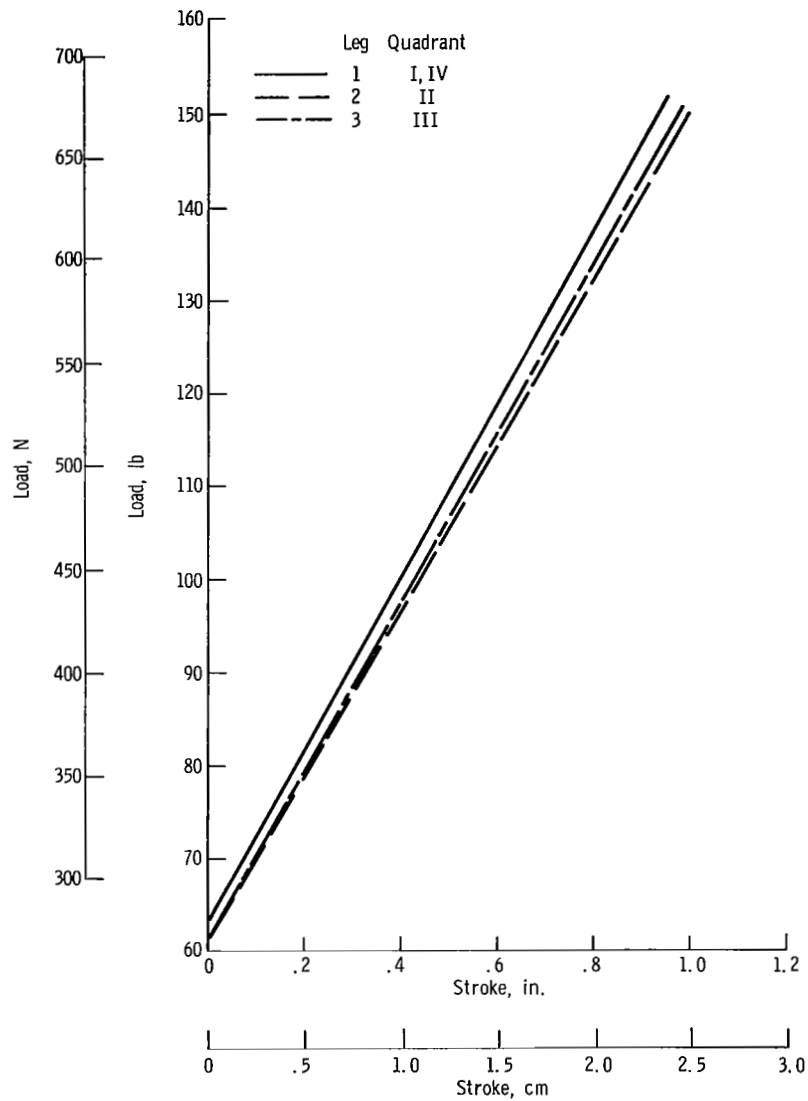
Figure V-54. – Surveyor jettison springs calibration, AC-12.
Stroke is from spring fully extended position.
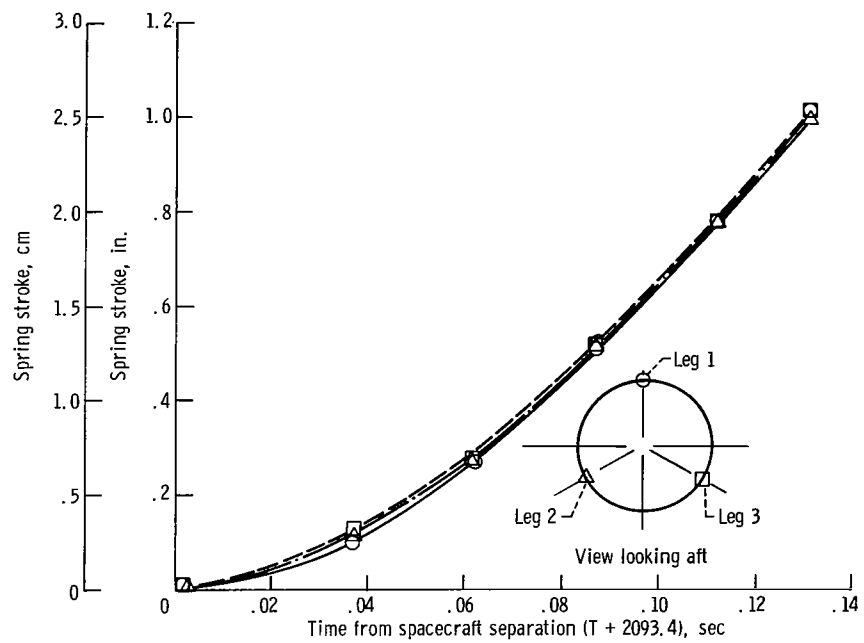
Figure V-55. – Centaur-Surveyor separation spring motion, AC-12. Stroke is from spring compressed position.

y axis

z axis

Quadrant I

Quadrant IV

x axis

-x axis

Quadrant II

Quadrant III

Hinge arm

-y axis

Hinge fitting
(typical eight
places)

Flexible, linear, shaped charge

Longitudinal seam shaped-charge installation
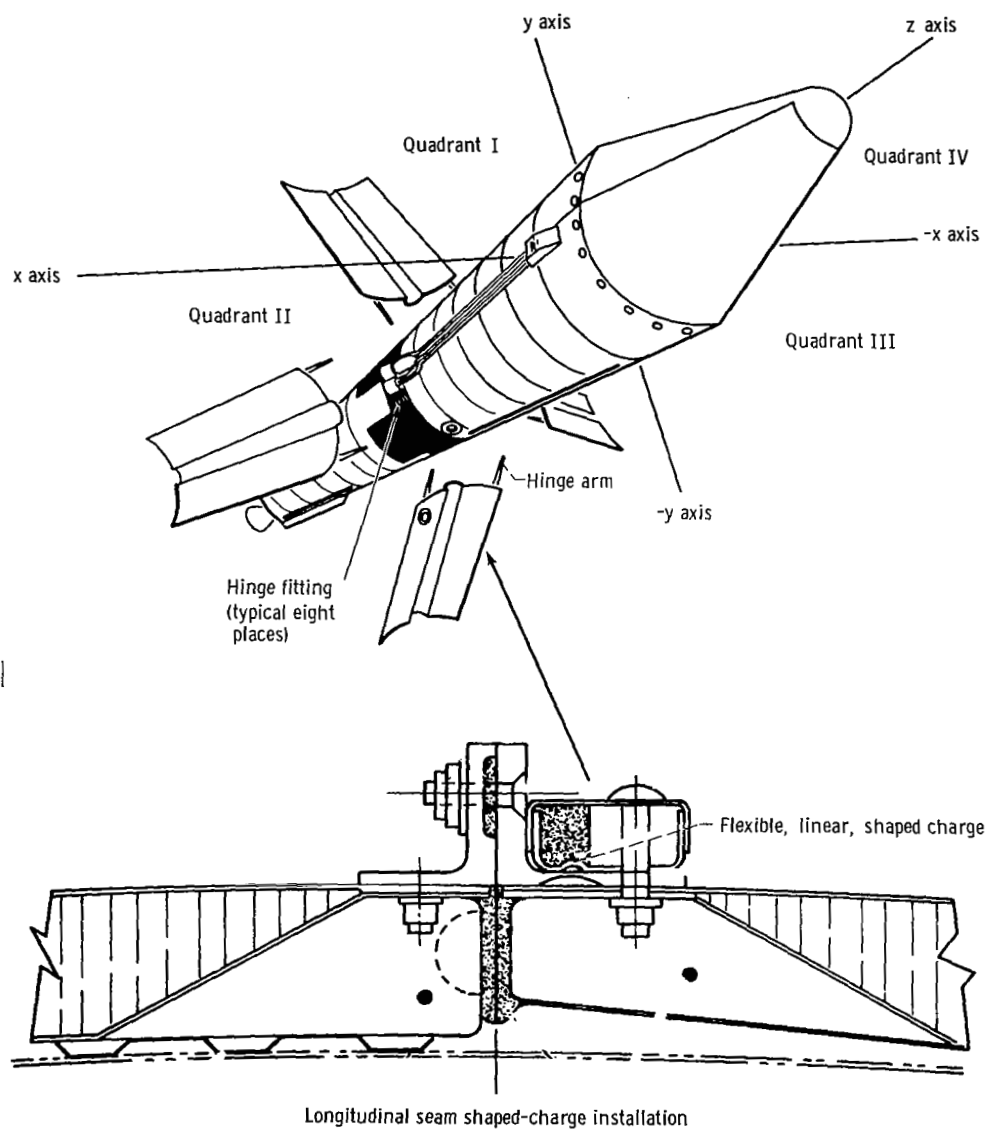
Figure V-56. - Hydrogen tank insulation jettison system, AC-12.

109

Section A-A

Four insulation
panel sensing
wires

A

Typical
four
hinges

A

9734-S
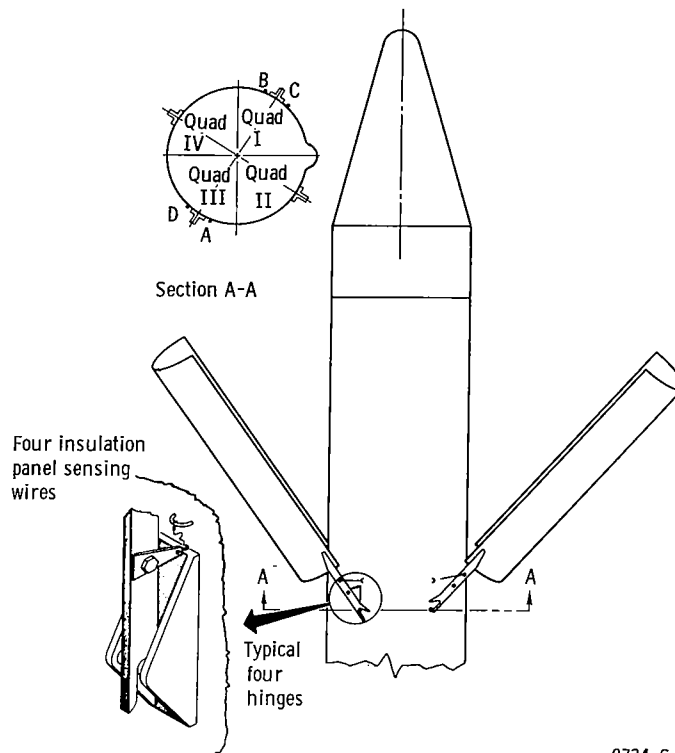
Figure V-57. - Insulation panel breakwire locations, AC-12.

+y axis

Nitrogen gas thrusters (two)

Station 219,
shaped charge

Quadrant IV

Quadrant I

+x axis

Explosive pin puller latches (eight)

-x axis

Hinge point

-y axis

Quadrant III

Quadrant II

Figure V-58. - Nose fairing jettison system, AC-12.

ELECTRICAL SYSTEMS

by John M. Bulloch and James Nestor

Power Sources and Distribution

Atlas system description. - The Atlas power requirements were supplied by a main power battery, two range safety command vehicle destruct system batteries, and a 400-hertz rotary inverter. Transfer of the Atlas electrical load from the external ground power supply to internal battery was accomplished by the main power changeover switch at T - 2 minutes. (See fig. V-59 for the system block diagram.)

Atlas system performance. - The Atlas main power battery supplied the requirements of all loads at normal voltage levels. The battery voltage was 28.2 volts at lift-off. It rose to 28.5 volts at sustainer engine cutoff, then dropped to a momentary low of 27.1 volts at retrorocket firing. This voltage profile was normal.

The rotary inverter, supplying the airborne 400 hertz power, operated within established voltage and frequency parameters. The voltage at lift-off was 115.3 volts. It reached a maximum of 115.6 volts at booster engine cutoff. The inverter frequency was 401.5 hertz shortly after startup at T - 2:30 minutes, increased to 402.2 hertz at lift-off, and rose to 402.6 hertz at the end of the programmed Atlas flight. The gradual rise in frequency is characteristic for the Atlas inverter. The required difference range of 1.3 to 3.7 hertz between Atlas and Centaur inverter frequencies was adequately maintained throughout the Atlas powered flight to avoid generation of undesirable beat frequencies in the autopilot system. If a beat frequency occurred in resonance with the "slosh" or natural frequencies of the vehicle, false commands could be given to the autopilot, resulting in possible degradation of vehicle stability.

Centaur system description. - The Centaur electric power system included three separate subsystems, powered by a main battery, two redundant range safety command (vehicle destruct) system batteries, and two pyrotechnic system batteries. A three-phase 400-hertz solid-state inverter was used to provide alternating current in the main power subsystem. This subsystem also included a power changeover switch which functioned to transfer the Centaur electrical system 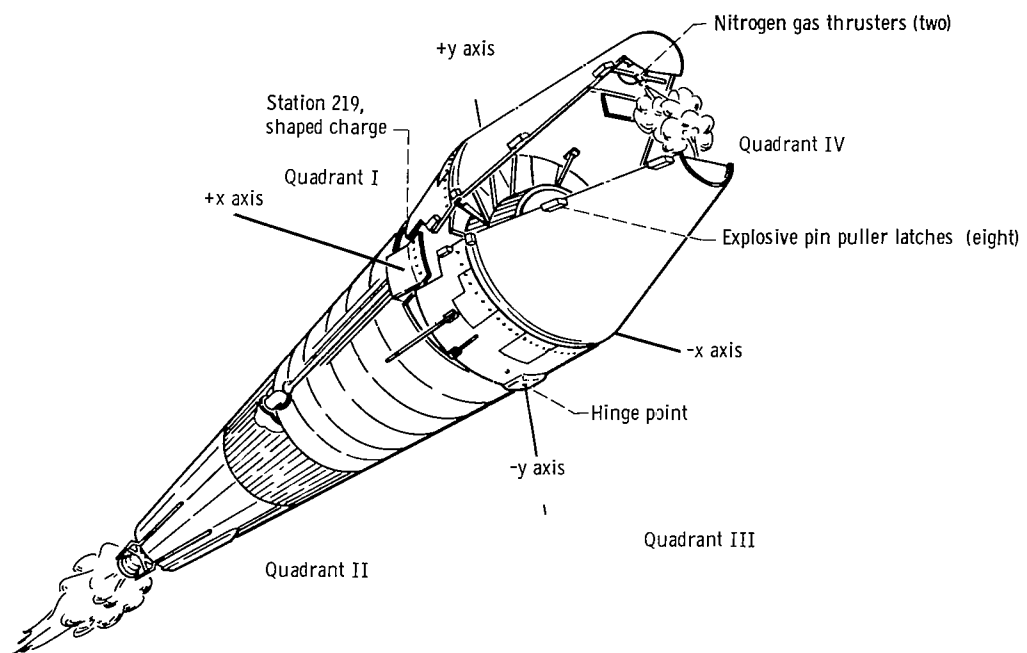to internal power at T - 4 minutes, and to turn off all systems except telemetry and tracking at approximately 100 seconds after completion of retrothrust.

Centaur system performance. - The Centaur electric system voltage and currents were normal at lift-off and satisfactorily supplied power to all loads throughout the flight.

The main battery voltage was 28.4 volts at lift-off. A low of 27.7 volts was recorded during the main engine first start sequence and a high of 28.5 volts was reached during the coast phase. The voltage decreased to 28.3 volts at main engine second start and recov-

ered to 28.8 volts by final power turnoff.

Main battery current was 44 amperes at lift-off. The maximum current was 63 amperes at main engine first and second starts. The main battery current profile during flight was consistent with data obtained during ground test and is shown in figure V-60.

Reliability of the pyrotechnic system operation had been improved by providing for squib firing by redundant relays. Both pyrotechnic system battery voltages were 35.7 volts at lift-off. Minimum specification limit is 34.7 volts. Proper operation of the pyrotechnic subsystem was verified by the successful jettison of the insulation panels and nose fairing.

Performance of the range safety command (vehicle destruct) subsystem batteries was satisfactory, as verified by telemetered data of the two receivers during launch and flight. The battery voltages at lift-off were 32.3 and 32.4 volts with receivers operating. The minimum specifications limit is 30 volts.

The Centaur solid-state inverter, supplying 400 hertz power to the guidance, flight control, and propellant utilization systems, operated satisfactorily throughout the flight. Telemetered voltage levels compared closely with the values recorded during preflight testing. Inverter voltages at lift-off were as follows: phase A, 115.8 volts, phase B, 115.5 volts; and phase C, 115.2 volts. Voltage levels rose slightly during flight (0.4 V for phase A, 0.8 V for phase B, and 0.2 V for phase C). The inverter frequency remained constant at 400.0 hertz throughout the flight.

Inverter temperature was 105° F (313.5 K) prior to hydrogen tanking and cooled gradually to 86° F (303 K) at lift-off. The temperature rose to a maximum of 139° F (332.5 K) at T + 2684 seconds when power changeover was effected. At end of data acquisition (T + 2940 sec), the inverter temperatures had dropped to 119° F (321.5 K). Inverter temperatures are plotted in figure V-61.

Instrumentation and Telemetry

Atlas system description. - The Atlas telemetry system consisted of a single PAM/FM/FM unit. A block diagram of this system is shown in figure V-62. This system transmitted at 229.9 megahertz. The letter designation PAM refers to Pulse Amplitude Modulation, a technique of sampling data to allow better utilization of the data handling capacity of the telemetry system. The designation FM/FM (Frequency Modulation/Frequency Modulation) refers to the combination of a frequency modulated radio frequency carrier upon which has been superimposed a number of frequency modulated subcarriers. All operational measurements were transmitted with two antennas, one in each Atlas equipment pod. Location of ground stations used in the AC-12 flight are shown in figure V-63. Telemetry coverage was obtained as shown in figure V-64.

112

TABLE V-14. - ATLAS MEASUREMENT SUMMARY, AC-12

Airborne systems	Number and measurement type										
	Acceleration	Rotation rate	Current	Deflection	Pressure	Frequency	Rate	Temperature	Voltage	Discrete	Totals
Airframe	1				3			2		4	10
Range safety									3	1	4
Electrical			1			1			2		4
Pneumatics					7			2			9
Hydraulics					6						6
Propulsion		3		2	19			2		6	32
Flight control				11			3		1	12	27
Telemetry								1			1
Propellants	1				2				1		4
Totals	2	3	1	13	37	1	3	7	7	23	97

Atlas system performance. - A summary of the 97 Atlas instrumentation measurements transmitted is given in table V-14. The only failure was in the sustainer hydraulic return pressure measurement (AH601P) which indicated that pressures were 25 psi (17.24 N/cm^2) high throughout the countdown and during flight. Comparison of telemetry and landline data of sustainer return pressures verified that the transducer was biased high by 25 psi (17.24 N/cm^2) prior to lift-off.

Centaur system description. - The Centaur telemetry system consisted of a single PAM/FM/FM unit operated at a frequency of 225.7 megahertz. The radiated power output was approximately 4 watts. The PAM/FM/FM modulated system transmitted from a single telemetry antenna mounted on a ground plane atop the umbilical island. Figure V-65 shows antenna locations on the Centaur. Locations of ground and ship receiving stations are shown in figure V-63. A block diagram of the Centaur telemetry system is shown in figure V-66. A new solid-state events conditioning module was incorporated in the AC-12 Centaur telemetry package. The function of the module was to superimpose on telemetry data the discrete occurrences of Atlas vernier engine cutoff, sustainer engine cutoff, and booster engine cutoff.

Centaur system performance. - Telemetry coverage was virtually continuous through T + 4000 seconds, as shown in figure V-67. Low signal levels at Carnarvon receiving stations did not allow proper data processing. A summary of the 163 instrumentation

TABLE V-15. – CENTAUR MEASUREMENT SUMMARY, AC-12

Airborne systems	Number and measurement type												
	Acceleration	Rotation rate	Current	Deflection	Vibration	Pressure	Frequency	Rate	Temperature	Voltage	Discrete	Digital	Totals
Airframe				1					2		3		6
Range safety										2	3		5
Electrical			1				1		1	4			7
Pneumatics						5			3		2		10
Hydraulics						2			2				4
Guidance									1	16		1	18
Propulsion		4				12			22		19		57
Flight control								3		4	35		42
Propellants				2						2			4
Spacecraft				3	4	1			1			1	10
Totals		4	1	6	4	20	1	3	32	28	62	2	163

measurements transmitted is given in table V-15. Over 98 percent of the data was successfully obtained. The following data were not obtained:

(1) The C-2 engine fuel pump temperature measurement (CP123T) had a slow response and the indicated temperature was about 70° F (295 K) warmer than expected.

(2) The liquid-hydrogen pump-inlet pressure measurement (C-1 engine, CP52P) did not return to zero after main engine first cutoff as expected. An offset of 4 percent information bandwidth was noted thereafter, coincident with the expected large pressure transient. It is believed the transducer was damaged at this time causing the 4 percent offset.

(3) The liquid-hydrogen pump-inlet pressure measurement (C-2 engine, CP54P) did not return to zero after main engine first cutoff as expected. An offset of 10 percent was noted thereafter, coincident with the expected large pressure transient. It is believed the transducer was damaged at this time, causing the 10 percent offset.

(4) The rate gyro spin motors on/off indication measurement (CS82X), changed from 103 to 96 percent of full scale at the approximate time of Centaur nose fairing jettison. Five seconds later the measurement dropped to zero. The measurement should have remained at full scale until power changeover, after Centaur retrothrust.

Tracking System

C-band beacon description. - A C-band radar subsystem with associated ground stations provided real-time position and velocity data to the range safety tracking system impact predictor. These data were also used by the Deep Space Network for acquisition of the spacecraft and for guidance and flight trajectory data analysis. The airborne equipment included a lightweight transponder, circulator (to channel receiving and sending signals), power divider, and two antennas located on opposite sides of the tank. The locations of the Centaur antennas are shown in figure V-65. The ground and ship stations are standard radar sets and are located as shown in figure V-63. A block diagram of the C-band system is shown in figure V-68.

C-band system performance. - C-band radar tracking was satisfactory, coverage was obtained up to T + 6791 seconds. The tracking ship Twin Falls did not provide C-band coverage. Grand Bahama reported intermittent track because of balance point shift (antenna pattern problems). Antigua, Pretoria, and Carnarvon radar tracking stations provided data for near-real-time orbit calculations. Cape Kennedy, Grand Bahama Island, and Bermuda radar tracking stations provided redundant tracking coverage early in flight. C-band radar coverage is shown in figure V-69.

Range Safety Command Subsystem

(Vehicle Destruct Subsystem)

Airborne subsystem description. - The Atlas and Centaur stages each contained independent vehicle destruct systems. These subsystems were designed to function simultaneously on command from the ground stations. Each system included redundant receivers, power control units, destructors, and batteries which operated independently of the main vehicle power systems. Block diagrams of the Atlas and Centaur vehicle destruct subsystems are shown in figures V-70 and V-71, respectively.

The Atlas and Centaur vehicle destruct subsystem provided highly reliable means of shutting down the engines only, or shutting down the engines and destroying the vehicle. To destroy a vehicle in the event of a flight malfunction, the propellant tanks would be ruptured with a shaped charge and the liquid propellants of the Atlas and Centaur stages dispersed.

Subsystem performance. - The Atlas and Centaur range safety command vehicle destruct subsystems were prepared to execute destruct commands throughout the flight. Engine cutoff or destruct commands were not sent by the range transmitters. The command from Antigua ground station to disable the range safety command system shortly

after Centaur main engine first cutoff was properly received and executed. Figure V-72 depicts ground transmitter coverage to support the vehicle destruct systems.

Signal strength at the Atlas and Centaur range safety command receivers was excellent throughout the flight, as indicated by telemetry measurements. Telemetered data indicated that both the Centaur receivers were turned off at approximately T + 597.2 seconds, thus confirming that the disable command was transmitted from the Antigua station.
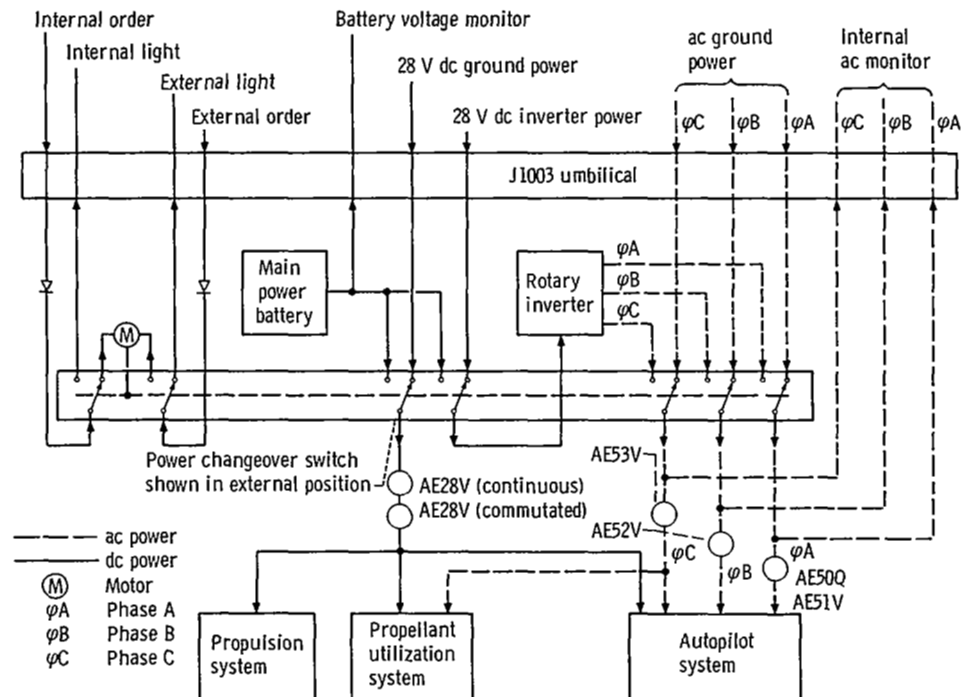
Figure V-59. - Atlas electrical system block diagram, AC-12.
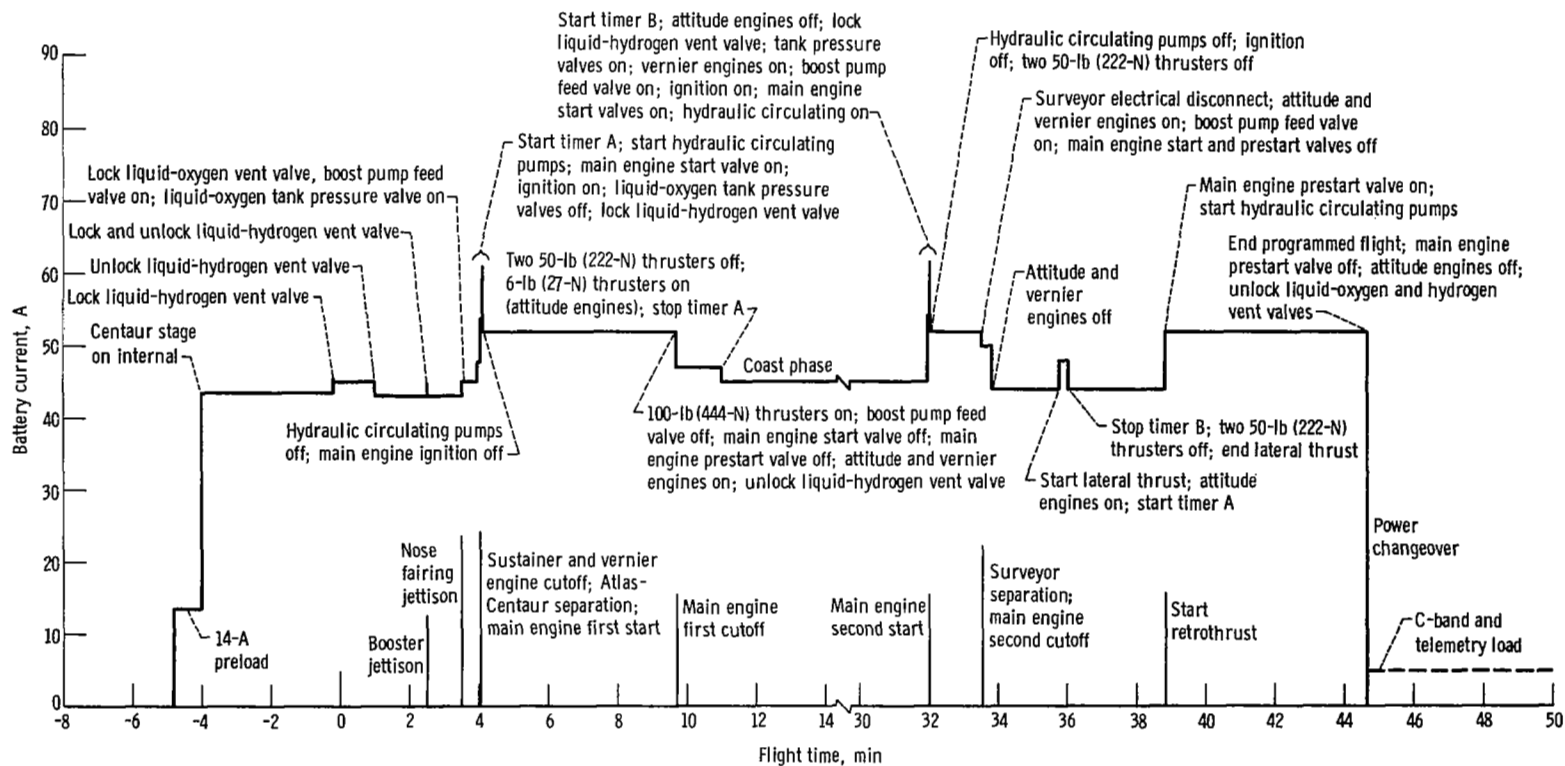
Figure V-60. - Main battery current profile, AC-12.
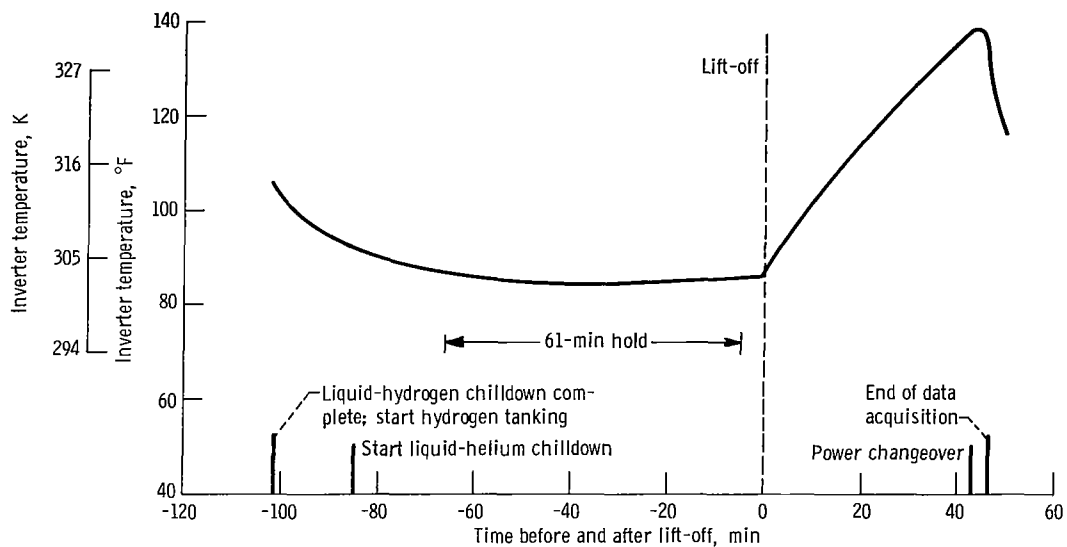
Figure V-61. - Centaur inverter temperature, AC-12.
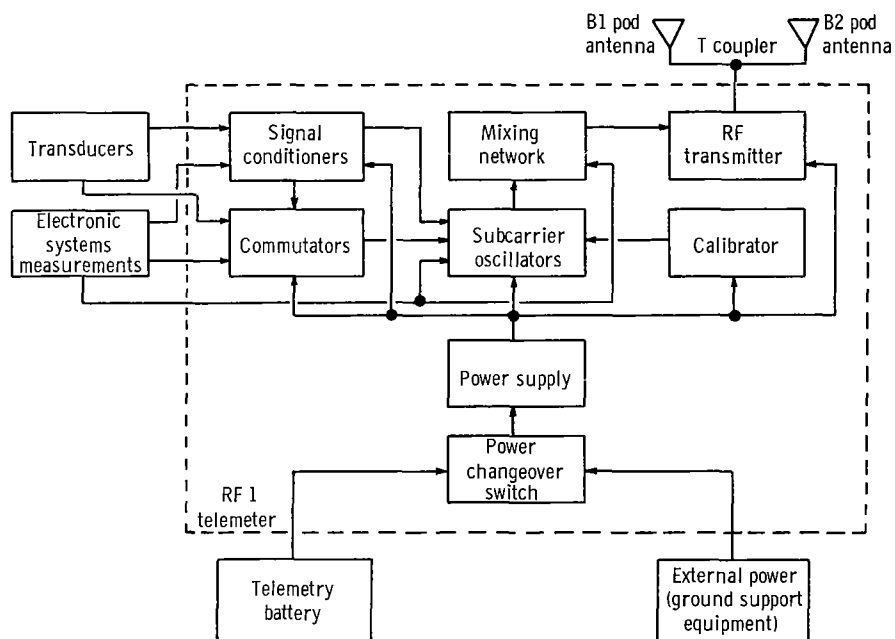
Figure V-62. - Atlas telemetry system block diagram, AC-12.
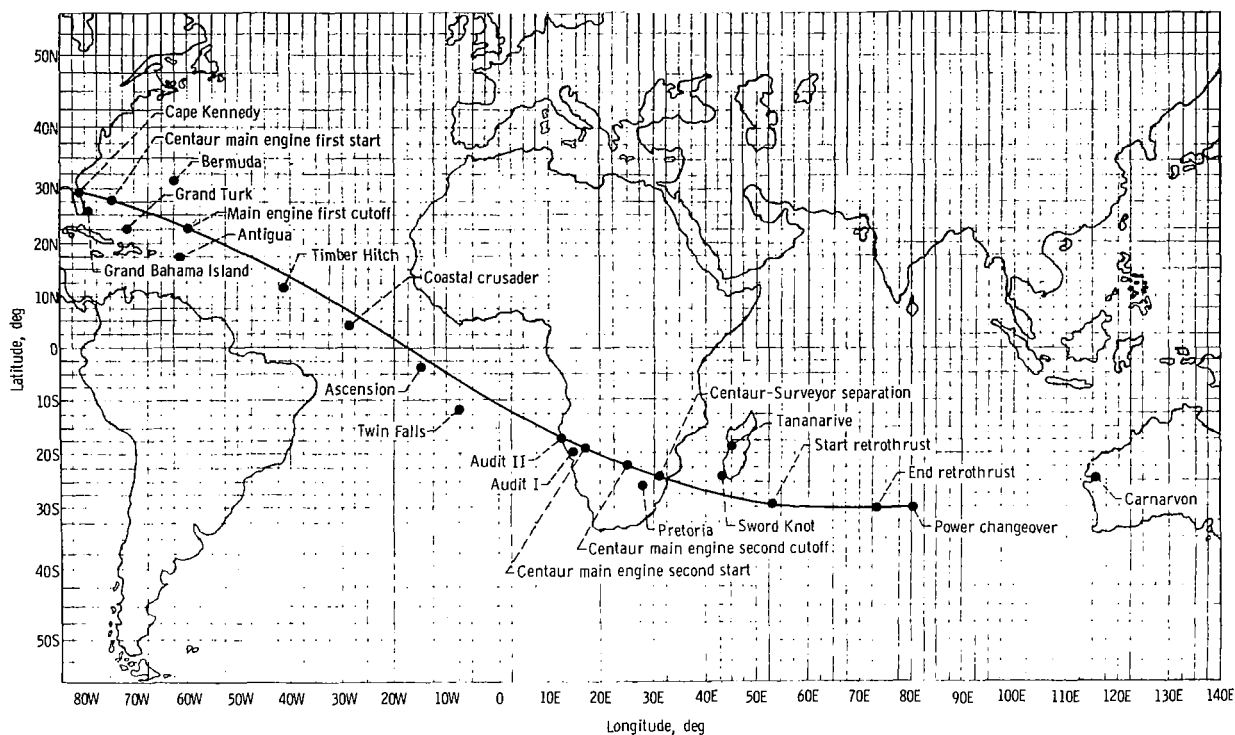
Figure V-63. - Tracking station locations and vehicle trajectory Earth track, AC-12.
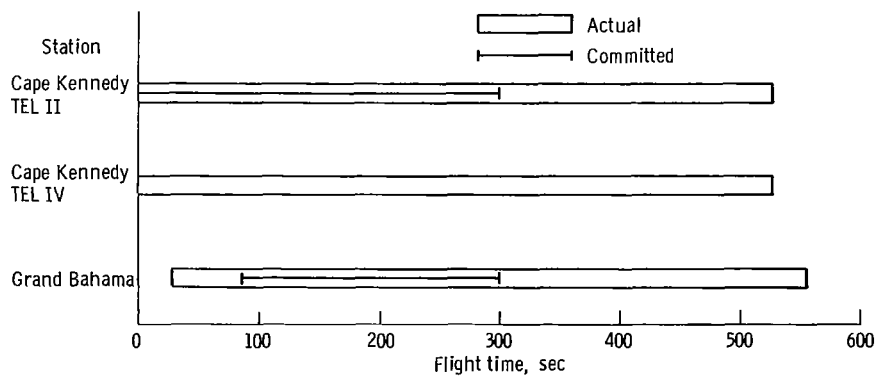
Figure V-64. - Atlas telemetry coverage, AC-12.

Figure V-65. - Centaur antenna locations and radio frequency subsystems, AC-12.

Figure V-66. - Centaur telemetry subsystem block diagram, AC-12.

Figure V-67. – Centaur telemetry coverage, AC-12.
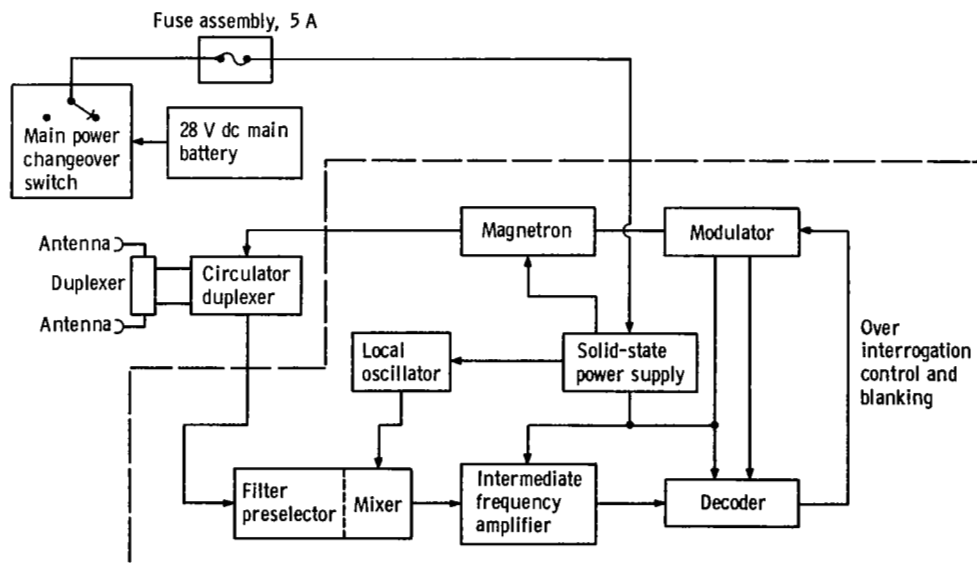
Figure V-68. – Centaur C-Band beacon subsystem, AC-12.

121
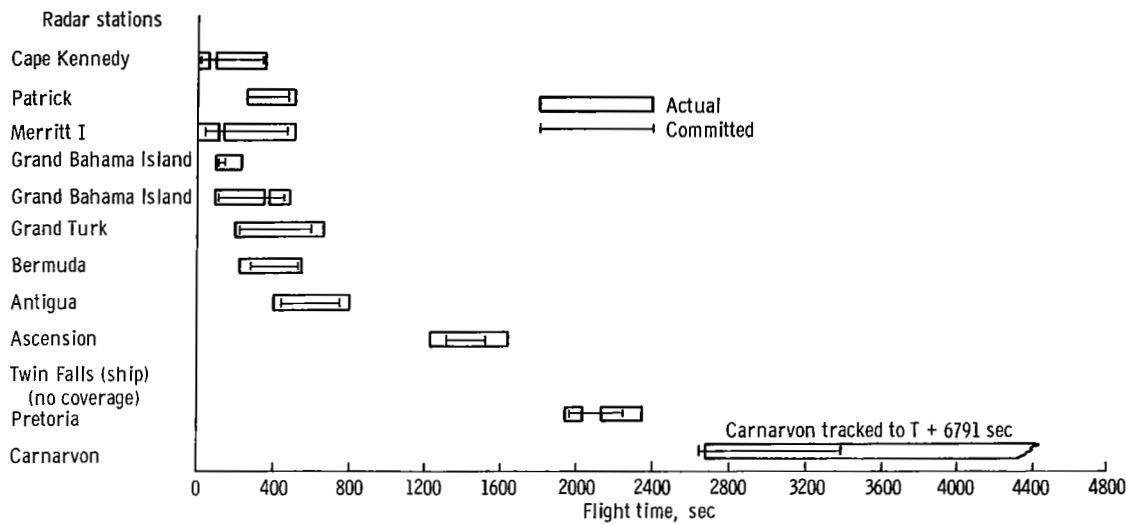
Figure V-69. – C-band radar coverage (auto beacon track only), AC-12.
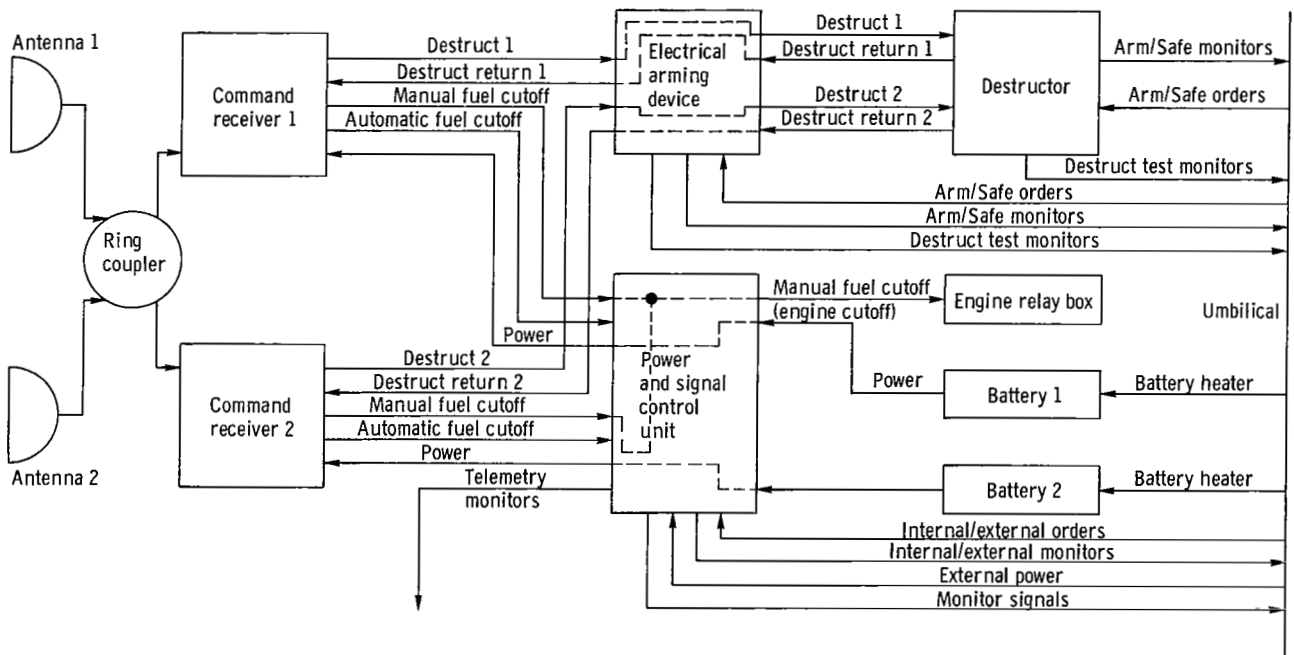
Figure V-70. – Atlas vehicle destruct subsystem block diagram, AC-12.
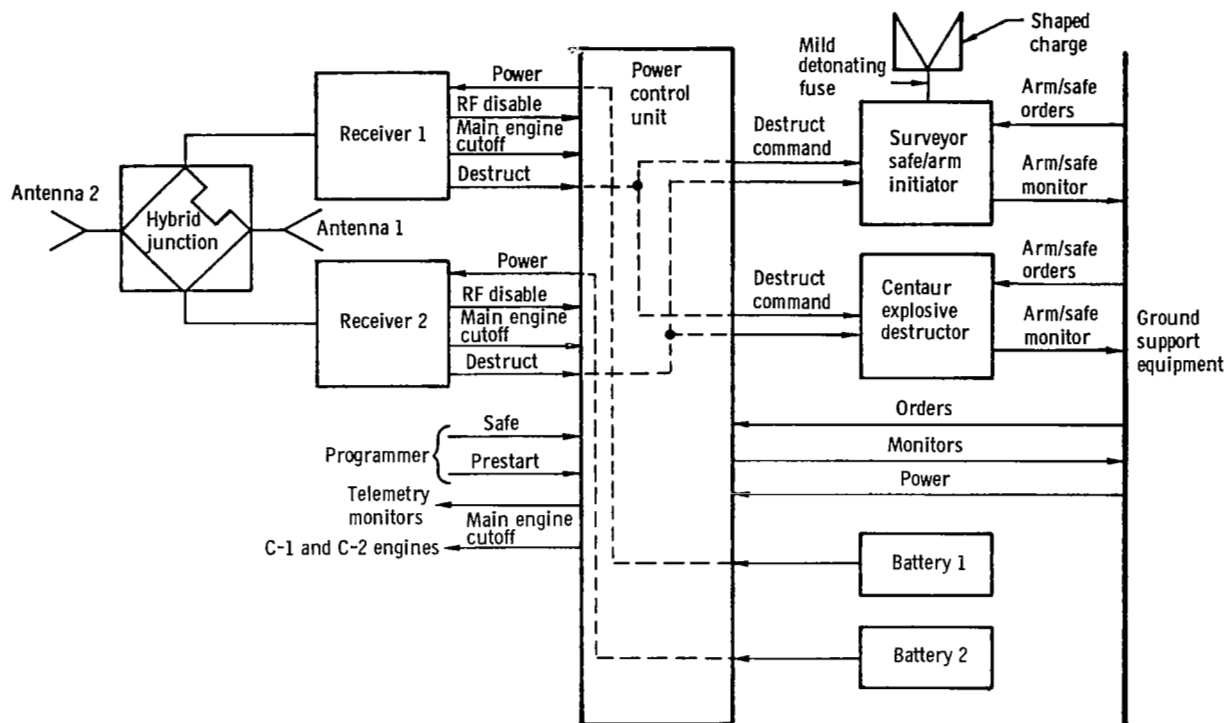
Figure V-71. – Centaur vehicle destruct subsystem block diagram, AC-12.
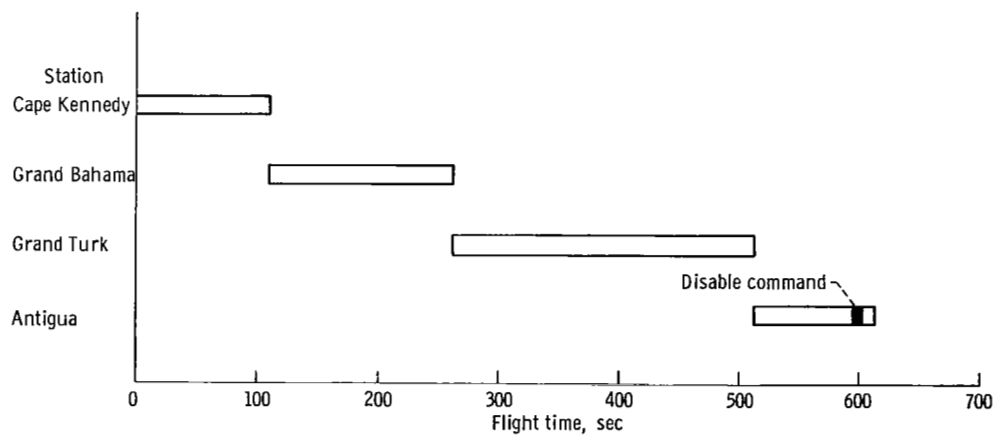
Figure V-72. – Range safety command system transmitter utilization, AC-12.

GUIDANCE AND FLIGHT CONTROL SYSTEMS

by Michael Ancik, Larry Feagan, Paul W. Kuebeler, and Corrine Rawlin

The objectives of the guidance and flight control systems were to guide the launch vehicle to the orbit injection point and establish the vehicle velocity necessary to place the Surveyor spacecraft in a lunar-transfer orbit. In accomplishing these objectives the guidance and flight control systems provided vehicle stabilization, controlled and guided the vehicle flight path, and sequenced flight events of the launch vehicle. These functions were performed at specified time periods from vehicle lift-off through completion of the Centaur retromaneuver after spacecraft separation. An inertial guidance system was installed on the Centaur stage. Separate flight control systems were installed on the Atlas and on the Centaur stages. The guidance system, operating with the flight control systems, provided the capability to stabilize the vehicle and compensate for trajectory dispersions resulting from thrust misalinement, winds, and vehicle performance variations.

Three modes of control were used for stabilization, control, and guidance of the launch vehicle. These modes were "rate stabilization only," "rate stabilization and attitude control," and "rate stabilization and guidance control." Block diagrams of the three modes are shown in figure V-73. The flight times during which a particular mode was used are shown in figure V-74 along with the modes of operation of the hydrogen peroxide attitude control sys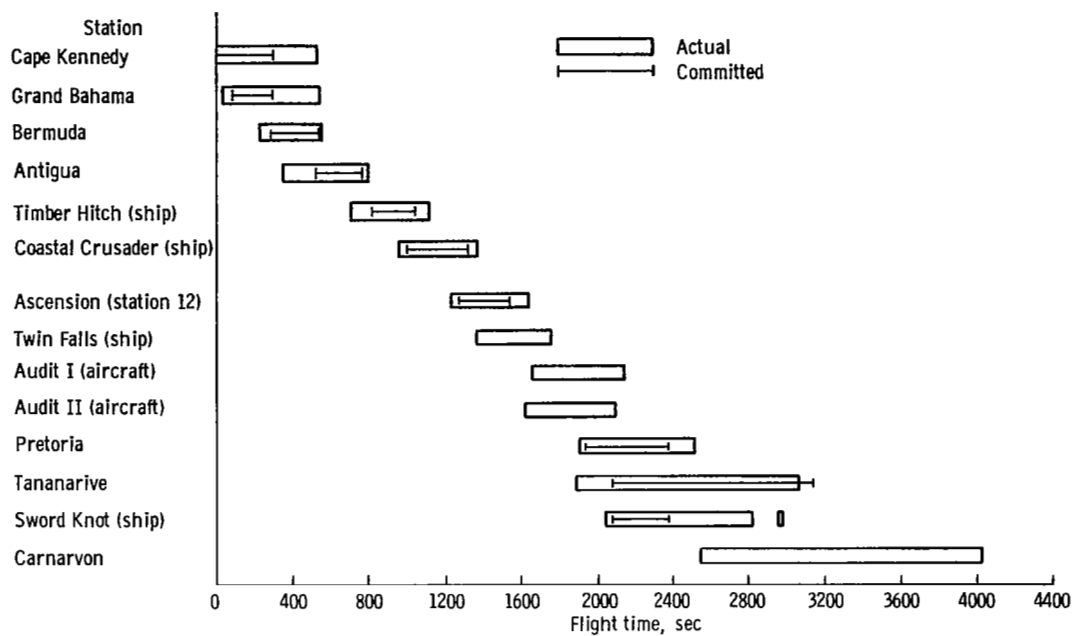tem, which are discussed later in this section. The rate-stabilization-only mode used output signals from rate gyros to control gimbaling of the engines. The output signal of each rate gyro was proportional to the angular rate of rotation of the vehicle about the input axis of the rate gyro. The engines provided directional thrust to minimize angular rate and thus stabilize the vehicle. During coast phases of the flight, the stabilizing directional thrust was provided by the hydrogen peroxide engines of the attitude control system. The rate-stabilization-only mode stabilized the roll axis of the Centaur stage continuously after Atlas sustainer engine cutoff. This mode was also used to stabilize the pitch and yaw axes of the Centaur stage during Atlas-Centaur separation, for 4 seconds following main engine second start, and for the period between main engine second cutoff and spacecraft separation. Rate stabilization was also combined with position (attitude) information in the other two modes of operation.

The rate-stabilization-and-attitude-control mode was used only during Atlas booster phase of flight. This mode is termed attitude control since the displacement gyros (one each for pitch, yaw, and roll axes) provided a reference attitude and controlled the vehicle to aline to that reference attitude. However, if the actual flight path differed from the desired flight path, there was no way of determining the difference and correcting the flight path. The reference attitude was programmed to change during booster phase. These changes in reference attitude caused the vehicle to roll to the programmed flight azimuth

124

angle and to pitch downward. Vehicle stabilization was accomplished in the same manner as in the rate-stabilization-only mode. The rate stabilization signals were algebraically summed with the attitude reference signals. These summed signals controlled gimbaling of the engines. These engines then provided directional thrust to stabilize and position the vehicle.

Rate stabilization and guidance control of the pitch and yaw axes were used during the Atlas sustainer and Centaur phases of flight. During this mode, the guidance system provided the attitude and direction reference. If the resultant flight path, as measured by the guidance system, was not the desired flight path, the guidance system issued steering signals to direct the vehicle to the desired flight path. Vehicle stabilization was accomplished in the same manner as in the rate-stabilization-only mode. The pitch and yaw rate stabilization signals were algebraically summed with the appropriate pitch and yaw steering signals of the guidance system to provide servocommands to the engines. The roll-rate-stabilization signal was algebraically summed with the Atlas roll attitude signal during the sustainer phase. During the Centaur phase, the roll axis was in the rate-stabilization-only mode. The summed pitch and yaw signals and the Centaur roll rate signal controlled gimbaling of the engines. These engines then provided directional thrust to stabilize the vehicle and direct the vehicle to the desired flight path. During coast phases of flight, thrust for attitude control was provided by the hydrogen peroxide engines.

Figure V-75 is a simplified diagram of the interface between the guidance system and the flight control systems.

Guidance

System description. - The AC-12 Centaur guidance system was an inertial system which was completely independent of ground control after entering flight condition approximately 9 seconds before lift-off of the vehicle. The guidance system performed the following functions:

(1) Measured vehicle acceleration in fixed inertial coordinates
(2) Computed the values of actual vehicle velocity and position and computed the vehicle flight path to attain the trajectory injection point
(3) Compared the actual position to the desired flight path and issued steering signals
(4) Issued discrete commands

A simplified block diagram of the guidance system is shown in figure V-76.

Inertial measuring unit: Vehicle acceleration was measured by the following three units:

(1) The inertial platform unit containing the platform assembly, gyros and accelerometers

(2) The pulse rebalance, gyro torquer and power supply unit containing the electronics associated with the accelerometers

(3) The platform electronics unit containing the electronics associated with the gyros

The platform assembly used four gimbals which provided a three-axis coordinate system. The use of four gimbals instead of three, allowed complete rotation of all three vehicle axes about the platform without gimbal lock. Gimbal lock is a condition in which two axes coincide causing loss of 1 degree of freedom. A gimbal diagram is shown in figure V-77. The azimuth gimbal was isolated from movements of the vehicle airframe by the other three gimbals. The inertial components (three gyros and three accelerometers) were mounted on the azimuth or inner gimbal. A gyro and an accelerometer were mounted as a pair with the sensing axes of each pair parallel. The gyro and accelerometer pairs were also alined on three mutually perpendicular (orthogonal) axes corresponding to the three axes of the platform.

The three gyros were identical and were of the single-degree-of-freedom, floated-gimbal, rate-integrating type. Each gyro monitored one of the three axes of the platform. These gyros were elements of control loops, the sole purpose of which was to maintain each axis fixed in inertial space. The output signal of each gyro was connected to a servoamplifier whose output controlled a direct-drive torque motor which moved a gimbal of the platform assembly. The orientation of the azimuth gimbal was fixed in inertial space and the outer roll gimbal was attached to the vehicle. The angles between the gimbals provided a means for transforming steering signals from inertial coordinates to vehicle coordinates. The transformation was accomplished by electromechanical resolvers, mounted between gimbals, to produce analog electrical signals proportional to the sine and cosine functions of the gimbal angles. These electrical signals were used for an analog solution of the mathematical equations for coordinate transformation by interconnecting the resolvers in a multiple resolver chain.

The three accelerometers were identical and were of the single-axis, viscous-damped, hinged-pendulum type. The accelerometer associated with each axis measured the change in vehicle velocity along that axis by responding to acceleration. Acceleration of the vehicle caused the pendulum to move off center. The associated electronics then produced precise current pulses to recenter the pendulum. These rebalance pulses were either positive or negative pulses depending on an increase or decrease in vehicle velocity. These pulses, representing changes in velocity (incremental velocity), were then routed to the navigation computer unit for computation of vehicle velocity.

Proper flight operation required alinement and calibration of the inertial measuring unit during launch countdown. The azimuth of the platform, to which the desired flight trajectory was referenced, was alined by ground-based optical equipment. The platform was alined perpendicular to the local vertical by using the two accelerometers in the horizontal plane. Each gyro was calibrated to determine its characteristic constant torque

drift rate and mass unbalance along the input axis. The scale factor and zero bias offset of each accelerometer were determined. These prelaunch determined calibration constants and scale factors were stored in the navigation computer for use during flight.

Navigation computer unit: The navigation computer unit was a serial, binary, digital machine with a magnetic drum memory. The memory drum had a capacity of 2816 words (25 bits per word) of permanent storage, 256 words of temporary storage, and six special purpose tracks. Permanent storage was prerecorded and could not be altered by the computer. The temporary storage was the working storage of the computer.

Incremental velocity pulses from the accelerometers were the information inputs to the navigation computer. The operation of the navigation computer was controlled by the prerecorded program. This program directed the computer to use the prelaunch equations, navigation equations, and guidance equations.

The prelaunch equations established the initial conditions for the navigation and guidance equations. Initial conditions included (1) a reference trajectory, (2) launch site values of geographical position, (3) initial values of navigation and guidance functions. Based on these initial conditions, the guidance system started flight operation approximately 9 seconds prior to lift-off.

The navigation equations were used to compute vehicle velocity and actual position. Velocity was determined by algebraically summing the incremental velocity pulses from the accelerometers. An integration was then performed on the computed velocity to determine actual position. Corrections for the prelaunch determined gyro and accelerometer constants were also made during the velocity and position computation to improve the navigation accuracy. For example, the velocity data derived from the accelerometer measurements were adjusted to compensate for the accelerometer scale factors and zero offset biases measured during the launch countdown. The direction of the velocity vector was also adjusted to compensate for the gyro constant torque drift rates measured during the launch countdown.

The guidance equations continually compared actual position and velocity with the position and velocity desired at the time of injection. Based on this position comparison, steering signals were generated to guide the vehicle along an optimized flight path to obtain the desired injection conditions. The guidance equations were used to generate eight discrete commands: (1) booster engine cutoff, (2) sustainer engine cutoff backup, (3) Centaur main engine first cutoff, (4) hydrogen peroxide settling engines cutoff, (5) B timer start (Centaur main engine second start sequence), (6) Centaur main engine second cutoff, (7) telemetry calibration on, and (8) telemetry calibration off. The booster engine cutoff command and the sustainer engine cutoff backup command were issued when the measured vehicle acceleration equaled predetermined values. The Centaur main engine first cutoff command was issued when the vehicle orbital energy equaled the energy required for injection into the parking orbit. At a predetermined time interval after main engine first

cutoff, the hydrogen peroxide settling engines cutoff command was issued. The B timer start command was issued when the angle between the position and target vectors, as computed by the guidance system, equaled a prelaunch determined angle. When the measured vehicle orbital energy equaled the predetermined value required for injection into the proper lunar trajectory, the Centaur main engine second cutoff command was issued. The telemetry calibration commands were issued at fixed time intervals after the B timer start command was issued.

During the booster phase of flight, the navigation computer supplied an incremental pitch signal and the total yaw signal for steering the Atlas stage. From a series of predetermined programs, one pitch program and one yaw program were selected based on prelaunch upper air wind soundings. The selected programs were entered and stored in the computer during launch countdown. The programs consisted of discrete pitch and yaw turning rates for specified time intervals from T + 15 seconds until booster engine cutoff. These programs permitted changes to be made in the flight reference trajectory during countdown to reduce anticipated aerodynamic heating and structural loading conditions on the vehicle.

Signal conditioner unit: The signal conditioner unit was the link between the guidance system and the vehicle telemetry system. This unit modified and scaled guidance system parameters to match the input range of the telemetry system.

System performance. - The performance of the AC-12 guidance system was satisfactory. The system performance was evaluated in terms of the resultant flight trajectory and the midcourse correction that would have been required by the spacecraft to impact the target for which the trajectory was designed. In addition, the issuance of discrete commands, operation of the guidance steering loops, gyro control loops, accelerometer loops, and other measurements were evaluated in terms of general performance.

Trajectory and midcourse requirements: The overall accuracy of the AC-12 guidance system was satisfactory. The parking orbit altitude was designed to be 90±5 nautical miles (166.7±9.3 km), based on spacecraft heating and payload considerations. The launch vehicle and spacecraft were injected into the parking orbit at an altitude of 85.9 nautical miles (159.2 km). The perigee and apogee altitudes were 85.7 nautical miles (158.7 km) and 91.5 nautical miles (169.5 km), respectively.

After coasting for 22.13 minutes, the Centaur engines were restarted, burned for 111.3 seconds, and the spacecraft was successfully injected into the proper lunar-transfer ellipse. Data from tracking information indicated that a midcourse correction (20 hr after injection) of 3.94 meters per second (miss only)[2] or 6.07 meters per second (miss plus

---

[2]The velocity correction required to hit the aiming point.

time of flight)[3] would have been required to impact the target for which the trajectory was designed. These corrections were well within the established specification that a Surveyor spacecraft would not be required to perform a midcourse correction greater than 50 meters per second.

The slight inaccuracies at injection were primarily introduced by three main sources:

(1) Dispersions due to the computational limitations

(2) Dispersion between predicted and actual engine shutdown impulse

(3) Dispersions related to the guidance equipment limitations and to variations from the predicted values of the thrust produced by the hydrogen peroxide engines

The contribution of these sources to the midcourse correction that would have been required 20 hours after injection are shown in the following table:

Error	Miss only, m/sec	Miss plus time of flight, m/sec
Computational limitations	2.01	2.77
Engine shutdown impulse dispersion	1.01	1.38
Guidance equipment and hydrogen peroxide engines	1.21	2.10
Total error (vector summation)	3.94	6.07

The landing conditions for which the trajectory was designed and the landing conditions which would have resulted had no midcourse maneuver been made are listed in the following table:

Landing conditions	Designed	No midcourse correction
Selenographic latitude	3.33° S	10.05° S
Selenographic longitude	23.17° W	37.00° W
Unbraked impact velocity	2670 m/sec	2671 m/sec
Flight time to Moon	2 days 16 hr 3 min 48.5 sec	2 days 16 hr 53 min 18.0 sec

[3]The velocity correction required to hit the aiming point at the specified time.

These data reflect a projected miss of the designed target of about 253 nautical miles (468 km), an unbraked impact velocity error of 3. 28 feet per second (1. 0 m/sec) high, and a flight time difference of 49 minutes 29. 5 seconds late.

Performance of the guidance system was not evaluated in terms of the midcourse correction actually executed. The actual midcourse correction was different from that required to impact the target for which the trajectory was designed (see section IV and the appendix). The new target was selected, based on actual spacecraft position and velocity measurements, to optimize the meeting of mission objectives.

Discrete commands: All eight discrete commands were issued within the expected range. Table V-16 lists the discretes, the criteria used by the navigation computer for

TABLE V-16. - DISCRETE COMMANDS, AC-12

Discrete command	Criteria for discrete to be issued	Discrete issued at this computed value	Actual time, T + sec	Predicted time, T + sec
Booster engine cutoff	When the square of vehicle thrust acceleration is greater than 29. 72 $(g's)^2$ $(5. 45 \ g's)^a$	31. 58 $(g's)^2$ (5. 62 g's)	142. 3	142. 4
Sustainer engine cutoff backup	When the square of vehicle thrust acceleration is less than 0. 53 $(g's)^2$	0. 18 $(g's)^2$	239. 9	232. 8 to 250. 3
Centaur main first engine cutoff	When extrapolated orbital energy-to-be-gained is equal to zero	-24 000 $(ft/sec)^2$; 7315 $(m/sec)^2$	589. 7	574. 9
Hydrogen peroxide set-tling engines cutoff	When time from main engine first cutoff discrete is greater than 74. 45 sec	75. 5 seconds after Centaur main engine first cutoff discrete	665. 2	650. 9
B timer start (Centaur main engine second start sequence)	When sine of angle between the position and target vectors is greater than -0. 036758	-0. 036439	1857. 3	1854. 6
Centaur main engine second cutoff	When extrapolated orbital energy-to-be-gained is equal to 131 500 $(ft/sec)^2$ (40 081 $(m/sec)^2$)	76 000 $(ft/sec)^2$; 23 165 $(m/sec)^2$	2028. 6	2022. 2
Telemetry calibration on	When time from B timer start discrete is greater than 260. 5 sec	261. 5 sec after B timer start dis-crete	2118. 6	2118. 3
Telemetry calibration off	When time from B timer start discrete is greater than 264. 5 sec	264. 7 after B timer start discrete	2122. 1	2122. 3

[a]This value is lower than the vehicle thrust acceleration of 5. 7±0. 08 g's required for booster engine shutdown. However, the vehicle acceleration was increasing during the predicted time delay in executing the test and the discrete command, at a rate such that, when 5. 62 g's was attained, the booster engines shut down.

the issuance of the discrete command, and the computed value at the time of issuance of the discrete command. Actual and predicted times from lift-off are also shown for reference.

Guidance steering loop: Guidance steering was activated 8 seconds after the booster engine cutoff command. At this time an 11° pitch-down maneuver was commanded. A 1^O yaw-right maneuver was also commanded. This vehicle attitude change was required to correct for errors accumulated during the booster phase of flight when the vehicle was under open loop control. The steering signals were less than 1^O throughout the remainder of the sustainer phase of flight. Guidance steering was deactivated at sustainer engine cutoff in preparation for staging. When guidance steering was reactivated, 4 seconds after Centaur main engine first start, a pitch-down maneuver of less than 1^O was commanded. A yaw-left maneuver of 1^O was also commanded. During the remainder of the Centaur powered phase of flight, the steering signals were less than 1^O. During the coast phase of flight, the maximum steering signals were 4° in pitch and 3° in yaw. Table V-17 lists the magnitude of the steering signals after each period of guidance system deactivation.

Guidance steering was deactivated at Centaur main engine second start and was reactivated 4 seconds after Centaur main engine second start. At this time, 1^O pitch-down and 6° yaw-left maneuvers were commanded. The steering signals were negligible during the remainder of the Centaur powered phase of flight.

Guidance steering was deactivated at Centaur main engine second cutoff and was reactivated at T + 2098.5 seconds for the retromaneuver. At this time, the steering signals commanded the vehicle to turn 180° to the vehicle velocity vector at injection. The sig-

TABLE V-17. - ATTITUDE COMMAND AT START OF GUIDANCE STEERING

AFTER EACH PERIOD OF SYSTEM DEACTIVATION, AC-12

Event	Time since end of last period of steering, sec	Flight time at start of steering, T + sec	Pitch command magnitude and direction	Yaw command magnitude and direction
Atlas sustainer phase, enable guidance steering	Lift-off	150.3	11° Nose down	1^O Nose right
Enable guidance steering after Centaur main engine first start	15.5	253.2	Less than 1^O nose down	1^O Nose left
Enable guidance steering after Centaur main engine second start	4	1921.3	1^O Nose down	6° Nose left

nals caused the vehicle to pitch up and yaw to the right to accomplish the turnaround maneuver.

Gyro control loops and accelerometer loops: The inertial platform was stable throughout the flight. The platform gimbal control loops operated satisfactorily. The maximum displacement errors were less than 20 arc-seconds (the dynamic accuracy tolerance was 60 arc-sec). Normal low-frequency oscillations (less than 2 Hz) were observed in all four loops and are attributed to vehicle dynamics. The accelerometer loops operated satisfactorily throughout the flight.

Other measurements: All the guidance system signals and measurements which were monitored during flight were normal and indicated satisfactory operation of the guidance system.

Flight Control

Atlas system description. - The Atlas flight control system provided the primary functions required for vehicle stabilization, control, execution of guidance steering signals, and timed switching sequences.

The Atlas flight control system consisted of the following major units:

(1) The displacement gyro unit which consisted of three single-degree-of-freedom, floated, rate-integrating gyros and associated electronic circuitry for gain selection and signal amplification. These gyros were mounted to the vehicle airframe in an orthogonal triad configuration alining the input axis of a gyro to its respective vehicle axis of pitch, yaw, or roll. Each gyro provided an electrical output signal proportional to the difference in angular position of the measured axis from the gyro reference axis.

(2) The rate gyro unit which contained three single-degree-of-freedom, floated, rate gyros and associated electronic circuitry. These gyros were mounted in the same manner as the displacement gyro unit. Each gyro provided an electrical output signal proportional to the angular rate of rotation of the vehicle about the gyro input (reference) axis.

(3) The servoamplifier unit which contained electronic circuitry to amplify, filter, integrate, and algebraically sum engine position feedback signals with position and rate signals. The electrical outputs of this unit directed the hydraulic controllers which in turn controlled the gimbaling of the engines.

(4) The programmer unit which contained an electronic timer, arm-safe switch, high, low, and medium power electronic switches, the fixed pitch program, and circuitry to set the roll program from launch ground equipment. The programmer issued discrete commands to the following systems: other units of the Atlas flight control system, Atlas propulsion, Atlas pneumatic, vehicle separation systems, Centaur flight control, and Centaur propulsion.

Atlas system performance. - The flight control system performed satisfactorily throughout the Atlas phase of flight. The corrections required to control the vehicle because of disturbances were well within the system capability. The vehicle dynamic response resulting from each flight event was evaluated in terms of amplitude, frequency, and duration, as observed on rate gyro data, and is shown in table V-18. In this table, the control capability is the ratio in percent of engine gimbal angle used to the available total engine gimbal angle. The control used at all times of the flight events includes that necessary for correction of the vehicle transient disturbances and for steady-state requirements.

The programmer was started at 42-inch (1.1-m) rise which occurred at approximately T + 1 second. This permitted the flight control system to gimbal the engines and thereafter control the vehicle. The vehicle transients were damped out by T + 2.5 seconds and required 14 percent of the control capability. The roll program was initiated at approximately T + 2.5 seconds to roll the vehicle to the desired flight azimuth of 100.809°. An average rate of 1.04 degrees per second clockwise was sensed. The pitch program was observed to start at T + 15.2 seconds with a pitch rate of -0.56 degree per second nose down.

Rate gyro data indicated that the period of maximum aerodynamic loading for this flight was approximately from T + 75 to T + 90 seconds. During this period, a maximum of 44 percent of the control capability was required to overcome both steady-state and transient loading.

The Atlas booster engines were cut off at T + 142.3 seconds. The rates imparted to the vehicle by this transient required a maximum of 14 percent of the sustainer engine gimbal capability. The Atlas booster engines were jettisoned at T + 145.3 seconds. The rates imparted by this disturbance were nearly damped out by the time Centaur guidance was admitted.

During the Atlas booster phase of flight, the Atlas flight control system provided the vehicle attitude reference. At T + 150.3 seconds the Centaur guidance system was used as the attitude reference. Fifty-six percent of the total control capability was required to move the vehicle to the new reference. The maximum vehicle rate transient during this change was a pitch rate of 2.48 degrees per second, peak to peak, with a duration of 15.5 seconds.

Insulation panels and nose fairings were jettisoned at T + 176.2 and T + 202.9 seconds, respectively. The maximum vehicle rate transient observed due to these disturbances was a pitch rate of 2 degrees per second peak to peak. The maximum control capability used to overcome these disturbances was 10 percent.

Sustainer engine cutoff occurred at T + 237.7 seconds. Atlas-Centaur separation was smooth with no noticeable transients.

TABLE V-18. - VEHICLE DYNAMIC RESPONSE TO FLIGHT DISTURBANCES, AC-12

Event	Time,[a] sec	Measure-ment	Rate gyro peak-to-peak am-plitude, deg/sec	Transient frequency, Hz	Transient duration, sec	Required percent control capability
Lift-off	T - 0	Pitch	0.24	2.5	(b)	(b)
		Yaw	.40	1.1	2.0	(b)
		Roll	.40	8.3	2.0	(b)
42-in. (1.1-m) rise	T + 1	Pitch	0.48	3.0	0.5	6
		Yaw	.56	3.3	.7	14
		Roll	1.68	1.43	1.5	14
Maximum dynamic pressure	Included period from T + 75 to T + 90	Pitch	0.96	0.36	14	44
		Yaw	1.36	.59	10	16
		Roll	.8	.50	7	16
Booster engine cutoff	T + 142.44	Pitch	1.04	4.76	3.0	14
		Yaw	1.0	9.1	3.0	10
		Roll	.96	2.22	3.0	10
Booster engine jettison	T + 145.5	Pitch	1.28	0.91	3.0	(b)
		Yaw	1.0	.72	4.5	(b)
		Roll	.88	.83	4.0	(b)
Admit guidance	T + 150.4	Pitch	2.48	0.667	15.5	56
		Yaw	.72	.72	4.0	10
		Roll	.80	1.11	15.5	6
Insulation panel jettison	T + 176.2	Pitch	0.32	5.0	0.5	2
		Yaw	.32	6.67	.5	10
		Roll	1.36	2.86	1.3	6
Nose fairing jettison	T + 203.0	Pitch	2.00	5	1.5	0
		Yaw	.64	33	.4	10
		Roll	1.12	1.43	1.5	6
Sustainer engine cutoff	T + 236.7	Pitch Yaw Roll	No significant transients			
Atlas-Centaur separation	T + 240	Pitch Yaw Roll	No significant transients			
Main engine first start	T + 250.6	Pitch	1.44	0.20	13	20
		Yaw	1.04	.31	7	8
		Roll	1.84	.56	9	8
Admit guidance	T + 254.6	Pitch	1.35	0.20	9	14
		Yaw	1.04	.15	6	4
		Roll	.33	1.0	4	4
Main engine first cutoff	T + 589.8	Pitch	2.02	35	0.40	10
		Yaw	1.04	33	.20	26
		Roll	.92	.42	2.0	26
Main engine second start	T + 1918.6	Pitch	1.69	0.83	2.5	16
		Yaw	1.13	.50	2.8	8
		Roll	2.16	1.25	2.8	8
Admit guidance	T + 1921.4	Pitch	0.42	0.55	3	2
		Yaw	2.09	.42	8	16
		Roll	.33	.72	2	16
Main engine second cutoff	T + 2028.7	Pitch	2.67	30	2.3	16
		Yaw	1.31	30	.4	8
		Roll	1.08	.63	1.4	8

[a]Initiation of disturbances as seen on rate gyro data.
[b]Indicates no measurable data.

Centaur system description. - The Centaur flight control system provided primary means for vehicle stabilization and control, execution of guidance steering signals, and timed switching sequences for programmed flight events. A simplified block diagram of the Centaur flight control system is shown in figure V-78.

The Centaur flight control system consisted of the following major units:

(1) The rate gyro unit which contained three single-degree-of-freedom, floated, rate gyros with associated electronics for signal amplification. These gyros were mounted to the vehicle in an orthogonal triad configuration alining the input axis of each gyro to its respective vehicle axis of pitch, yaw, or roll. Each gyro provided an electrical output signal proportional to the angular rate of rotation of the vehicle about the gyro input (reference) axis.

(2) The servoamplifier unit which contained electronics to amplify, integrate, and algebraically sum engine position feedback signals with position and rate signals. The electrical outputs of this unit directed the hydraulic actuators, which in turn controlled the gimbaling of the engines. In addition, this unit contained the logic circuitry controlling the engines of the hydrogen peroxide attitude control system.

(3) The electromechanical timer unit which contained a 400-hertz synchronous motor to provide the time reference. Two timer units designated A and B were needed because of the large number of discrete commands required for the parking-orbit mission.

(4) The auxiliary electronics unit, which contained logic, relay switches, transistor power switches, power supplies, and an arm-safe switch. The arm-safe switch electrically isolated valves and pyrotechnic devices from control switches. The combination of the electromechanical timer units and the auxiliary electronics unit issued discretes to the following systems: other units of the flight control system, propulsion, pneumatic, hydraulic, separation system, propellant utilization, telemetry, spacecraft, and electrical.

Vehicle steering during Centaur powered flight was by thrust vector control through gimbaling of the main engines. There were two actuators for each engine to provide pitch, yaw, and roll control. Pitch control was accomplished by moving both engines together in the pitch plane. Yaw control was accomplished by moving both engines together in the yaw plane, and roll control was accomplished by moving the engines differentially in the yaw plane. Thus, the yaw actuator responded to an algebraically summed yaw-roll command. By controlling the direction of thrust of the main engines, the flight control system maintained the flight of the vehicle on a trajectory directed by the guidance system. After main engine cutoff, control of the vehicle was maintained by the flight control system using selected constant thrust hydrogen peroxide engines. A more complete description of the engines and the propellant supply for the attitude control system is presented in the PROPULSION SYSTEMS section of this report.

The logic circuitry which commanded the 14 hydrogen peroxide engines, either on or

TABLE V-19. - ATTITUDE CONTROL SYSTEM MODES OF OPERATION, AC-12

[V engines, 50 lb (222.4 N) thrust; S engines, 3.0 lb (13.3 N) thrust; A engines, 3.5 lb (15.6 N) thrust; P engines, 6.0 lb (26.7 N) thrust.]

Mode	Flight period	Description
All off	1. Powered phases 2. 5 sec during spacecraft separation sequence	This mode prevents the operation of all attitude control engines regardless of error signals.
Separate on	1. Main engine second cutoff until start of spacecraft separation sequence 2. End of lateral thrust during turnaround until end of retrothrust	When in the separate on mode, a maximum of 2 A and 2 V engines and 1 P engine fire. These engines fire only when appropriate error signals surpass their respective thresholds. A engines: when 0.2 deg/sec threshold is exceeded, suitable A engines fire to control in yaw and roll. A_1A_4 and A_2A_3 combinations are inhibited. P engines: when 0.2 deg/sec threshold is exceeded, suitable P engine fires to control in pitch. P_1P_2 combination is inhibited. S engines: off V engines: when 0.3 deg/sec threshold is exceeded, suitable engines fire (as a backup for higher rates). V_1V_3 and V_2V_4 combinations are inhibited.
A and P separate on	End of spacecraft separation sequence until start of lateral thrust	This mode is the same as separate on mode, except V engines are inhibited.
V half on	1. Main engine first cutoff until main engine first cutoff plus 75 sec 2. Main engine second start minus 40 sec until main engine second start 3. During lateral thrust phase 4. Last 100 sec prior to Centaur power turnoff	In the V half on mode, only the V engines are in the half on mode. A engines: when 0.2 deg/sec threshold is exceeded, suitable A engines fire to control in roll only. P engines: off S engines: off V engines: when there are no error signals, V_2V_4 combination fires continuously. This continuous firing serves various purposes: to settle propellants in flight periods 1 and 2, to provide lateral and added longitudinal separation between Centaur and spacecraft in flight period 3, and in order to deplete hydrogen peroxide supply to determine the amount of usable propellant remaining at end of mission in flight period 4. When 0.2 deg/sec threshold is exceeded, a minimum of 2 and a maximum of 3 V engines fire to control in pitch and yaw.
S half on	1. Main engine first cutoff plus 75 sec until main engine second start minus 40 sec	This mode is described as follows: A engines: when 0.2 deg/sec threshold is exceeded, suitable A engines fire to control in roll only. P engines: off S engines: when there are no error signals, S_2S_4 combination fires continuously for propellant retention purposes. When 0.2 deg/sec threshold is exceeded, a minimum of 2 and a maximum of 3 S engines fire to control in pitch and yaw. V engines: when 0.3 deg/sec threshold is exceeded, a minimum of 1 and a maximum of 2 V engines fire to control in pitch and yaw. When a V engine fires, a corresponding S engine is commanded off.

136

off, was contained in the servoamplifier unit of the flight control system. Figure V-79 shows the alphanumeric designations of the engines and their locations on the aft end of the vehicle. Algebraically summed position and rate signals were the inputs to the logic circuitry. The logic circuitry provided five modes of operation designated: "all off," "separate on," "A and P separate on," "V half on," and "S half on." These modes of operation were used during different periods of the flight which were controlled by the timer unit. A summary of the modes of operation is presented in table V-19. In this table "threshold" designates the vehicle rate in degrees per second that had to be exceeded before the engines were commanded "on."

Centaur system performance. - The Centaur flight control system performance was satisfactory. Vehicle stabilization and control were maintained throughout the flight. All events sequenced by the timers were executed at the required times. The following evaluation is presented in paragraphs related to timed-sequenced portions of flight. For the time periods of guidance-and-flight-control mode of operation and attitude-control-system mode of operation (refer to fig. V-74). Vehicle dynamic response for selected flight events is tabulated in table V-18.

Sustainer cutoff through main engine first cutoff (T + 237.7 to T + 589.7 sec): The Centaur A timer was started at sustainer engine cutoff by a discrete command from the Atlas programmer. Appropriate commands were issued to separate the Centaur stage from the Atlas stage and to initiate the main engine first firing sequence. Disturbing torques were created prior to main engine start by boost pump exhaust and chilldown flow through the main engines. Vehicle control was maintained by the hydrogen peroxide system and by gimbaling the main engines. There were no significant transients during separation. Centaur main engine first start was commanded at T + 249.2 seconds. The maximum angular rates due to engine start transients were 1.84 degrees per second and were corrected by gimbaling the engines less than 1^O. When guidance steering was enabled 4 seconds after main engine start, the Centaur vehicle was oriented less than 1^O nose high and 1^O nose right of the steering vector. Transients due to this difference and the main engine start disturbances to the vehicle were damped out within 9 seconds. Vehicle steady-state angular rates during the period of closed loop control were under 0.5 degree per second. The angular rates imparted to the vehicle at main engine cutoff indicated a small value of differential cutoff impulse. The maximum rate measured was 2.02 degrees per second in pitch.

Main engine first cutoff to main engine second prestart (T + 589.7 to T + 1900 sec): After main engine first cutoff, the hydrogen peroxide attitude control system was activated. During the 22.13-minute coast period, the control requirements were well within the capability of the attitude control system. Except for periods of noisy data, the rate gyros indicated maximum rates of 0.68 degree per second about the roll axis and 0.51 degree per second about the pitch and yaw axes.

Main engine second prestart through main engine second cutoff (T + 1900 to T + 2028. 6 sec): The hydraulic recirculating pumps were activated 28 seconds prior to main engine second start, and the Centaur main engines were centered. Main engine second start occurred at T + 1917. 3 seconds. The maximum angular rate observed at this time was 2. 16 degrees per second about the roll axis. Prestart and start operations resulted in a vehicle attitude 1^O nose high and 6° nose right. These attitude errors were corrected when guidance steering was enabled at approximately T + 1921 seconds. The control capability used to control these disturbances was 16 percent maximum. Angular rates were low during the second powered phase which ended with main engine second cutoff (T + 2028. 6 sec).

Main engine second cutoff to electrical power turnoff (T + 2028. 6 to 2683. 4 sec): At the time of Centaur main engine cutoff, guidance-generated steering signals were temporarily discontinued. The hydrogen peroxide attitude control system damped the low angular rates created by the main engine cutoff transient to within the 0. 2 degree per second control threshold. At T + 2093. 2 seconds (the attitude control system having been deactivated for 5 sec), the Surveyor spacecraft was successfully separated from Centaur. The deactivation of the attitude control system during this time was to preclude a possibility of the Centaur interfering with the spacecraft during the separation phase. Angular rates prior to the retromaneuver did not exceed 0. 51 degree per second.

The retromaneuver sequence was initiated at T + 2098. 4 seconds. The Centaur was commanded to turn approximately 180°. The attitude control system was activated which started turing the vehicle to the new steering vector. Approximately half way (90°) through the turnaround, the V engines were commanded to the V-half-on mode to provide 100 pounds (444 N) of thrust for 20 seconds. This maneuver increased the lateral separation between Centaur and the spacecraft and minimized impingement of the residual propellants on the spacecraft during the period of retrothrust. Guidance gimbal resolver data indicated that the vehicle turned through a total angle of 162° in approximately 100 seconds.

At T + 2333. 7 seconds, the engine prestart valves were opened to allow the residual propellants to discharge through the main engines. Coincident with this propellant discharge, the engine thrust chambers were gimbaled to aline the thrust vector through the vehicle center of gravity. Thrust from the propellant discharge provided additional separation between Centaur and the Surveyor spacecraft. Separation distance at the end of 5 hours was 1436 kilometers. This was more than 4. 3 times the separation distance required for a Surveyor mission.
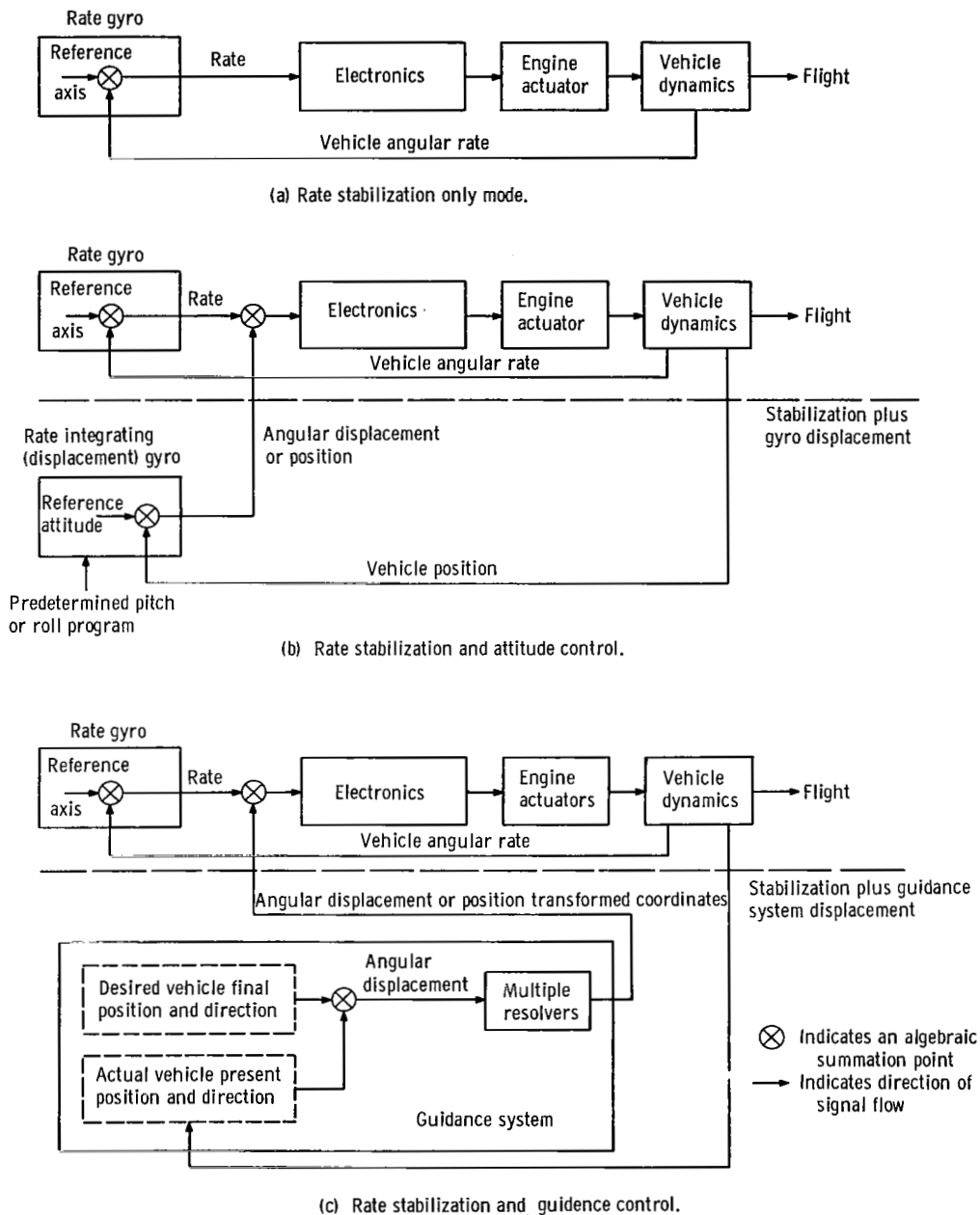
(a) Rate stabilization only mode.

(b) Rate stabilization and attitude control.

(c) Rate stabilization and guidance control.

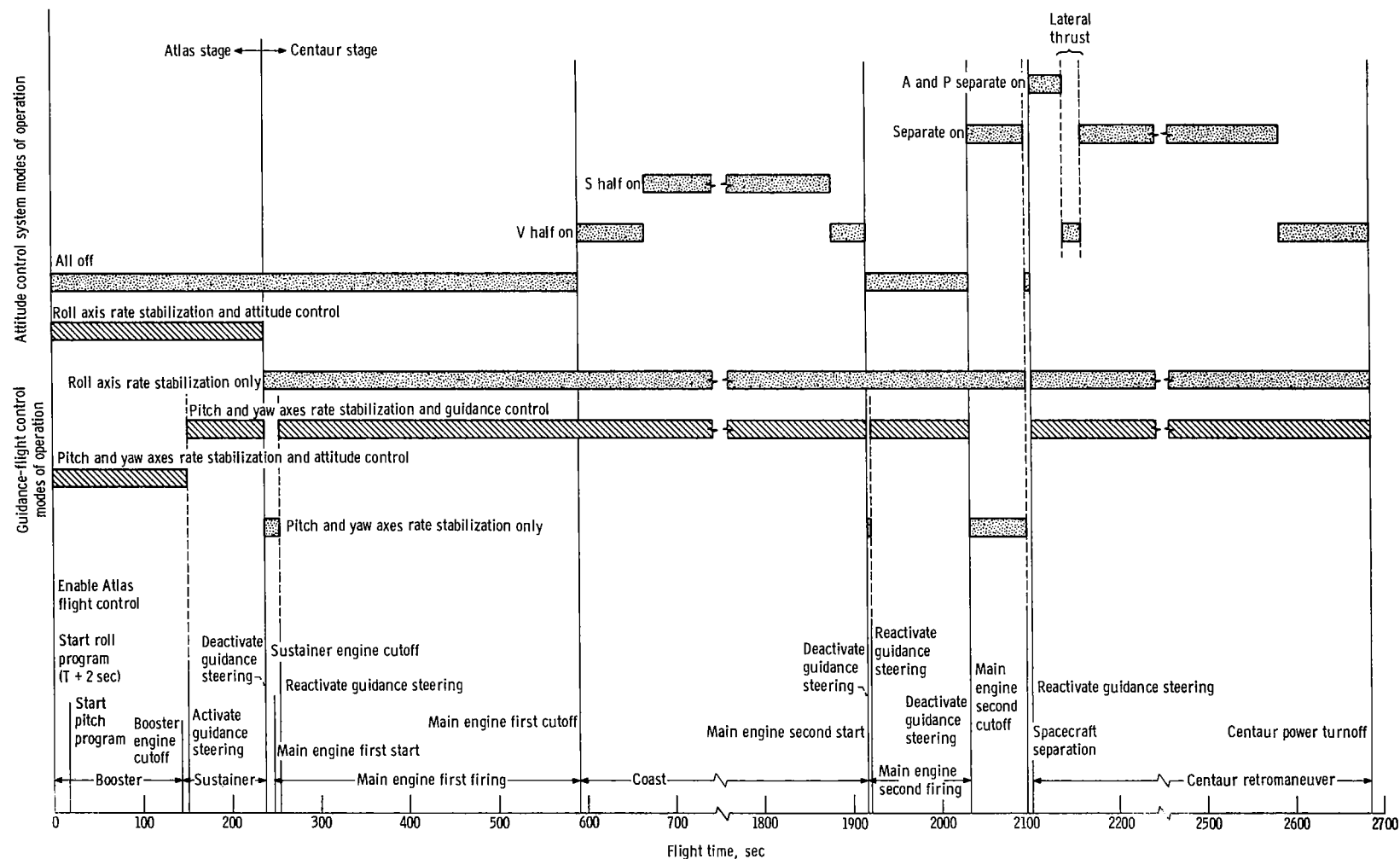Figure V-73. - Guidance and flight control modes of operation, AC-12.

Figure V-74. – Time periods of guidance – flight-control mode and attitude control system mode of operation, AC-12.
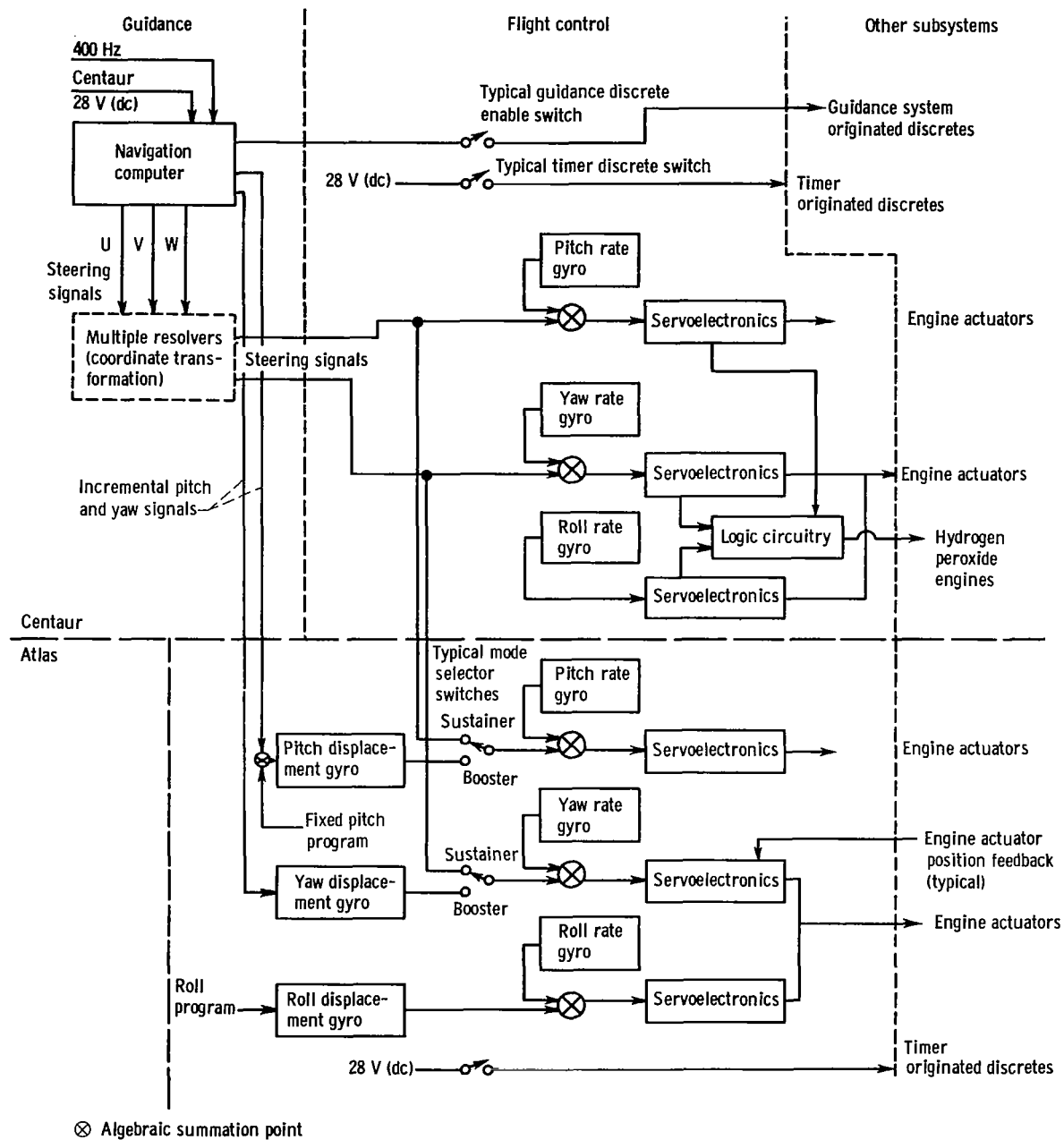
Figure V-75. – Simplified guidance and flight control systems interface, AC-12.
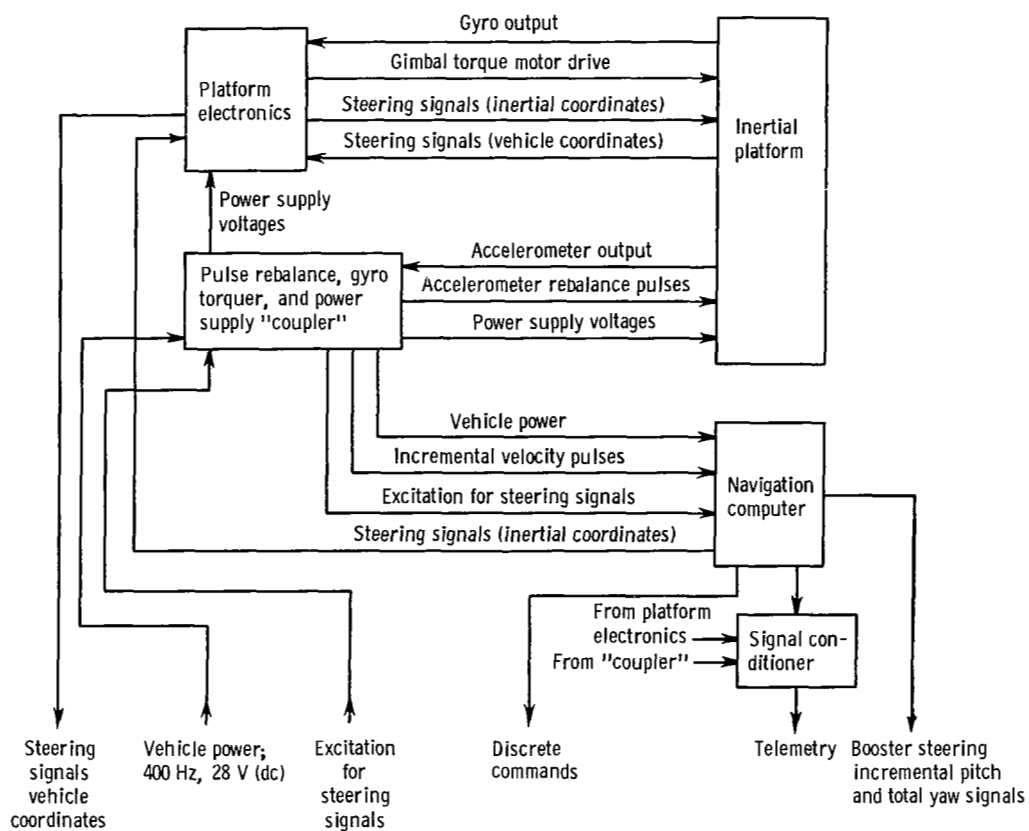
⊗ Algebraic summation point

Figure V-76. – Simplified block diagram of Centaur guidance system, AC-12.

The diagram contains the following labeled elements:

Platform electronics
Inertial platform
Pulse rebalance, gyro torquer, and power supply "coupler"
Navigation computer
Signal con- ditioner

Connections between Platform electronics and Inertial platform:
- Gyro output
- Gimbal torque motor drive
- Steering signals (inertial coordinates)
- Steering signals (vehicle coordinates)

Power supply voltages

Connections between Pulse rebalance, gyro torquer, and power supply "coupler" and Inertial platform:
- Accelerometer output
- Accelerometer rebalance pulses
- Power supply voltages

Connections to Navigation computer:
- Vehicle power
- Incremental velocity pulses
- Excitation for steering signals
- Steering signals (inertial coordinates)

From platform electronics
From "coupler"

Bottom labels:
Steering signals vehicle coordinates
Vehicle power; 400 Hz, 28 V (dc)
Excitation for steering signals
Discrete commands
Telemetry
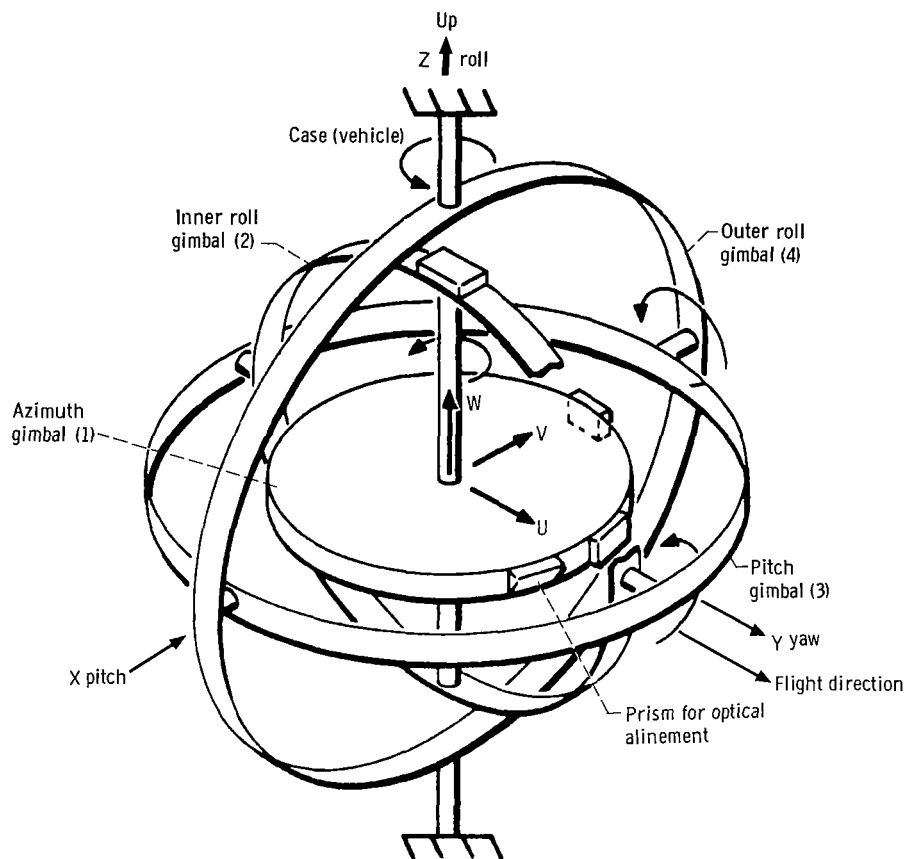Booster steering incremental pitch and total yaw signals

Figure V-77. – Gimbal diagram. Launch orientation: inertial platform coordinates, U, V, and W; vehicle coordinates, X, Y, and Z, AC-12.
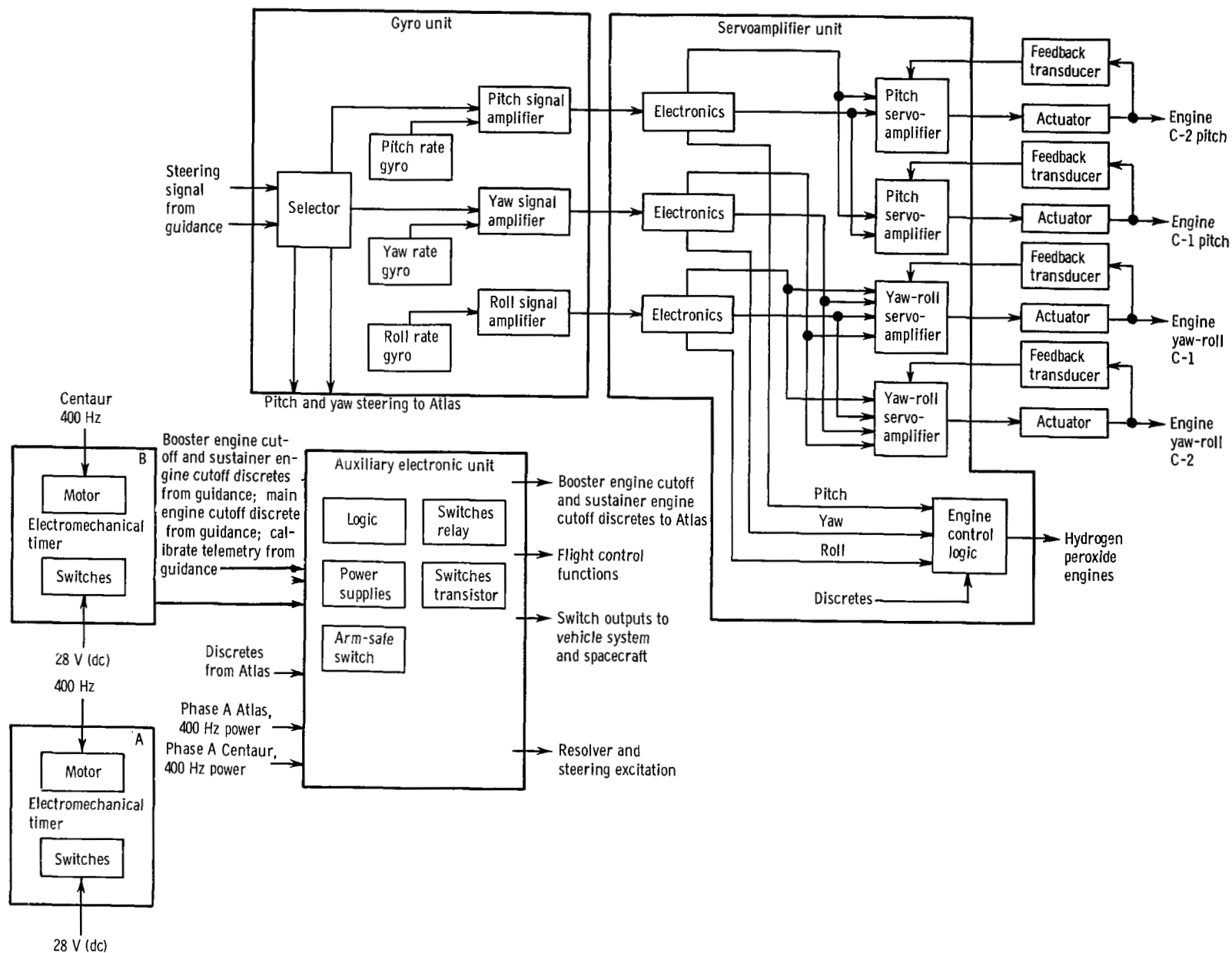
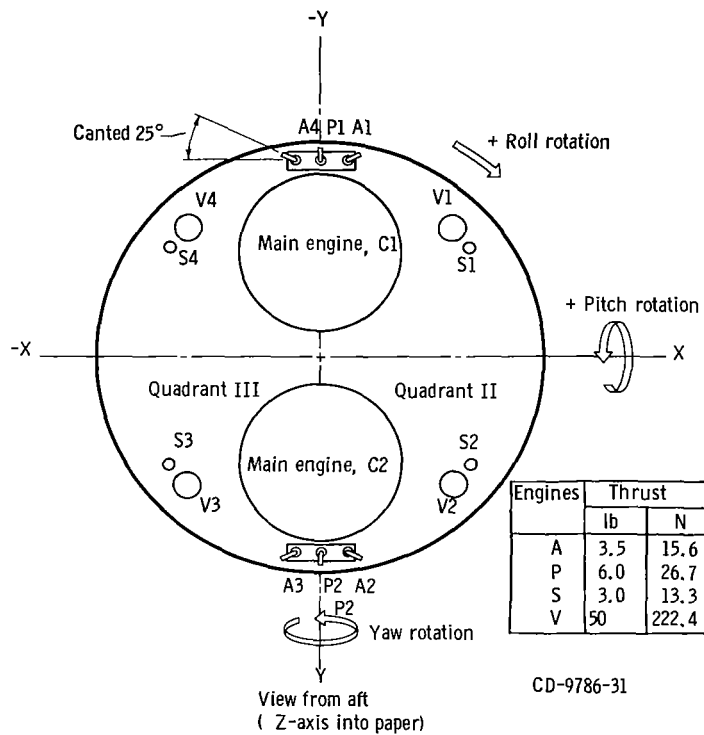Figure V-78. - Centaur flight control system, AC-12.

Figure V-79. – Attitude engines alphanumeric designations and locations, AC-12. Signs of axes are convention for flight control system.

VI. CONCLUSIONS

The Atlas-Centaur AC-12 was the first operational launch vehicle to use the indirect (parking-orbit) mode of ascent. This vehicle boosted Surveyor III – the second Surveyor to land successfully on the Moon. The actual touchdown point on the Moon was 2.94^O South latitude and 23.3^O West longitude. This position was within 5.6 kilometers of the final targeted aiming point.

Centaur main engines were restarted successfully after the 22-minute coast period in the parking orbit and all systems performed within specifications for a normal two-burn mission.

Lewis Research Center,
National Aeronautics and Space Administration,
Cleveland, Ohio, June 12, 1968,
491-05-00-02-22.

APPENDIX

SUPPLEMENTAL FLIGHT, TRAJECTORY, AND PERFORMANCE DATA

by John J. Nieberding

POSTFLIGHT VEHICLE WEIGHT SUMMARY

The postflight weight summary for the Atlas-Centaur vehicle AC-12 with the Surveyor III spacecraft is presented in tables A-I and A-II.

TABLE A-I. - ATLAS POSTFLIGHT VEHICLE WEIGHT

SUMMARY, AC-12

	Weight	
	lb	kg
Booster jettison weight:		
Booster dry weight	6 111	2 772
Oxygen residual	523	237
Fuel (RP-1) residual	538	244
Unburned lubrication oil	28	13
Total	7 200	3 266
Sustainer jettison weight:		
Sustainer dry weight	5 443	2 469
Oxygen residual	715	324
Fuel (RP-1) residual	561	254
Interstage adapter	997	452
Unburned lubrication oil	17	8
Total	7 733	3 507
Flight expendables:		
Main impulse fuel (RP-1)	75 429	34 214
Main impulse oxygen	171 938	77 990
Helium panel purge	6	3
Oxygen vent loss	15	7
Lubrication oil	174	79
Total	247 562	112 293
Ground expendables:		
Fuel (RP-1)	534	242
Oxygen	1 700	771
Lubrication oil	3	1
Exterior ice	50	23
Liquid nitrogen in helium shrouds	140	64
Pre-ignition gaseous oxygen loss	450	204
Total	2 877	1 305
Total Atlas tanked weight	265 372	120 371
Minus ground run	-2 877	-1 305
Total Atlas weight at lift-off	262 495	119 066

TABLE A-II. - CENTAUR POSTFLIGHT VEHICLE WEIGHT

SUMMARY, AC-12

	Weight	
	lb	kg
Basic hardware:		
Body	950	431
Propulsion group	1 229	558
Guidance group	338	153
Control group	151	68
Pressurization group	187	84
Electrical group	286	130
Separation group	81	37
Flight instrumentation	258	117
Miscellaneous equipment	145	66
Total	3 625	1 644
Jettisonable hardware:		
Nose fairing	1 993	904
Insulation panels	1 213	550
Ablated ice	50	23
Total	3 256	1 477
Centaur residuals:		
Liquid hydrogen	166	75
Liquid oxygen	532	241
Gaseous hydrogen	116	53
Gaseous oxygen	170	77
Hydrogen peroxide	36	16
Helium	5	2
Ice	12	5
Total	1 037	470
Centaur expendables:		
Main impulse hydrogen	4 864	2 206
Main impulse oxygen	24 581	11 150
Gas boiloff on ground hydrogen	6	3
Gas boiloff on ground oxygen	21	9
In-flight chill hydrogen	42	19
In-flight chill oxygen	50	22
Booster phase vent hydrogen	40	18
Booster phase vent oxygen	80	36
Sustainer phase vent hydrogen	18	8
Sustainer phase vent oxygen	30	13
Engine shutdown loss hydrogen:		
First shutdown loss	6	3
Second shutdown loss	6	3
Engine shutdown loss oxygen:		
First shutdown loss	18	8
Second shutdown loss	18	8
Parking-orbit vent hydrogen	13	6
Parking-orbit vent oxygen	0	0
Parking-orbit leakage hydrogen	0	0
Parking-orbit leakage oxygen	0	0
Hydrogen peroxide	201	91
Helium	5	2
Total	29 999	13 608
Total tanked weight	37 917	17 199
Minus ground vent	-27	-12
Total Centaur weight at lift-off	37 890	17 187
Spacecraft	2 280	1 034
Total Atlas-Centaur-spacecraft lift-off weight	302 665	137 287

ATMOSPHERIC SOUNDING DATA

Ambient Temperature and Pressure

The atmospheric conditions at the launch site were determined from data obtained from several Rawinsonde sounding balloons sent aloft on the day of launch up until approximately 02:10 hours eastern standard time. Profiles of measured temperature and pressure are compared with the predicted values on the basis of characteristic weather for the Cape Kennedy area. The largest dispersion between predicted and actual temperatures in figure A-1 occurred at an altitude of about 6.6 nautical miles (12.2 km). At this altitude the actual temperature was approximately 10.0^O R (5.6 K) lower than predicted. The average temperature variation over the entire altitude range was about 4.9^O R (2.7 K) lower than predicted. The measured pressures in figure A-2 were in very close agreement with the predicted values at all altitudes. Consequently, these small dispersions in atmospheric temperatures and pressures had no adverse affects on the Atlas-Centaur flight.

Atmospheric Winds

Wind speed and azimuth data as a function of altitude are compared with the normal April wind data for the Cape Kennedy area in figures A-3 and A-4, respectively. The erratic pattern of the wind data curves actually occurred; the data should not be smoothed.

Although absolute agreement between the magnitudes of actual and predicted wind speeds was not always close, the basic characteristics of the predicted and actual data curves are similar. The maximum wind speed measured was 72 feet per second (22 m/sec) at an altitude of 7.5 nautical miles (13.9 km). This measured maximum occurred at an altitude approximately 1 nautical mile (1.8 km) higher than predicted. The maximum wind speed of 104 feet per second (31.8 m/sec) was predicted to occur at an altitude of 6.5 nautical miles (12.02 km). Over the entire 18-nautical-mile (33.2-km) altitude range, the actual wind speeds averaged approximately 16.4 feet per second (5.0 m/sec) lower than predicted.

Wind azimuth is defined as the direction toward which the wind is blowing. Wind azimuth differs from wind direction by 180°. Between approximately 0.75 nautical mile (1.39 km) and 11.3 nautical miles (20.9 km) all actual wind azimuths are higher than predicted. Except for the peaks in actual data at 1.8 and 9.75 nautical miles (3.3 and 18.0 km, respectively), the characteristics of the actual curve are as predicted over the total altitude range. The average difference between actual and predicted data in this range was approximately 80°. Above 11.3 nautical miles (20.9 km), the actual wind azimuths

were more erratic than they were below this altitude. This pattern of rapid azimuth fluctuation was predicted. No wind data were available above about 18 nautical miles(33.2 km).

SURVEYOR LAUNCH WINDOWS AND COUNTDOWN HISTORY

The April 1967 launch period for AC-12 spanned seven days: April 15 to April 21. If launched on April 15, because of the design of the lunar trajectory for that day, the only possible landing site for Surveyor III would have been very near the center of the visible face of the Moon. This area, known as Sinus Medii, is a region of very rugged terrain. Because of the failure of Surveyor II, the Jet Propulsion Laboratory decided not to risk a Surveyor III landing in such a potentially dangerous region. Consequently, April 15 was eliminated as a possible launch day.

There were two possible landing sites for an April 16 launch, one was Sinus Medii and the other was much farther west, at 3.33° South latitude, 23.17° West longitude. Sinus Medii had previously been eliminated as a possible target. With an April 16 launch for the western landing site, however, it was possible for the Surveyor to land just prior to lunar sunrise. Consequently, it would have violated its constraint to land no earlier than 1 hour after lunar sunrise. For a launch to this site on April 17, however, the lunar lighting criteria could be met. Thus, April 17 was chosen for the first launch day.

The launch window on April 17 opened at 0114 eastern standard time when the required time for the parking-orbit coast became less than the maximum allowable of 25 minutes. The window closed at 0225 eastern standard time because of a telemetry coverage constraint. The opening and closing launch azimuths were 94.9° and 103.0°, respectively. Two built-in holds were scheduled in the countdown: one at T - 90 minutes of 60 minutes duration and one at T - 5 minutes of 10 minutes duration. It became necessary to extend the T - 5 hold to investigate an indicated spacecraft anomaly in the position transducer of the roll actuator. Results of testing on Surveyor V and study of data from Surveyor II verified that the behavior of the roll actuator position signal was characteristic of the system and that Surveyor III was ready for launch. The countdown was resumed at 0200 eastern standard time. Lift-off occurred at 0205:01.059 eastern standard time, approximately 51 minutes into a 71-minute window.

FLIGHT EVENTS RECORD

The major flight events for the AC-12 flight are listed in table A-III. Programmer times, when given, are for those flight events sequenced and commanded by an in-flight

Event	Programmer time, sec	Preflight time, sec	Actual time, sec
Lift-off (2-in. (5.08-cm) motion)	T + 0.0	T + 0.0	T + 0.0
Start roll	T + 2.0	T + 2.0	T + 2.0
End roll	T + 15.0	T + 15.0	T + 15.0
Start pitchover	T + 15.0	T + 15.0	T + 15.0
Booster engine cutoff	BECO	T + 143.0	T + 142.3
Jettison booster engines	BECO + 3.1	T + 146.1	T + 145.3
Jettison insulation panels	BECO + 34.0	T + 177.0	T + 176.2
Jettison nose fairing	BECO + 61.0	T + 204.0	T + 202.9
Start Centaur boost pumps	BECO + 62.0	T + 205.0	T + 203.9
Sustainer engine cutoff; vernier engine cutoff; start Centaur programmer	SECO	T + 236.8	T + 237.7
Atlas-Centaur separation	SECO + 1.9	T + 238.7	T + 239.6
Centaur main engine first start (MES - 1)	SECO + 11.5	T + 248.3	T + 249.2
Centaur main engine first cutoff	MECO 1	T + 574.9	T + 589.7
Start propellant settling engines	MECO 1	T + 574.9	T + 589.7
Stop propellant settling engines; start propellant retention engines	MECO 1 + 76.0	T + 650.9	T + 664.8
Stop propellant retention engines; start propellant settling engines	MES 2 - 40.0	T + 1873.8	T + 1877.0
Start Centaur boost pumps	MES 2 - 28.0	T + 1885.8	T + 1889.3
Centaur main engine second start	MES 2	T + 1913.8	T + 1917.3
Stop propellant settling engines	MES 2	T + 1913.8	T + 1917.3
Centaur main engine second cutoff	MECO 2	T + 2022.2	T + 2028.6
Preseparation arming signal; extend landing gear signal	MES 2 + 134	T + 2047.8	T + 2051.3
Unlock omniantennas on signal	MES 2 + 144.5	T + 2058.3	T + 2061.8
High power transmitter on signal	MES 2 + 165	T + 2078.8	T + 2082.3
Electrical disconnect	MES 2 + 170.5	T + 2084.3	T + 2087.8
Spacecraft separate	MES 2 + 176.0	T + 2089.8	T + 2093.2
Start turnaround	MES 2 + 181.0	T + 2094.8	T + 2098.5
Start propellant settling engines[a]	MES 2 + 221.0	T + 2134.8	T + 2138.4
Stop propellant settling engines[a]	MES 2 + 241.0	T + 2154.8	T + 2158.4
Start discharge of Centaur residual propellants	MES 2 + 416	T + 2329.8	T + 2333.7
End discharge of Centaur residual propellants; start propellant settling engines[b]	MES 2 + 666	T + 2579.8	T + 2583.5
End propellant settling engines firing (hydrogen peroxide depleted)	Not applicable	No applicable	T + 2627.7
Energize power changeover	MES 2 + 766	T + 2679.8	T + 2683.4

[a]Lateral thrust imparted to Centaur for additional longitudinal separation from spacecraft (V engines).
[b]Postmission hydrogen peroxide depletion experiment.

timer. Preflight times are based on the best estimate of the flight sequence for the actual flight azimuth. Actual times listed are the measured times of the given flight events.

TRAJECTORY DATA

Dynamic Pressure and Mach Number

Dynamic pressure and Mach number data for AC-12 are presented in figures A-5 and A-6, respectively. These data were calculated from downrange tracking data obtained during flight and from atmospheric sounding data taken from a Rawinsonde balloon launched approximately 5 minutes after launch. The agreement between actual and predicted values of dynamic pressure was good except during the time interval from approxi-

mately T + 64 to T + 78 seconds when slight discrepancies were present. The maximum difference between actual and predicted values of dynamic pressure occurred at T + 70 seconds when the actual pressure was about 34.5 pounds per square foot (0.165 N/cm^2) higher than predicted. Even this maximum difference represents a dispersion from predicted values of only 4.7 percent. This dispersion was not considered detrimental to the Atlas-Centaur flight. Beyond T + 78 seconds, actual values were consistently lower than predicted. The average deviation was approximately 16.6 pounds per square foot (0.079 N/cm^2).

Dynamic pressure, q is defined as $1/2 \rho V^2$, where ρ is the atmospheric density and V is the vehicle velocity relative to the atmosphere (air speed). Since ρ depends on atmospheric pressure P and on atmospheric temperature T, dispersions in q can only result from dispersions in P, T, or V. Deviations of actual from predicted values of these three parameters completely explain all dynamic pressure dispersions. Every actual data point which disagreed with the value predicted at that time can be precisely correlated with this predicted value if known dispersions in ambient pressure and temperature and vehicle relative velocity are considered.

Variation of the actual Mach number values (velocity ratios) from the expected values was negligible over the entire time interval shown in figure A-6. At about T + 58 seconds, the vehicle reached a relative velocity of Mach 1 and thus entered the transonic region (see fig. A-7). The slight decrease in slope, which represents a decrease in acceleration, at T + 142.3 seconds reflects the loss of booster thrust at booster engine cutoff.

Axial Load Factor

The axial load factor for the Atlas and Centaur powered phases of flight is shown in figure A-7. Axial load factor is defined as the ratio of the quantity vehicle thrust minus drag divided by vehicle weight. A plot of the axial load factor is equivalent to a plot of the acceleration, in g's, supplied to the vehicle by thrust alone (thrust acceleration). It does not include the gravitational component of acceleration. Actual and predicted data showed good agreement at all times except in the brief interval between about T + 236 and T + 252 seconds.

A flattening of the curve occurs from approximately T + 52 to T + 60 seconds. This interval of relatively constant acceleration reflects the severe vibrations experienced by the vehicle when it passed through Mach 1 (see fig. A-6). A very abrupt decrease in acceleration from 5.62 to 1.07 g's occurred at booster engine cutoff, 0.7 second earlier than expected. A small but very sudden increase in acceleration occurred about 3.0 seconds later when the booster engines were jettisoned. Following booster jettison, the constantly decreasing vehicle propellant weight caused the thrust acceleration to increase

smoothly, except for small perturbations caused by sudden weight losses at insulation panel and nose fairing jettison (T + 176.2 and T + 202.9 sec, respectively). Sustainer engine cutoff was expected at T + 236.8 seconds; it actually occurred at T + 237.7 seconds. Consequently, the abrupt decrease in the curve reflecting the loss of all thrust occurred about 0.9 second later than expected. Since Centaur main engine first start is a timed function from sustainer engine cutoff, the Centaur main engines fired slightly later than expected. As a result, the rise in axial load factor which reflects the Centaur main engine thrust, occurred at T + 249.2 seconds, 0.9 second later than expected. After the main engines started, the uniformly decreasing Centaur propellant weight caused the curve again to increase smoothly until termination of the Centaur main engine first firing at T + 589.7 seconds. This firing period was 13.9 seconds longer than predicted (see PROPULSION SYSTEMS in section V).

Inertial Velocity

Inertial velocity data for the AC-12 flight are presented in figure A-8. Inertial velocity is referenced to a coordinate system which does not rotate with the Earth. As expected, abrupt changes in the vehicle total acceleration, the slope of the inertial velocity curve, coincided with the sharp changes in axial load factor, or thrust acceleration in g's (see fig. A-7). From lift-off to booster engine cutoff, agreement between actual and predicted data is excellent. Between booster engine cutoff and sustainer engine cutoff, actual inertial velocities averaged less than 0.5 percent low. The sudden flattening of the curve at sustainer engine cutoff indicates the loss of all thrust. The actual curve shows that the sustainer engine shut off almost exactly at the time expected (0.9 sec late). The velocities again began to increase 11.5 seconds later when the Centaur main engines started for the first time.

During the Centaur first firing period, the actual velocities were lower than expected. A major contributor to these low velocities was the lower than expected thrust (see PROPULSION SYSTEMS in section V). The maximum difference between predicted and actual data occurred at about T + 576 seconds when the actual velocities were about 800 feet per second (244 m/sec) lower than predicted. By the time the Centaur shut down, however, the actual velocities were about 50 feet per second (15.3 m/sec) higher than expected. Because the altitude at this time was lower than expected (see fig. A-9), these high velocities were essential to ensure the proper energy for the parking orbit.

Attitude and Range Tracking Data

Altitude as a function of time and ground range are shown in figures A-9 and A-10, respectively. The ground trace of the vehicle subpoint, latitude against longitude, is given in figure A-11.

Actual and predicted altitudes are in close agreement until about T + 300 seconds. Beyond this time, actual altitudes were lower than expected. The maximum deviation occurred at Centaur main engine first cutoff (T + 589.7 sec) when the actual altitude was approximately 3 nautical miles (5.5 km) lower than expected. The lower than predicted altitude at this time was compensated for by higher than expected inertial velocity at the same time. Consequently, the proper parking-orbit energy was attained. Although not shown by the data, after T + 589.7 seconds, the altitudes are almost constant, indicating that a nearly circular parking orbit had been achieved.

The plot of altitude against ground range in figure A-10 shows good agreement between actual and predicted data until the vehicle was approximately 300 nautical miles (555 km) down range. Beyond this range, the altitudes are slightly lower than expected. This deviation of actual from predicted data is consistent with that observed in figure A-9.

Geocentric latitude against longitude in figure A-11 shows good agreement between predicted and actual data for the data interval plotted. The maximum dispersion in latitude occurred at a longitude of about 58° West, when the latitude was 0.75° more southernly than expected. At Centaur main engine first cutoff, the longitude was 60.7° West. At this time (T + 589.7 sec) the latitude dispersion was 0.70°.

Orbital Parameters

Orbital parameters for the Surveyor III lunar-transfer orbit, the Centaur parking orbit, and the Centaur postretromaneuver orbit are presented in tables A-IV, A-V, and A-VI, respectively.

The data defining the Surveyor orbit is based on approximately 22 hours of tracking data. The Centaur parking orbit is based on data obtained early in the coast phase, 15.5 seconds after the Centaur propellant settling engines were shut down. The postretromaneuver orbit is based on Eastern Test Range tracking data. The reference time for this orbit occurred about 51 minutes after lift-off.

TABLE A-IV. - SURVEYOR ORBIT PARAMETERS, AC-12

Parameter	Value
Time from 2-in. (5.08-cm) motion, sec	78 904
Epoch (Greenwich mean time), hr	0500:05.0 (Apr. 18)
Apogee altitude, n mi; km	268 571; 497 393
Perigee altitude, n mi; km	91; 168.53
Injection engergy, C_3, ft^2/sec^2; km^2/sec^2	-1.6816×10^7; -1.56223
Semimajor axis, n mi; km	137 769; 255 149
Eccentricity	0.97443161
Orbital inclination, deg	30.533157
Injection (spacecraft separate) true anomaly, deg	10.959
Injection (spacecraft separate) flight path angle, deg	5.624
Period, days	14.85
Longitude of ascending mode, deg	125.154
Argument of perigee, deg	223.04754
Geocentric latitude at Centaur main engine second cutoff, deg South	21.97
Longitude at Centaur main engine second cutoff, deg East	25.02

TABLE A-V. - CENTAUR PARKING-ORBIT PARAMETERS, AC-12

Parameter	Value
Time from 2-in. (5.08-cm) motion, sec	680.3
Epoch (Greenwich mean time), hr	0716:21.3 (Apr. 17)
Apogee altitude, n mi; km	94; 174.09
Perigee altitude, n mi; km	88; 162.98
Injection energy, C_3, ft^2/sec^2; km^2/sec^2	-65.574×10^7; -60.92
Semimajor axis, n mi; km	3532; 6541
Eccentricity	0.0008309
Orbital inclination, deg	29.96244
Period, min	87.7
Inertial velocity at Centaur main engine first cutoff, ft/sec; m/sec	25 924; 7902
Earth relative velocity at Centaur main engine first cutoff; ft/sec; m/sec	24 534; 7478
Geocentric latitude at Centaur main engine first cutoff, deg North	22.99
Longitude at Centaur main engine first cutoff, deg West	60.68

Parameter	Value
Time from 2-in. (5.08-cm) motion, sec	3091.9
Epoch (Greenwich mean time), hr	0756:32.9 (Apr. 17)
Apogee altitude, n mi; km	190 828; 353 413
Perigee altitude, n mi; km	90; 166.68
Injection energy, C_3, ft^2/sec^2; km^2/sec^2	-2.3358×10^7; -2.17
Semimajor axis, n mi; km	98 902; 183 167
Eccentricity	0.9642721
Orbital inclination, deg	29.96997
Period, days	9.03

Surveyor III Midcourse Velocity Correction

The accuracy with which the Surveyor III spacecraft was injected into the lunar-transfer orbit was such that a midcourse velocity correction of only 12.91 feet per second (3.94 m/sec) would have been required to ensure arrival at the preflight designed target. This velocity correction is known as the "miss only" correction. In order to ensure arrival at the preflight designed target at the designed arrival time, a correction of 19.90 feet per second (6.07 m/sec) would have been required. This velocity correction is known as the "miss plus time of flight" correction. However, during the flight of Surveyor III, the Jet Propulsion Laboratory chose to alter the aiming point slightly from 3.33° South latitude, 23.17° West longitude, to 2.92° South, 23.25° West. Consequently, the midcourse velocity correction actually made to ensure arrival at the new target was 13.7 feet per second (4.19 m/sec). No correction was made to adjust the arrival time. Therefore, the total midcourse velocity correction performed by Surveyor III approximately 22 hours after lift-off was 13.7 feet per second (4.19 m/sec).
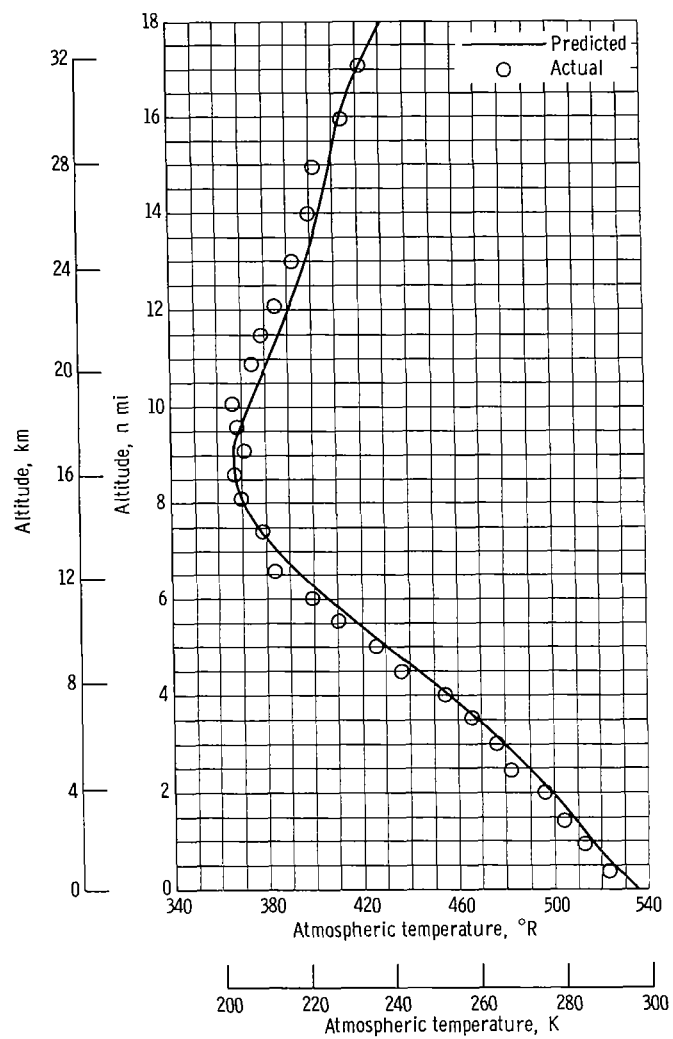
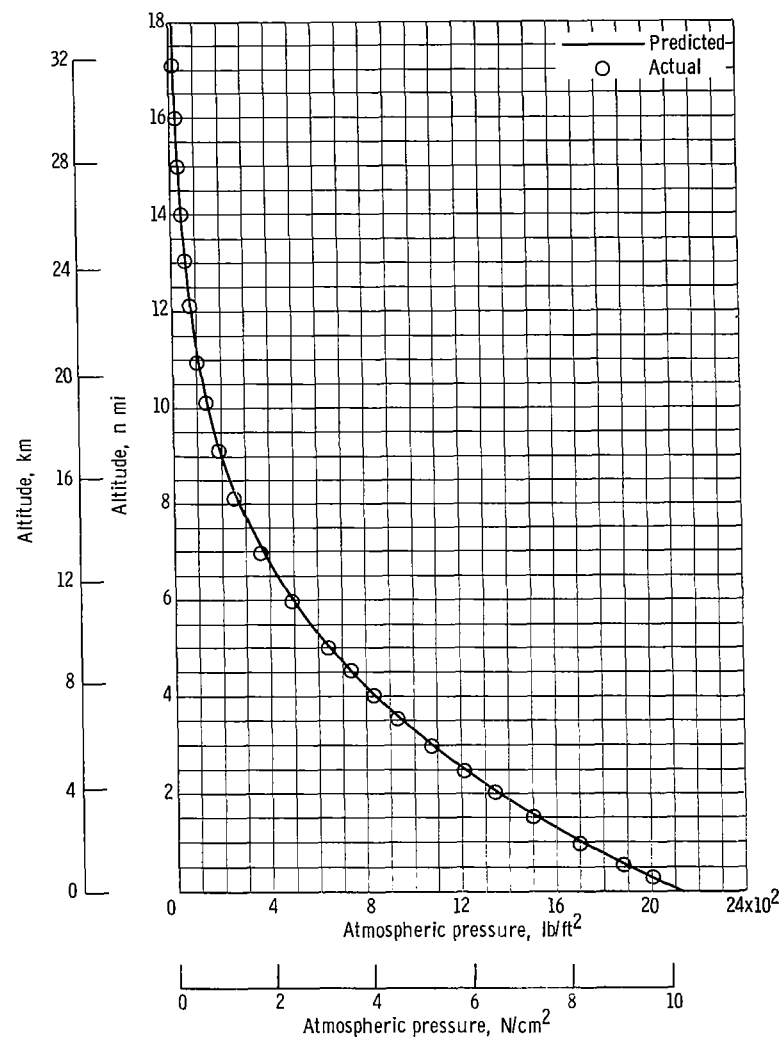Figure A-1. - Altitude as function of temperature, AC-12.

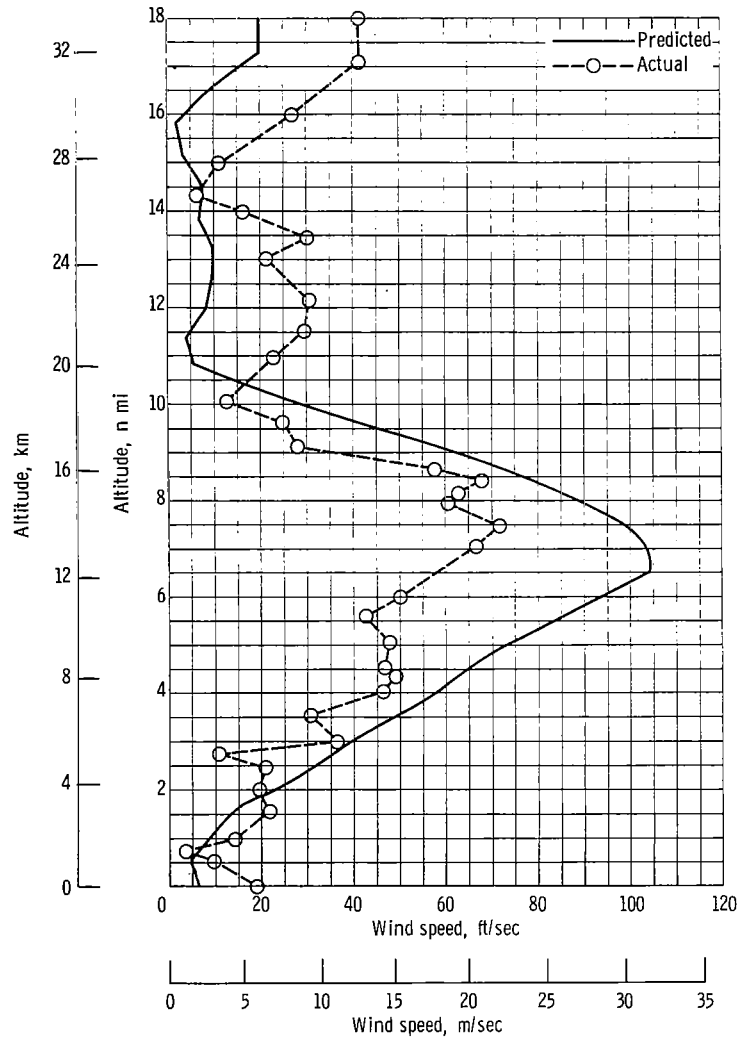Figure A-2. - Altitude as function of pressure, AC-12.

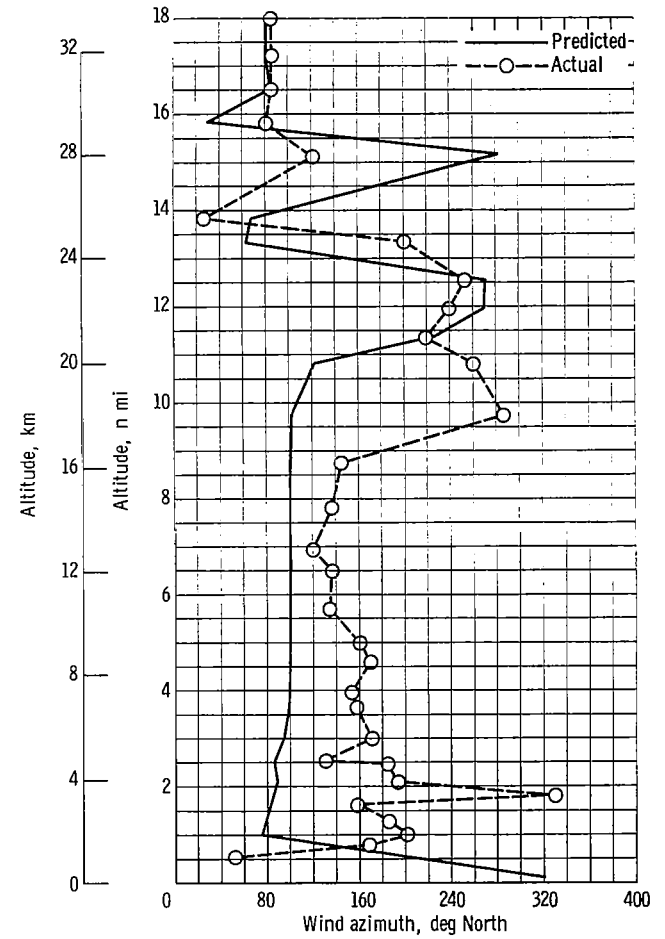Figure A-3. - Altitude as function of wind speed, AC-12.

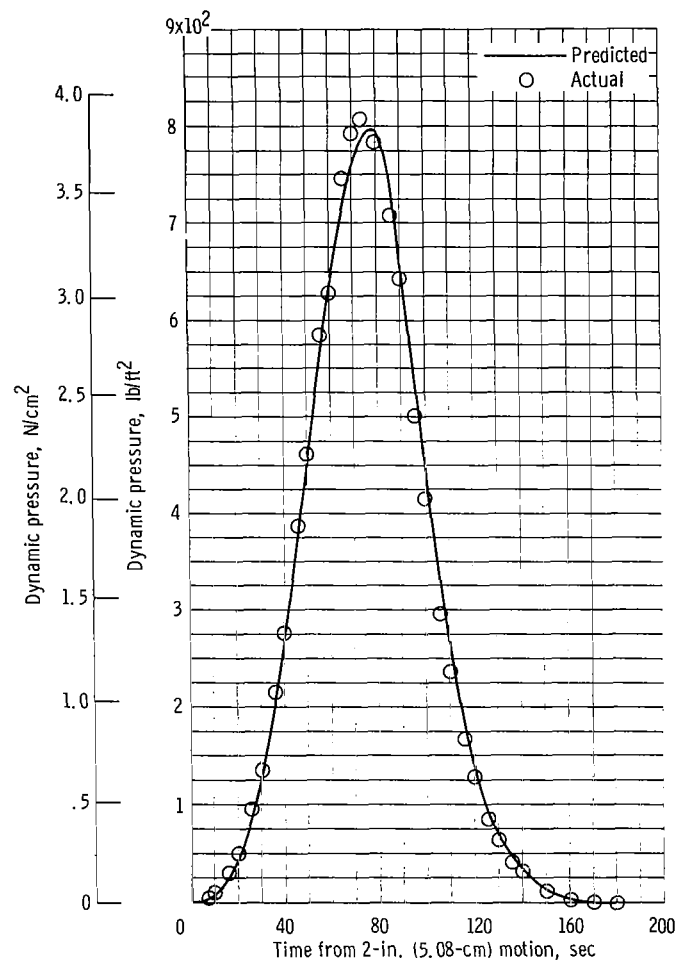Figure A-4. - Altitude as function of wind azimuth, AC-12.

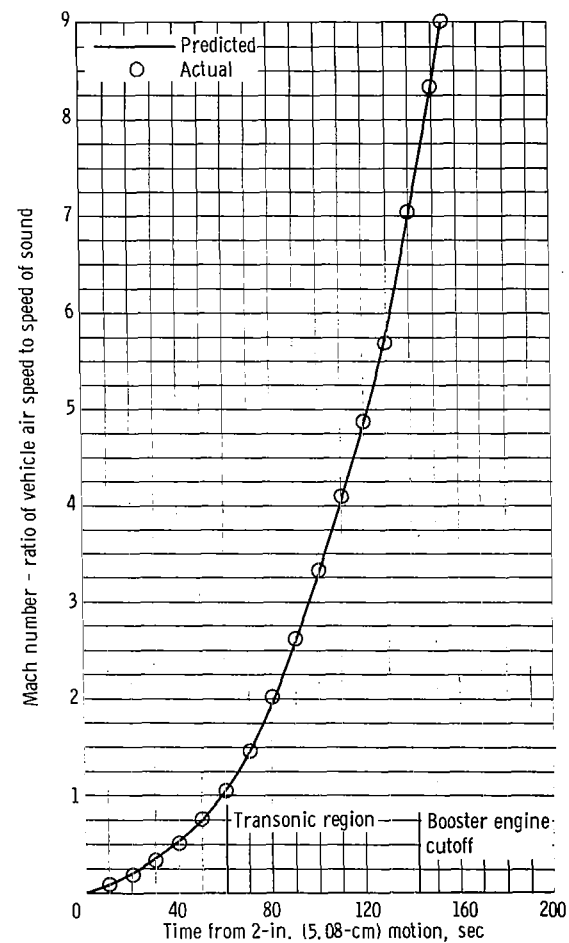Figure A-5. - Dynamic pressure as function of time, AC-12.

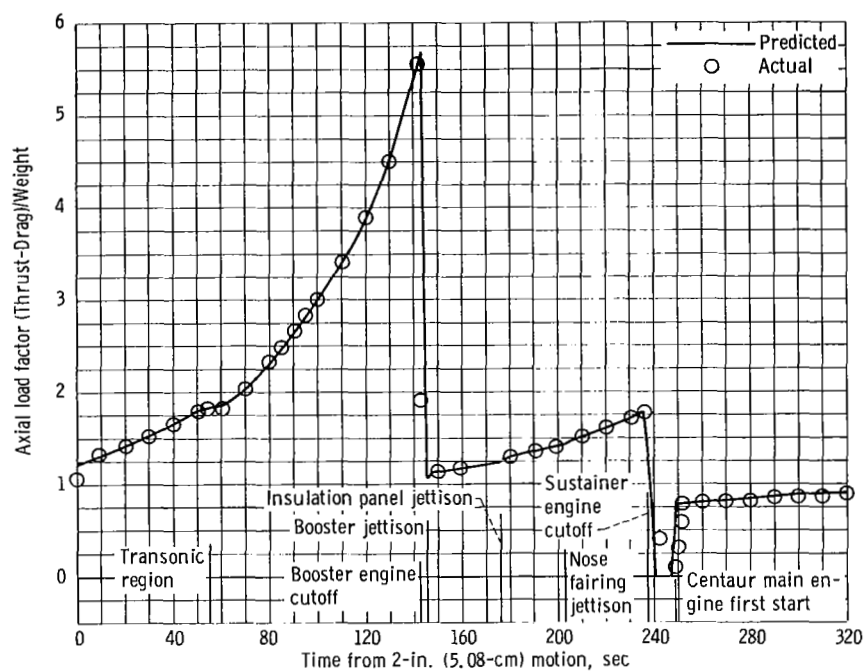Figure A-6. - Mach number as function of time, AC-12.

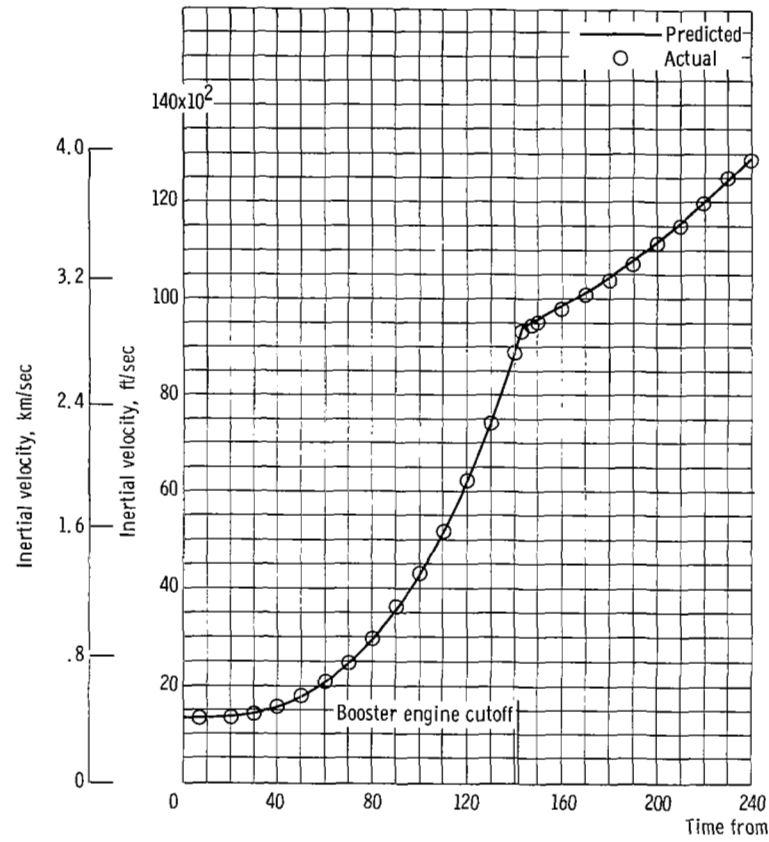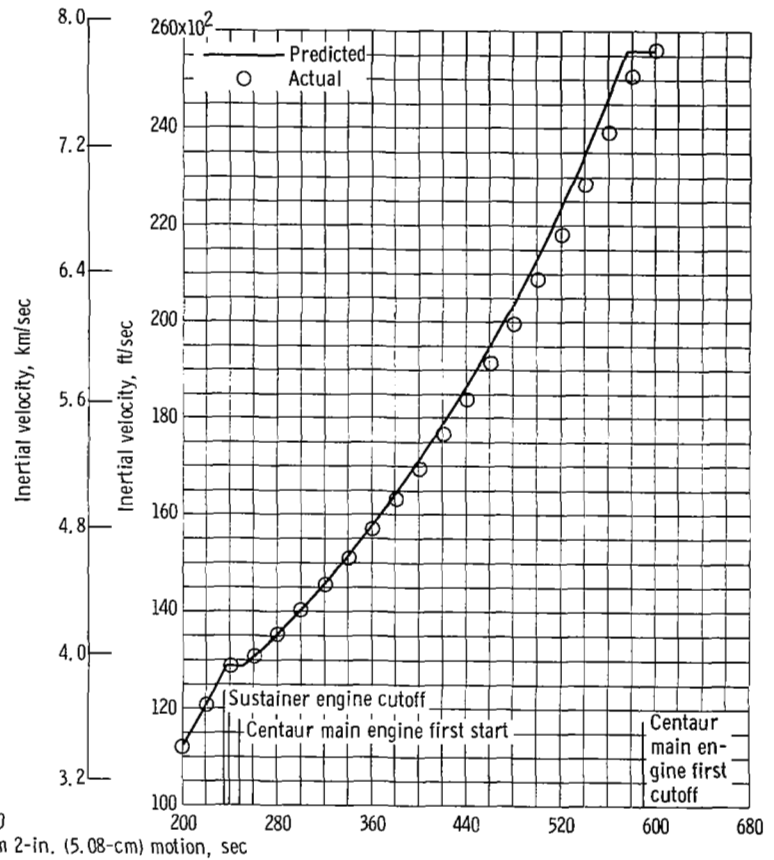Figure A-7. - Axial load factor as function of time, AC-12.

(a) Time, 0 to 240 seconds.

(b) Time, 200 to 680 seconds.

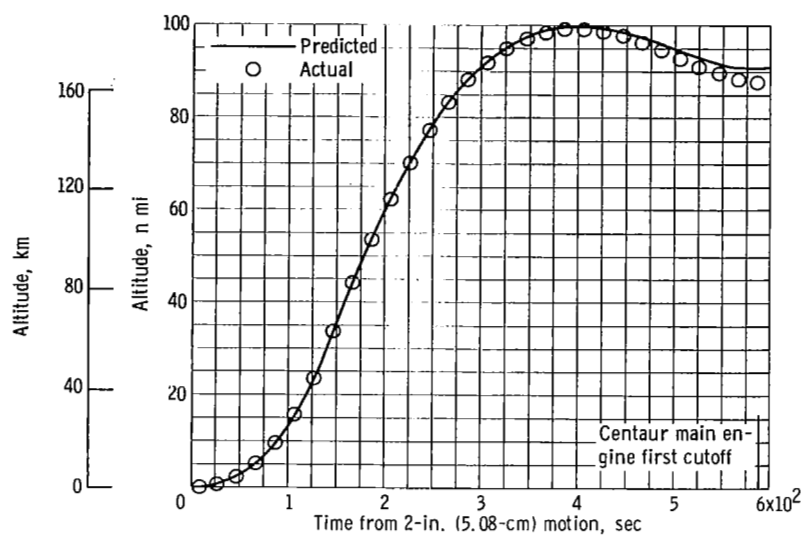Figure A-8. - Inertial velocity as function of time, AC-12.
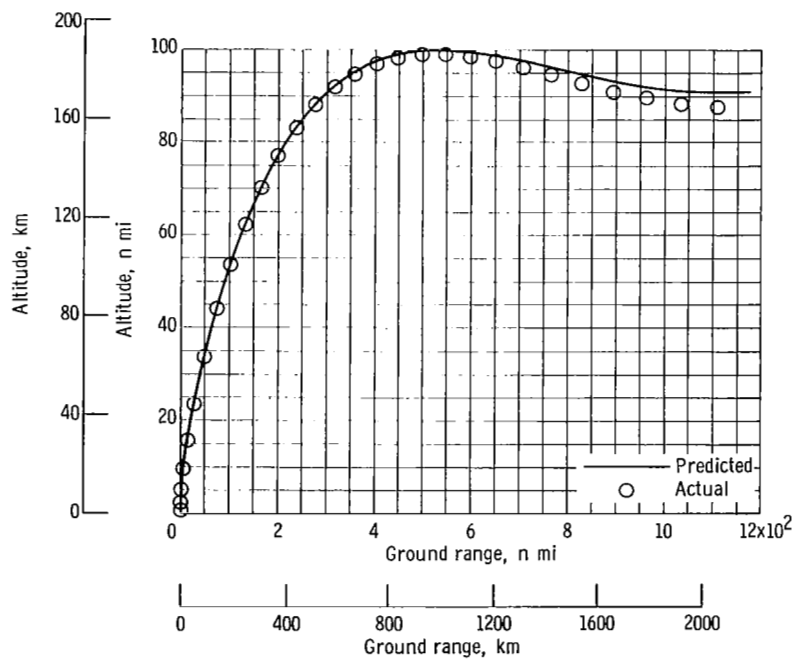
Figure A-9. – Altitude as function of time, AC-12.

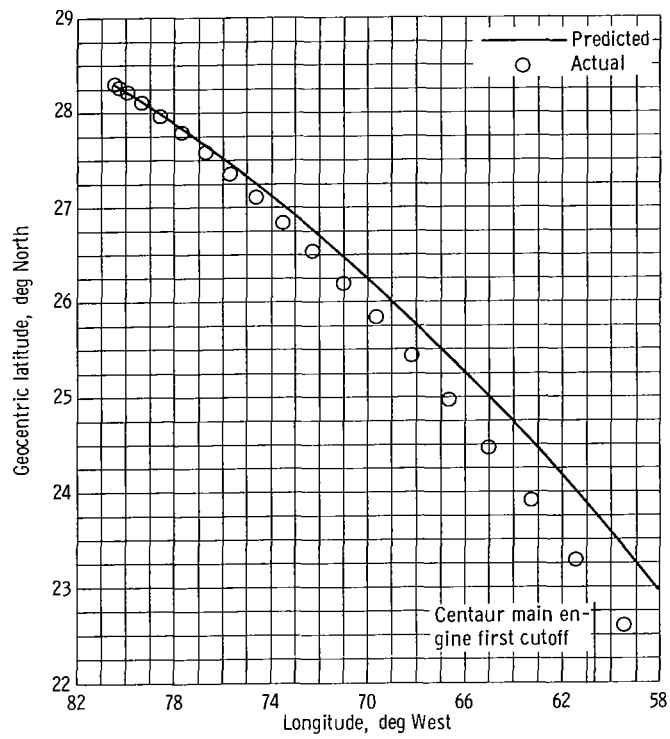Figure A-10. – Altitude as function of ground range, AC-12.

Figure A-11. - Ground trace of vehicle subpoint, AC-12.

REFERENCES

1. Lewis Research Center: Performance Evaluation of Atlas-Centaur Restart Capability in Earth Orbit. TM X-1647, 1968.

2. Foushee, B. R.: Liquid Hydrogen and Liquid Oxygen Density Data for Use in Centaur Propellant Loading Analysis. Rep. AE62-0471, General Dynamics Corp., May 1, 1962.

3. Pennington, K., Jr.: Liquid Oxygen Tanking Density for the Atlas-Centaur Vehicles. Rep. BTD 65-103, General Dynamics Corp., June 3, 1965.

4. Gerus, Theodore F.; Housely, John A.; and Kusic, George: Atlas-Centaur-Surveyor Longitudinal Dynamics Tests. NASA TM X-1459, 1967.